Crystal Nucleation of Poorly Soluble Drugs

II. Experimental results and new knowledge

Alexandra Franzén

Supervisor: Lennart Lindfors, Medicines Evaluation, Astra Zeneca, Mölndal

Examiner: Ulf Olsson, Department of Physical Chemistry, Lund University

Master of Science Thesis, 30hp, 2011

Abstract

This report is a continuation of the report, *Crystal nucleation of poorly soluble drugs, I Method development and initial results. [1]*

The aim of the studies was to experimentally investigate the crystallization process. The focus has been on crystal growth, crystal dissolution and primary nucleation.

For three model substances, Bicalutamide, Linaprazan and Felodipine, experiments have been carried out. The experimental results have been compared to existing theoretical models to see how well the models can describe these processes.

For crystal growth and dissolution, a surface integration/disintegration constant, λ, can be used to try to describe the processes. The dissolution experiments could be well described by this model, while growth could not. The model does however work better at high supersaturations than low ones, concerning growth.

The Hillig- Nielsen, polynuclear surface nucleation model was also used to evaluate the growth experiments. The model was able to describe the growth process better.

Obretenov interpolation, a model where both mono- and polynuclear growth are included, was also used to try to describe crystal growth. This model gave the best agreement between experimental results and theory so far.

Nucleation experiments were also conducted, and from the experiments the interfacial tension was to be determined. The development of this experimental method has been an important part of this work.

Table of Contents

1. Introduction

Many drugs developed today are poorly soluble in water. To be able to administer these drugs at high doses, formulations with enhanced dissolution are required. This can be achieved by use of drug nanoparticles. Nanoparticles have a small radius and thus a large surface to volume ratio providing fast dissolution. [2]

Nanoparticles can be either amorphous or crystalline. Amorphous material has an apparent solubility that is higher than the crystalline solubility. [3][4] Amorphous nanoparticles may, due to the solubility, increase the dissolution rate in the stomach and intestinal system and thus provide an improved bioavailability.

The bulk concentration in a system where amorphous particles dissolve, is above the equilibrium solubility for the most stable crystalline phase, i.e. it is supersaturated. The dissolved substance will potentially nucleate in the solution forming crystalline material. Since crystallization is unfavorable for the bioavailability, there is a need to study and understand crystallization, in order to be able to reduce it. [5]

Nanoparticles have a tendency to aggregate. In order to prevent aggregation polymer and, or surfactant is often present in the process of forming nanoparticles.

Due to its stabilizing properties polymers may decrease the rate of crystal growth. The decrease is thought to be due to polymer adsorption to crystals. The adsorption gives slower surface integration kinetics and also influences the particle shape. Polymers do however not affect the nucleation rate significantly. The reason for this is thought to be the small size of the critical clusters that form the nucleus. There is no polymer adsorption to particles of this size. [5]

Crystallization is often initiated at rough surfaces such as dust, remaining crystals or a scratched glass beaker; this is referred to as heterogeneous nucleation. [6] It is however of interest to determine the nucleation rate when the only driving force is the chemical potential. This type of nucleation is referred to as homogenous nucleation. [6] To reduce heterogeneous nucleation it is important to remove foreign particles from experimental systems. Heterogeneous nucleation may also take place at an interface, for example between air and liquid. This is a major drawback with most methods using solutions.

Crystallization consists of two different processes, nucleation and crystal growth, usually occurring simultaneously in a supersaturated solution. [5]

In classic nucleation theory, the main parameter of interest is the interfacial tension between the crystal and the surrounding solution, γ_{sl}. The interfacial tension can be interpreted as the free energy cost required creating a new surface between a solid and a liquid (per area unit).

When the supersaturation in a solution is high so is the crystallization rate. When lowering the supersaturation, it will eventually reach a concentration where nucleation ceases but crystal growth continues. The concentration range between this limit and the equilibrium solubility is called the metastable zone. [5]

Attempts to determine the nucleation rate have previously been done for proteins, pharmaceutical substances and different inorganic materials, using methods involving nucleation in the vapor-liquid phase or measurements of the induction time, the time required for formation of detectable crystals in liquids. [7][8][9]

Lately, attempts have been made to separate nucleation from crystal growth for proteins. [10][11][12][13] Galkin and Vekilov used temperature to control the degree of supersaturation during the nucleation process. In such experiments a supersaturated solution is generated. After a predetermined time, the nucleation time, the temperature is lowered to decrease the supersaturation into the metastable zone. This method has the advantage of allowing a large number of experiments to be performed simultaneously with identical conditions. The results can therefore be statistically evaluated, which is important since nucleation is a stochastic process. [14]

Other attempts to determine the nucleation rate have also been made for the substance Bicalutamide. [5] Lindfors et al. used dilution with a substance saturated solution to lower the concentration into the metastable zone.

In this paper the methods developed by Galkin, Vekilov and Lindfors et al. has been modified further in order to get more understanding of the nucleation process and to be able to determine the nucleation rate with higher accuracy. This would convey information about the interfacial tension and correspondence between experimental results and theory.

Crystal growth in supersaturated solutions has been studied previously by use of fluorescence. [4][5] The same is valid in this paper, but different supersaturations are to be investigated.

The way of stabilizing the initial nanoparticles have also been altered in order to see how the stabilization affects crystal growth in the experimental system. [5]

The experimental result gives information about the surface integration kinetics. Three different theories have been used to evaluate the experimental results.

The λ-model describes growth as incorporation of monomers. The rate of incorporation can be described by the surface integration factor, λ.

The other theoretical models describe crystal growth as a surface nucleation process. The Hillig-Nielsen theory uses a polynuclear model to describe the growth from a supersaturated solution. [15] The Obretenov interpolation model describes crystal growth by interpolating mono- and poly nuclear growth mechanisms in a continuous mode. [16]

Crystal dissolution in water has previously been investigated by Lindfors et. al. [4] Here, the same has been done for a range of undersaturations. The aim was to determine that previous results indicating that the dissolution process is diffusion controlled, i.e. $\lambda=0$, were correct and applying for all tested substances, regardless of the concentration in the solution.

2. Theory

Knowledge of the crystallization process is rather poor regarding the nucleation and crystal growth separately since the two processes normally occur simultaneously.

The theory below is based on classic nucleation theory and spherical symmetry.

2.1 Nucleation

In a supersaturated solution crystals will eventually form in order to minimize the free energy in the system. Clusters are formed when free monomers, M, by diffusion meet and form dimers, M_2. Dimers can then either grow by addition of further monomers giving trimers, M_3, or they can dissolve to free monomers again. The formation of clusters can be described by the following equation:

$$M_n + M \leftrightarrows M_{n+1} \quad (1)$$

The nucleation process has an energy barrier. Before the cluster reaches the critical size, R*, it is a subcritical cluster with larger probability to dissolve since its existence is thermodynamically unfavorable. When the size exceeds the critical radius, it becomes supercritical and then it is thermodynamically favorable for the cluster to continue to grow.

A critical cluster has equal probability to grow and dissolve.

Nucleation from a liquid phase can be described by considering the free energy change of forming a solid sphere of radius, R.

$$\Delta G = -n_c * k_B * T * ln\left(\frac{C}{S_0}\right) + 4\pi R^2 \gamma_{sl} \quad (2)$$

where ΔG is the free energy change, n_c is the number of aggregating molecules, k_B is the Boltzmann constant, T is the temperature in Kelvin, C is the molar concentration, S_0 is the intrinsic solubility, and γ_{sl} is the interfacial tension, between a solution and a crystal.

The number of aggregating molecules can be obtained from equation 3.

$$n_c = \frac{4\pi R^{*3}}{3\nu} \tag{3}$$

where R* is the critical radius and ν is the molecular volume of the solute. The molecular volume is obtained from the following relation; $\nu = V_m/N_A$, where V_m is the molar volume and N_A is Avogadro's number, $6.022*10^{23}$ mol^{-1}.

When the concentration is higher than the intrinsic solubility, $C>S_0$, there is a maximum in free energy at the critical radius, R*. At the maximum, the relation between the concentration and the critical radius is the following.

$$k_B * T * ln\left(\frac{C}{S_0}\right) = \frac{2\gamma_{sl}*(\nu/N_A)}{R^*} \tag{4}$$

Equation 4 is known as the Kelvin equation, N_A is Avogadro's constant, $6.022*10^{23}$. The critical radius, R*, depends on the supersaturation, which is a measure of the chemical potential, and the cost of creating a new surface.

By combining the equations above (2-4), a new expression for the free energy cost to form a critical nucleus can be written.

$$\Delta G^* = \frac{16\pi*\gamma_{sl}^3*\nu^2}{3\left(k_B*T*ln\left[C/S_0\right]\right)^2} \tag{5}$$

Classic nucleation theory describes the formation of a nucleus as addition of monomers, as written above in equation 1. The formation of a critical nucleus is thus described as follows.

$$M_n + M \xrightarrow{k_{n^*}^+} M_{n^*} \tag{6}$$

where n* is the number of monomers in a critical cluster.

The rate expression for the reaction described in equation 6 is:

$$\frac{d[M_{n^*}]}{dt} = k_{n^*}^{+}[M][M_n] \tag{7}$$

When clusters begin to form, a steady state is rapidly established. The steady state concentration of critical clusters is close to the equilibrium concentration. The steady state concentration is thus approximately

$$[M^*] \approx [M] * e^{\left(-\Delta G^*/k_{B*T}\right)} \tag{8}$$

where [M*] is the concentration of critical clusters, [M] is the total concentration of substance in the system which is approximately equal to the concentration of free monomer. The critical free energy is received from equation 5.

Combination of equation 7 and 8, gives an expression for the nucleation rate, J, the net production of a critical clusters per unit time and unit bulk volume.

$$J = \frac{d[M_{n^*+1}]}{dt} = k_{n^*}^{+}[M]^2 * e^{\left(-\Delta G^*/k_{B*T}\right)} \tag{9}$$

If the nucleation kinetics is diffusion controlled, the forward rate constant, k_n^+, for the formation of critical nuclei is given by the following equation. [17]

$$k_{n^*}^{+} = 4\pi(R_M + R_{n^*})(D_M + D_{n^*}) \tag{10}$$

where R_M and R_{n*} are the radius of a single monomer and a critical cluster. D_M and D_{n*} are the diffusion coefficients for the monomer and the critical cluster respectively.

For large critical clusters the following approximation can be done.

$$R_M + R_{n^*} \approx R_{n^*} = R^* \tag{11}$$

The diffusion of monomers is much larger than diffusion of clusters, $D_M >> D_{n*}$, from this relation and equation 11, equation 10 can be simplified.

$$k_{n^*}^{+} = 4\pi R^* D_M \tag{12}$$

When combining equation 4, 5, 9 and 12, the expression for the nucleation rate is the following:

$$J = \frac{8\pi\gamma_{sl}\nu}{k_B T ln\left[C/S_0\right]} [M]^2 D_M e^{\frac{-16\pi\gamma_{sl}^3\nu^2}{3(k_B T)\left(ln\left[C/S_0\right]\right)^2}} \tag{13}$$

As can be seen in this equation, the nucleation rate strongly depends on the interfacial tension of the solid/liquid interface.

2.3 Crystal Growth

2.3.1 Surface integration model

In a supersaturated solution the transport of monomers to a particle surface is diffusion controlled. This is true even with moderate stirring since there is a stagnant layer closest to the particle surface. Through this layer only diffusion is possible.

It is assumed in the theory below that the clusters are spherical and that the monomers are of negligible size compared to the clusters.

The concentration gradient in the steady-state diffusion field around a particle can be described as the concentration difference between the bulk, C_b, and the surface of a thin boundary layer outside the particle, divided by the radius of the particle, $(C_b\text{-}C')/R^*$

To determine concentration at the surface of the crystal the following equation can be used.

$$C' = AS_0 + (1 - A)C_b \tag{14}$$

Where S_0 is the intrinsic solubility and

$$A = \frac{1}{1+(\lambda/R)} \tag{15}$$

λ in equation 15 is a surface integration factor.

The chemical potential difference between the crystal surface and the solution is the driving force for crystal growth. The chemical potential difference can be received from the following equation:

$$\frac{\Delta\mu_{Surface}}{k_B T} = ln\left(\frac{C'}{S_0}\right) \tag{16}$$

Where $\Delta\mu_{Surface}$ is the difference in chemical potential between the bulk and the crystal surface.

Fick's first law can describe the flow of material into the crystal. The process is diffusion controlled and in one dimension, this law is given by:

$$J_D = -D_0 \frac{dC}{dx} \tag{17}$$

J_D is the flow of monomers, D_0 is the intrinsic diffusion coefficient for monomers and dC/dx is the concentration gradient.

In three dimensions and with the assumption that C' is equal to the solubility on the surface of the particle this law becomes

$$\frac{dM}{dt} = D_0 A \nabla C(R) = -D_0 4\pi R(S(R) - C_b) \tag{18}$$

where dM/dt is the molar flow of monomers to the particle surface, A is the surface area, ∇C(R) is the concentration gradient as a function of distance from the center of the particle, and S(R) is the concentration at the surface of the particle, that is equal to the solubility, S_0.

Crystal growth is not entirely controlled by diffusion. When a monomer reaches the crystal surface it has to find a suitable site for attachment and create or break bonds. This is known as surface integration and modeled as a thin boundary layer through which monomers must pass, resulting in a slower net flow of monomers to the surface.

The transport through the imagined layer can be said to be proportional to a surface integration factor, k_+, and the area of the layer. By defining the surface integration constant $\lambda=D_0/k_+$, equation 18 can be rewritten:

$$\frac{dM}{dt} = \psi 4\pi R D_0 (C_b - S_0) \tag{19}$$

Where, $\psi=r/(\lambda+R)$.

Equation 19 can be further reformulated into

$$\frac{dR}{dt} = \psi \frac{D_0 \nu}{R} (C_b - S_0) \tag{20}$$

If $R>>\lambda$, the growth process is controlled by diffusion and if, and if $\lambda>>R$ the growth will be limited by surface integration.

2.3.2 Surface nucleation

Another approach to the mechanisms behind crystal growth is the Hillig-Nielsen theory. According to this theory the growth of crystals occur by two-dimensional nucleation, so called surface nucleation. [6]

Surface nucleation occurs through nucleation and growth of layers on the crystal surface and can be compared to surface condensation events. [18] The growth occurs by formation of two-dimensional nuclei on the existing crystal surface and lateral spreading of the new crystal layer. According to the Hillig-Nielsen theory, multinuclear growth takes place. This means that several nuclei can be formed simultaneously, and that one layer does not have to be entirely covered before new nuclei are formed. [19]

To model crystal growth by multilayer 2D-nucleation, the flow of monomers to the surface has to be considered at first. The flow was derived in section 2.3 and is be described by equation 17.

Gibbs free energy for surface nucleation is described by:

$$\Delta G_{surfnuc} = 2\pi R a^2 \gamma_{sl} a^2 - n k_B T ln\left(\frac{C'}{S_0}\right) \quad (21)$$

The first term corresponds to the edge work of increasing the 2D nucleus circumference, the second term is the free energy gained by incorporating a monomer in to the 2D nuclei.

The free energy for creation of a critical two dimensional cluster can be derived from the equation above.

$$\Delta G^*_{surfnuc} = -n^* \Delta\mu + \frac{\gamma_{sl} a^2 (2R)(n^*)}{a} \quad (22)$$

The number of monomers in the critical 2D nuclei is thus

$$n^* = \frac{\pi \gamma_{sl}^2 a^2}{\left(k_B T ln\left(\frac{C'}{S_0}\right)\right)^2} \quad (23)$$

Equation 22 can by use of equation 23 and the relation $n=\pi R^2/a^2$ be reformulated into

$$\Delta G^* = \frac{\pi \gamma_{sl}^2 a^2}{k_B T ln\left(\frac{C'}{S_0}\right)} \quad (24)$$

Further, equation 24 can be reformulated into the following

$$\Delta G = \Delta G^* - \left(\sqrt{n} - \sqrt{n^*}\right)^2 k_B T ln\left(\frac{C'}{S_0}\right) \quad (25)$$

The total rate of crystal growth is also dependent of the rate of lateral spreading of the 2D nuclei.

Kink positions, positions where the surface energy is the same if a monomer is added or removed are the positions where monomers are incorporated into a crystal. According to the Hillig-Nielsen theory, the net flow of monomers to kink positions is:

$$J_{D(\infty)} = 2\nu_{in} v(C' - S_0) \tag{26}$$

Where ν_{in} is the frequency by which molecules are incorporated into the crystal. Assuming that kink positions are found at the edge of formed 2D nuclei, at an average distance χ_0 from one another, the probability that a 2D nuclei of radius R will gain a monomer is the following.

$$k_+(R) = 2\nu_{in}\left({}^{2\pi R}/_{\chi_0}\right)C'v \tag{27}$$

The average distance between the kink positions can be described by the equation below.

$$\chi_0 = a\left(\frac{C'}{S_0}\right)^{-1/2} exp\left({}^{\gamma_{sl}}/_{k_B T}\right) \tag{28}$$

By inserting equation 28 into equation 27, the following expression for the rate of monomer integration is derived.

$$k_+(\chi) = 4\nu_{in}\sqrt{\chi\pi}\left(\frac{C'}{S_0}\right)^{1/2} exp\left({}^{-\gamma_{sl}}/_{k_B T}\right) \tag{29}$$

By combining the lateral spreading rate and the rate of 2D nucleation, the total rate of crystal growth can be described according to equation, 30.

$$\frac{dR}{dt} = {}^{\pi^2}/_3\left(2\pi\sqrt{ln\left[{}^{C'^{1/2}}/_{S_0}\right]e\left(-\frac{\Delta G}{k_B T}\right)}\right)^{1/3} exp\left(-\frac{\gamma_{sl}a^2\sqrt{\frac{\pi}{6}}}{k_B T}\right)av^{4/3}[(C')^2 - C'S_0]^{2/3}\nu_{in}\left(\frac{C'}{S_0}\right)^{1/3} \tag{30}$$

There are two parameters in the equation that are to be determined for each substance; γ_{sl} is the apparent surface tension and ν_{in} is the integration frequency (Hz). [15]

The complete derivation can be found in Generalized *Hillig-Nielsen Theory, for crystalline nanoparticles*, by Rasmus Persson, see reference 19.

2.3.3 Obretenov interpolation

Obretenov describes crystal growth by 2D nucleation as a process that can occur either by mono- or multinuclear growth, depending on the supersaturation of the solution. The growth rate is described by a unified expression that combines known equations for mono- and multinuclear growth. [16]

The growth rate for mononuclear crystal growth is described by equation 31.

$$\left(\frac{dR}{dt}\right)_{mononuclear} = 2RJ_{2D}a \tag{31}$$

Where 2R is the monolayer height for spheres constructing a layer, J_{2D} is the rate of 2D nucleation and *a* is the crystal face area.

For the polynuclear growth mechanism the statistical theory of Kolmogorov-Avrami-Evans is incorporated in the theory. Due to the statistics used, the multinuclear growth expression is only valid for a sufficiently large number of nuclei per monolayer. The general form of the growth rate expression is:

$$\left(\frac{dR}{dt}\right)_{polynuclear} = 2R\beta(\pi J_{2D}w)^{1/3} \tag{32}$$

Where w is the spreading velocity of the monoatomic step and β is a constant numerical factor close to unity, 0.97, when polynuclear growth described by Hillig-Nielsen is used. [16]

In the middle region of the crystal growth curve, between mononuclear growth (beginning) and polynuclear growth (the end), each monolayer will be formed by several nuclei. The growth rate can thus be described by equation 33.

$$\left(\frac{dR}{dt}\right)_{Obretenov} = \frac{2RJ_{2D}a}{n} \tag{33}$$

Where n is the average number of nuclei taking part in the formation of one monolayer. n can be determined by the following equation.

$$n = 1 + \frac{a}{\beta \pi^{1/3}} \left(\frac{J_{2D}}{w}\right)^{2/3} \tag{34}$$

The steady state growth rate for combined mono- and multinuclear growth can thus be describes by the following equation. [16]

$$\left(\frac{dR}{dt}\right)_{Obretenov} = \frac{2RJ_{2D}a}{1+\frac{S_0}{\beta \pi^{\frac{1}{3}}}\left(\frac{J_{2D}}{w}\right)^{2/3}} \tag{35}$$

2.4 Secondary nucleation

Classic nucleation theory does not take into account the effects of existing crystals in the solution, so called secondary nucleation. [20] Large crystals are thought to stabilize small unstable clusters of monomers by van der Waals interactions when in close proximity and thus facilitate nucleation. [21]

Van der Waals forces between particles of the same material have stabilizing effects. Large crystals are thus thought to have stabilizing effects on subcritical nuclei, lowering the ΔG* and increasing the rate of forming supercritical nuclei. This secondary nucleation effect is given by

$$\Delta G^* = -n^* k_B T ln\left(\frac{C_b}{S_0}\right) + 4\pi r^{*2}\gamma_{sl} - A_{121}R^*/6l \tag{36}$$

where A_{121} is the Hamaker constant and l is the distance between the surface of the large crystal and the cluster. [21]

For a large crystal to stabilize a subcritical nucleus the distance between them has to be very small. Taking the short distance into account, the effect of surface integration on concentration profiles outside crystals becomes very important. Diffusion controlled growth of a particles means that the concentration very close to the surface of the large crystal is equal to the intrinsic solubility. This conveys that only monomers can exist in the solution

close to the surface and thus the effect of secondary nucleation would not be possible. If on the other hand, crystal growth is controlled by surface integration, the concentration profile is altered. The concentration very close to the crystal surface is then no longer equal to the intrinsic solubility, but higher. Subcritical nuclei will be able to come in close proximity of the large crystal and thus they can be stabilized for further growth. [21]

The stabilization of one subcritical nucleus results in more crystals formed that in turn can stabilize further subcritical nuclei resulting in a chain reaction. The effects of the stabilization on the critical radius, R*, depends on the distance to the large crystal. [21]

Other theories exist as well. Molecular build-up on the surface of the parent crystal that has not been well incorporated in the crystal lattice might be removed into the supersaturated solution where it will have the opportunity to grow. Diffusion effects or the shearing action of a stirred solution might apply force enough to remove the layer.

The parent crystal might also grow in a way, with dendrites, that the shearing action of the solution can tear off small clusters from the crystal surface and these can then develop in the supersaturated solution. [20]

2.5 Crystal dissolution

The process of crystal dissolution is in theoretical terms described the same way as the crystal growth. Since it is the reverse of crystal growth, the diversion from diffusion controlled dissolution rate is modeled by a surface disintegration step where the detachment rate constant, k_- is included. [4]

3. Experiments

3.1 Substances

Three model substances were used in the performed experimental studies. Bicalutamide, Linaprazan and Felodipine were provided from Astra Zeneca and used without any further purification.

3.1.1 Characteristics

Table 1. Substance characteristics that have been used in the report and in calculations. Reference, In-house data AstraZeneca R&D unless another reference is referred to.

	S_0 [uM]	$S_{amorphous}$ [uM]	M_w [g/mol]	D [m^2/s]	ν [cm^3/mol]
Bicalutamide	14.5	~ 800	430.4	5*10-10	281 [22]
Linaprazan	3.7	~ 1000	366.5	5*10-10	301
Felodipine	2.5	~ 30	384.3	5*10-10	265 [22]

Bicalutamide crystals are polymorph b, the crystal structure is called JAYCES02. [22] The molecular structures of the model substances are shown in appendix 1.

3.2 General procedures

All vials (borosilicate glass) used in the experiments were cleaned with 95% ethanol (three times), 70% ethanol (three times) and dried prior to use, in order to minimize the amount of contaminating particles. Ethanol from Kemetyl was used. Clean vials were stored upside down in a closed cabinet or closed with a lid, cleaned according to the same procedure.

Substance was weighed using an analytical scale from Mettler Toledo, XP205, delta range. The substances were dissolved in DMSO from Scharlau Chemie S.A., and filtered with a hydrophilic Dismic®-13 HP, PTFE, 0.20µm filters, from Advantec®. The DMSO concentration was kept constant, at 0.8% throughout all experiments.

MilliQ water, from the Elix 3 system from Millipore, was used in the experiments and filtered with hydrophilic Dismic®-13 HP, PTFE, 0.20µm filters from Advantec® prior to use.

Pipettes from the Eppendorf Reference Series were used for all pipetting.

All experiments were performed at room temperature, without stirring and in darkness at elevated experimental times.

3.3 pH adjustment

All experiments performed on Linaprazan contained 1µM NaOH, from Sigma Aldrich. This was done to keep the pH above the pKa of the molecule, to be certain that the molecule was uncharged. [1] The experimental pKa is 6.1. [23]

3.4 Preparation of substance solutions

This procedure applies for supersaturated solutions, growth solutions and undersaturated solutions.

The drug dissolved in DMSO was calmly added to water in a 10ml vial. Gentle mixing was performed by turning the closed vessel three times, giving a solution with a final DMSO concentration of 0.8(v/v) % and four milliliter supersaturated solution.

After creating the substance solution it was filtered to eliminate any solid material, such as initial crystals. As written above, 0.2µm hydrophilic PTFE filters were used for all substances.

3.5 Filtration

The choice of filters was investigated by use of fluorescence.

Experiments were carried out in the same way as crystal growth experiments; see section 3.3.5, to see if the filter used had any affect. Different amount of water was filtered with two different filters, PTFE and Millex- filters. Unfiltered water was used as reference.

3.6 Nanoparticles

3.6.1 Theoretical considerations

Crystalline nanoparticles, can effectively be prepared by use of precipitation-ultrasonication method [24] or by wet milling. [25]

Precipitation means that the drug is solved, often an organic solvent. The solution is rapidly added into a miscible non-solvent, usually an aqueous solution. [26] Use of ultrasound has proved to be an efficient way to control the nucleation and crystallization process. The mechanisms are thought to be cavitations and acoustic streaming. [24]

Milling is an attrition based way of making nanoparticles. The drug is dispersed in an aqueous solution with suitable stabilizators. The dispersion is mixed with beads of for example zirconium. The mixture is then milled and the procedure generates enough energy to convert the drug crystals into nanoparticles. [25]

To prevent aggregation and have stable crystalline particles, stabilization is needed. This can be received by steric hindrance and, or electrostatic stabilization.

Polymers are often used for steric stabilization, while surfactants often are used for electrostatic stabilization. If both types are used simultaneously, it is called electrosterical stabilization.

The stabilization, both type and specific species, that is suitable, depends on properties of the substance that should crystallize. Charge, pKa, and hydrophilicity, logP, are the most important properties to consider. [27] The stabilizer must of course have sufficient affinity for the particles surface and it must also have a rather high diffusion rate in order to cover the generated surface rapidly. [28]

A highly charged surface can often be properly stabilized by use of a polymer, while surfaces with low charge might need a mixture of a polymer and a surfactant. [27]

Polymers are known to decrease crystal growth rate when stabilizing crystalline particles. The decrease is thought to be due to polymer adsorption to the crystal giving slower surface integration kinetics and it is thought to influence the particle shape too. Thus, when experimentally investigating crystal growth it is important not to have polymers present stabilizing the particles. [5] It is however not yet known how surfactants impact the growth rate.

3.6.2 Preparation of nanoparticles

Several details in the process of making nanocrystals by use of the precipitation method and ultrasound were evaluated in the previous work, *Crystal nucleation of poorly soluble drugs, I. Method development and initial experimental results*. [1]

For Bicalutamide and Felodipine the ultrasonic treatment was performed in Biotage microwave vials 2-5ml with an S2 from Covaris for the ultrasonic treatment.

Bicalutamide nanoparticles were prepared by addition of drug dissolved in DMSO to the stabilizer solution, giving a final concentration of 1mM of Bicalutamide, 0,8% (v/v) of DMSO and 0.1% (w/w) AOT, Dioctyl sulfosuccinate, Mw= 444.6g/mol. The drug was rapidly added into the stabilizer solution when the ultrasonic treatment was just started.

Felodipine nanoparticles were prepared by addition of drug dissolved in DMSO, to a final concentration of 0.5mM of Felodipine, 0.8% (v/v) DMSO and 0.1 % (w/w) AOT. The drug was rapidly added to the stabilizer solution on an ultrasonic bath, Transsonic T460 from Elma®, with fresh and degassed water. The solution was then rapidly transferred to the Covaris S2 for ultrasonic treatment.

The protocols are attached, see appendix 2 and 4.

Linaprazan nanosuspension was prepared by wet milling. The substance was suspended in a stabilizer solution giving 1.33 (w/w) % PVP (K30) and 0.067% (w/w) AOT and 10 (w/w) % substance. The suspension was milled according to the procedure in appendix 3.

The substance concentration in the milled nanosuspension was determined to 101mM by use of LC.

3.6.3 Size measurements

Size measurements were performed in the Mastersizer 2000, from Malvern, where the entire particle size distribution is received. The refractive index was set to 1.59.

For Bicalutamide and Felodipine 18ml, 125µM solution was injected and for Linaprazan 20µL of high concentration, 101mM, was added to water in the sample cell.

If the nanoparticles were not freshly prepared, gentle mixing and ultrasonic treatment (30 seconds) was applied prior to the size measurement. This was done to disperse any aggregates and receive a homogeneous sample.

3.7 Fluorescence

3.7.1 Theoretical considerations

When a molecule absorbs light or electromagnetic radiation it can be excited to a higher energy level. As the molecule returns to its ground state light is emitted. The emitted light normally has less energy than the excited light and thus it has a longer wavelength, according to the equation below.

$$E = hf = \frac{hc}{\lambda} \tag{37}$$

where h is Planck´s constant, f is the frequency, c is the speed of light and λ, is the wavelength.

At low concentration the intensity of the fluorescence light is generally proportional to the concentration. This relation can be used when performing quantitative measurements on fluorescent substances.

$$I \propto [S] \tag{38}$$

I is the fluorescence intensity, and [S] is the concentration of substance in the sample.

Due to quenching molecules in solution have lower fluorescence than molecules incorporated in crystals. In favorable cases the intensity from the supersaturated solution can be neglected and the intensity from the sample is thus proportional to the fluorescence of the crystals.

$$I \propto [S]_{crystal} \tag{39}$$

3.7.2 Fluorescence measurements

The experiments that have been carried out and are described in this report have its foundation in experiments and method development that was presented in *Nucleation of poorly soluble drugs, I. Method development and initial experimental results*. [1]

All fluorescence measurements were performed in quarts cuvette from Hellma, prior to use washed thoroughly with 99.5% ethanol (shaking with fresh ethanol ten times), dried with nitrogen gas and left upside down when stored.

The measurements were performed on two milliliter samples using the LS 55 Luminescence Spectrometer from Perkin Elmer™ Instruments.

Information about excitation and emission wavelengths for the substances was already known for Bicalutamide and Felodipine. [1] For Linaprazan absorbance measurements and emission and excitation scans were performed to find wavelengths where the concentration dependence is linear for crystals and the influence of substance in solution is small enough to be neglected.

Table 2. Settings for growth fluorescence measurements of the studied substances.

	Excitation λ [nm]	Excitation slit width, Growth experiments [nm]	Excitation slit width, Dissolution experiments [nm]	Emission λ[nm]	Emission slit width, Growth experiments [nm]	Emission slit width, Dissolution experiments [nm]
Bicalutamide	234	5		323	2.5	
Linaprazan	300	5		378	2.5	
Felodipine	370	2.5		430	2.5	

3.8 Liquid Chromatography

Liquid chromatography, at a Waters system 2695 Separations module with a Waters 2998 Photodiode Array Detector, was used to perform quantitative measurements of the concentration of substance in samples in 1.5ml LC-vials from Waters.

For Bicalutamide an XTerra RP_8 column with a particle size of 3.5µM and column dimensions 3.9*100mm was used. The mobile phase used was 56% H_2O, 44% AcN, Acetonitrile, from Fisher Scientific and 10mM formic acid, from Merck, with a flow rate of 0.8ml/min.

For Linaprazan an XTerra RP_8 column with a particle size of 3.5µM and column dimensions 3.9*100mm was used. The mobile phase had the following components; A: 80% 0.1M sodium phosphate buffer at pH 6, from Sigma Aldrich and 20% AcN, and B contained 100% AcN. The flow rate was 0.8ml/minute and the gradient in table 3 was used.

Table 3. Gradient used for liquid chromatography of Linaprazan. The flow rate was 0.8ml/min. Mobile phase A contains 80% 0.1M sodium phosphate buffer pH 6, and 20% AcN. Mobile phase B contains 100% AcN.

Time [minute] / component	A [%]	B [%]
0	90	10
4	60	40
5	40	60
6	90	10

For Felodipine an XBridge C18 column with a particle size of 3.5µM and column dimensions 3.0*100mm was used. The mobile phase used was 55% AcN, 45% H2O and 0.025% trifluoric acid, TFA, from Merck, with a flow rate of 1.0 ml/min**.**

3.9 Crystal growth experiments

3.9.1 Starting point

Crystal growth experiments have been performed previously by Lindfors et al [4] and in the previous thesis work. [1] The experiments were performed by addition of a supersaturated solution to pre-formed nanocrystals.

The same method has been used here, but with PTFE-filters and also for Linaprazan.

3.9.2 Growth experiments

Growth experiments were performed by addition of nanocrystals, to the bottom of the rinsed quarts cuvette from Hellma, giving 10% (mol/mol) crystalline material in the final solution for Bicalutamide and Felodipine and 7.1% (mol/mol) for Linaprazan.

Solution of a certain supersaturation was added rapidly and the fluorescence measurement was then performed.

The settings used for each substance are shown in table 2. The protocols for the growth experiments are attached see appendix 5, 6 and 7.

3.9.3 Metastable zone for growth

As for crystal nucleation there is a metastable zone for crystal growth. To determine the metastable zone, growth experiments with solutions of low concentration was conducted for the chosen time range (3 hours). Where no increase in intensity was seen during this time, the limit of the metastable zone was determined.

3.10 Crystal Dissolution experiments

3.10.1 Starting point

Dissolution experiments have been performed previously on Felodipine by Lindfors et al. [4] The experiments were performed by addition of an under-saturated solution to pre-formed nanocrystals in a quarts cuvette, measuring the fluorescence.

3.10.2 Crystal Dissolution

The crystal dissolution experiments were performed by addition of nanocrystals to the bottom of the rinsed quarts cuvette from Hellma. Solutions with substance concentration below saturation were added rapidly to the running fluorescence measurements.

The total substance concentration varied between 3 and 90% of the solubility, with constant crystal concentration in all experiments.

The settings used for each substance are shown in table 2. The protocols for the dissolution experiments are attached see appendix 8, 9 and 10.

3.11 Crystal nucleation experiments

3.11.1 Starting point

As written above, the Vekilov and Galkin method, modified by Lindfors et al and further in the previous thesis work, has been the starting point for these experiments. The aim was to develop the method and to investigate more substances and supersaturations.

The method developed in the previous thesis work, was in a simplified way, the following for Bicalutamide. A supersaturated solution was created as described above. The supersaturated solution was filtered into a PVP coated polystyrene reagent reservoir. The solution was left ambient at room temperature during the nucleation time, after which the solution was transferred to a 96 microwell plate pre-filled with a substance saturated solution to lower the concentration into the metastable zone. In the metastable zone crystals were allowed to grow to detectable size (72 hours).

3.11.2 Growth solutions

The growth solution is substance saturated in order not to cause dissolution of nuclei. Polymer is included to slows down the growth rate and contribute to growth of spherically shaped crystals. The spherical shape is preferable since it makes it easier to count the crystals and also decreases the risk of secondary nucleation due to dendrites falling off. [5]

The solutions contain polymer as written in table 4.

Table 4. Specification of polymers used in the Growth solutions for each substance.

	Polymer	Polymer in the growth solution [%]	Specification	Brand
Bicalutamide	PVP, polyvinylpyrrolidine	0.021	360 kDa	Sigma Aldrich
Linaprazan	HPMC, hydroxypropyl methylcellulose	0.1	6cPs	Sigma Aldrich
Felodipine	-	-	-	-

3.11.3 Antivibration table

All nucleation experiments and metastable zone experiments have been performed on an antivibration table, from Technical Manufacturing Corporation, to decrease disturbance. [2]

3.11.4 Metastable zone experiments

Supersaturated solutions of different concentrations were prepared as described above. After filtration, the solutions were left for a certain time, 72 hours, in four milliliter vials. The solutions were stored in dark on the anti-vibration table.

After the nucleation time, the solutions were filtered to remove crystals and the concentration of the solution was determined by use of LC.

For Felodipine the metastable zone experiments were performed with nucleation time from three days to 21 days. Three different types of vials were tested. Borosilicate glass, borosilicate glass coated with substance from nanosuspension and silanized glass.

3.11.5 Coating of vials

Felodipine nanosuspension was prepared as written above. The suspension was diluted to 25μM with water. The solution was added to clean 4 ml vials, 3.5 ml per vial, and they were put on a shaking table for five days and turned upside down daily.

After the coating process the vials were washed thoroughly with water and dried prior to use.

3.11.6 Coating of plates

All polystyrene material was coated with polymer. This was done in order to minimize interactions with the material, and thus reduce possibilities of heterogeneous nucleation and absorption of substance to the polystyrene. [1] PVP was used for experiments performed on Bicalutamide and HPMC was used for experiments with Linaprazan.

The 96 microwell plates, from Nunc^{TM} Brand Products, were coated according to the following procedures. For plates used for Bicalutamide 1% (w/w) PVP, 360kDa, was used

and for plates where Linaprazan was used 1% HPMC (6 cPs) was used. The protocols for these procedures are attached, see appendix 11 and 12.

3.11.7 Crystal nucleation experiments

Supersaturated solutions were prepared as described above and filtered into 4 ml vials where the solution was left for the decided nucleation time. The nucleation was terminated by moving a certain amount of the supersaturated solution to wells on a 96-well plate, by use of a manual pipette. The plate was pre-filled with growth solution used to dilute the sample into the metastable zone.

The supersaturated solution was handled carefully and added in a controlled manner, followed by careful mixing by use of the pipette.

The samples were after dilution left in dark on the anti-vibration table for the growth time when the crystals grew to detectable size. The protocol for the experiment is attached, see appendix 11 and 12.

Results have to this point been received for one concentration for Bicalutamide and initial experiments have been conducted on Linaprazan.

3.11.8 Evaluation of nucleation experiments

The nucleation rate, J, can experimentally be calculated by the following equation

$$J = N_{tot}/(V\Delta t) \tag{40}$$

where V is the volume of the initial supersaturated solution prior to dilution, and Δt is the nucleation time. For short nucleation times the nucleation rate can be determined for a certain supersaturation, assuming that the nuclei that are formed do not change the bulk concentration significantly. Assuming that the nucleation of each crystal is independent of other crystals, the stochastic nucleation process can be described by a Poisson distribution. [5]

$$P(N) = \frac{\langle N \rangle^N}{N!} e^{-\langle N \rangle} \quad (41)$$

where N is the number of crystals, $\langle N \rangle$ is the average number of crystals.

A Poisson distribution was fitted the experimental data to receive the average number of crystals at each nucleation time. 16 wells per experiments have been used for each data point.

The number of crystals in each well was calculated manually by use of a DIC microscope, Axiovert 135 TV from Zeiss.

4. Results and discussion

4.1 General results

4.1.1 Effect of filters used to filter supersaturated solutions

Two different filters were tested, Millex-GV and PTFE filters. Growth experiments were carried out where the supersaturated solutions were prepared with water filtered in different ways; without filtration, filtered with PTFE filter and with a small or a large amount of water filtered through a Millex filter. The results can be seen in figure 1.

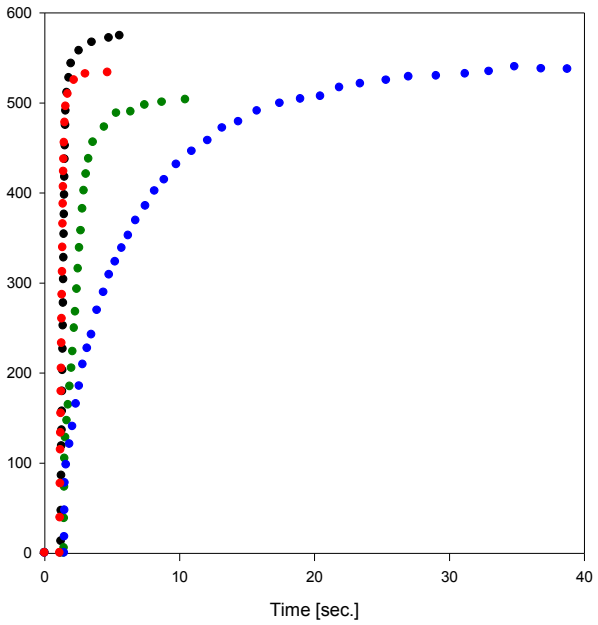

Figure 1. The effect of filtration on the crystal growth rate of Bicalutamide can be seen. The intensity is plotted against time for; ● not filtered water, ● water filtered with a PTFE filter, ● a small volume of water filtered with a Millex-GV filter, ● a large volume of water filtered with a Millex-GV filter.

The growth rate was significantly affected by filtration with Millex-filter. This result was unexpected and results presented in the first report can be questioned, where Millex-GV filters had been used.

4.1.2 Loss of material from filtration

Solutions with different degree of supersaturation were filtered with PTFE filters to determine the substance loss. The results can be seen in figure 2 a)-c).

For Bicalutamide the yield was 100±2.5% regardless of the initial concentration in the concentration range up to 500μM.

For Linaprazan the yield was constant, at 93±1.7% up to 35μM.

For Felodipine the yield was constant, at 82±4.5%, up to approximately 25uM, at higher concentration there was substantial substance loss. The loss above 25µM is probably due to creation of amorphous material. The amorphous solubility for Felodipine is around 30µM. Being above 25µM is very close to the amorphous solubility and it is thus almost certain that amorphous material is decreasing the yield.

The reproducible loss of substance when filtering supersaturated solutions of different concentrations was unexpected. It had been more reasonable if the loss increased with concentration, which could have been explained by more initial crystals being formed at higher supersaturations. The amount that is lost from the initial crystals are however very low and does thus not contribute significantly to the concentration loss.

It would also have been reasonable if the loss had decreased with increasing concentration, this could be explained by saturation of the filter, from adsorption of substance.

The most reasonable assumption is though that the even loss is due to being in the linear range of Langmuir absorption isotherm.

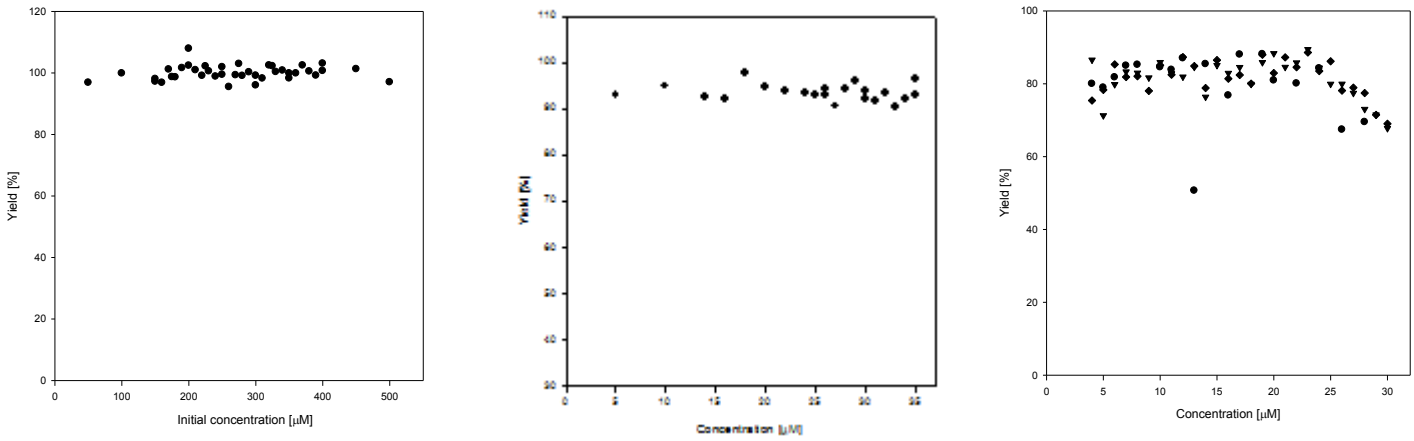

a) b) c)

Figure 2. Yield [%] after filtration against the initial concentration [µM] for a) Bicalutamide, giving 100% yield b) Linaprazan, giving 93% yield and c) Felodipine, giving 82% yield. Different symbols indicate different experiments.

4.2 Crystal growth and dissolution experiments

4.2.1 Preparation of nanocrystals

To obtain good experimental data that can be compared with theory, the experimental systems were designed to be as unaffected by additives as possible. One way of achieving this was to try to produce nanoparticles that had reasonable stability, without polymeric stabilizer present. This was achieved for Bicalutamide and Felodipine, but to prepare nanoparticles of Linaprazan without polymer became quite a challenge.

For unknown reasons it was not possible to measure growth on Linaprazan particles stabilized only with surfactant, even though they seemed to be of reasonable size and stability. Milling was thus used to get Linaprazan nanoparticles, stabilized with both surfactant and polymer. The concentration of stabilizer is however reasonably low.

Nanocrystals were evaluated with focus on size and stability. The particle size and size distribution were measured several times after the production to make sure that the particles were of reasonable size and stability.

Particles with intensity mean size up to 300 nm was accepted in these experiments.

The Bicalutamide particles had good stability for at least 14 days. The volume weighted mean diameter was 137nm, and the entire distribution can be seen in appendix 13.

The measurement data has been edited, due to a small signal at larger size. The results before the edit can be seen in appendix 14.

Milled Linaprazan particles had very good stability. The volume weighted mean diameter was 156nm, and the entire distribution can be seen in appendix 15.

The measurement data has been edited, due to a small signal at larger size. The results before the edit can be seen in appendix 16. The editing was justified since nothing was expected to be seen at the size, air bubbles might be a reasonable explanation.

Felodipine particles were stable up to between 24 and 48 hours. The volume weighted mean diameter was 181nm, and the size distribution can be seen in appendix 17.

The measurement data has been edited, due to a small signal at larger size. The results from before the edit can be seen in appendix 18.

The editing was justified since nothing was expected to be seen at the size. A reasonable explanation might be air bubbles or contamination. The latter is strengthened since the unexpected larger size particles are seen for all substances.

4.2.2 Fluorescence scan

The excitation wavelength for Linaprazan was chosen by looking at the absorbance curve showing a maximum at 300nm, thus it is certain that it is the correct substance that is being looked at in the experiments. Then an emission scan was performed, see appendix 19, from this data the graph below was constructed.

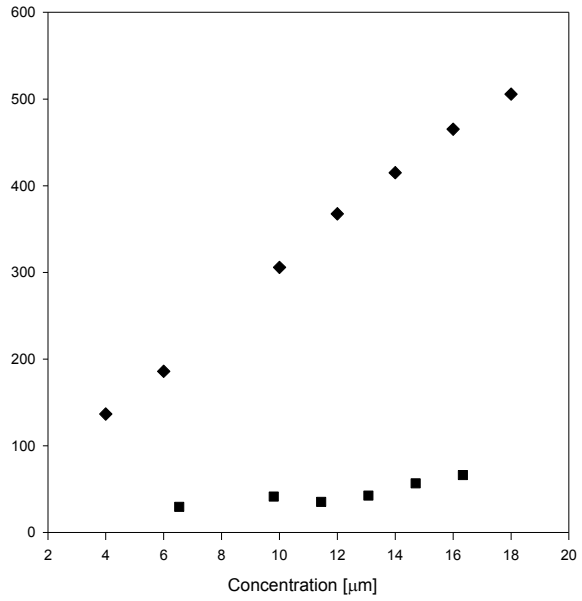

Figure 3. Result from fluorescence measurements on Linaprazan. The intensity is plotted against the sample concentration for supersaturated solutions ■ and crystals ♦. Excitation at 300 nm and measuring the emission at 378 nm.

The fluorescence measurements on Linaprazan gave linearity for the crystals and low influence from solution when excitation took place at 300 nm (5nm slit width) and the emission was measured at 378 nm (2.5 nm slit width).

Similar, linear results have previously been obtained for Bicalutamide and Felodipine. [1]

4.2.3 Crystal dissolution

The crystal dissolution experiments were performed as described in section 3.10.2. The results were normalized and display fraction of crystalline material as a function of time.

All results are shown in appendix 20, 21 and 22. The results and calculations for the highest and lowest concentrations are presented for all substances below.

Calculations were performed in a computer program based on equation 20 in which the polydispersity of the initial particles are taken into account.

In the equation the only unknown parameter is the integration factor, λ. When λ=0, the dissolution process is diffusion controlled.

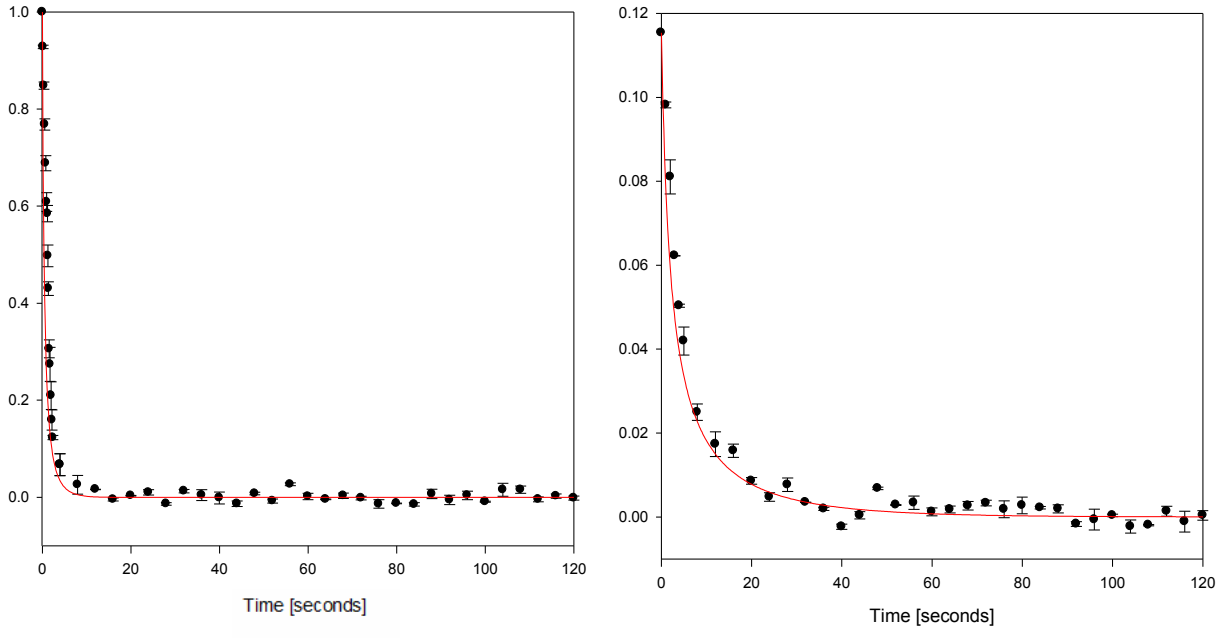

a) b)

Figure 4. Result from dissolution experiments on Bicalutamide. The fraction crystalline material is plotted vs. time for a) 1.5μM initial crystals in water, the theoretical curve (red) corresponds to λ=0nm, b) 1.5μM initial crystals and 11.5μM in the initial solution. The theoretical curve (red) corresponds to λ=0nm. Note the difference in the y-axis.

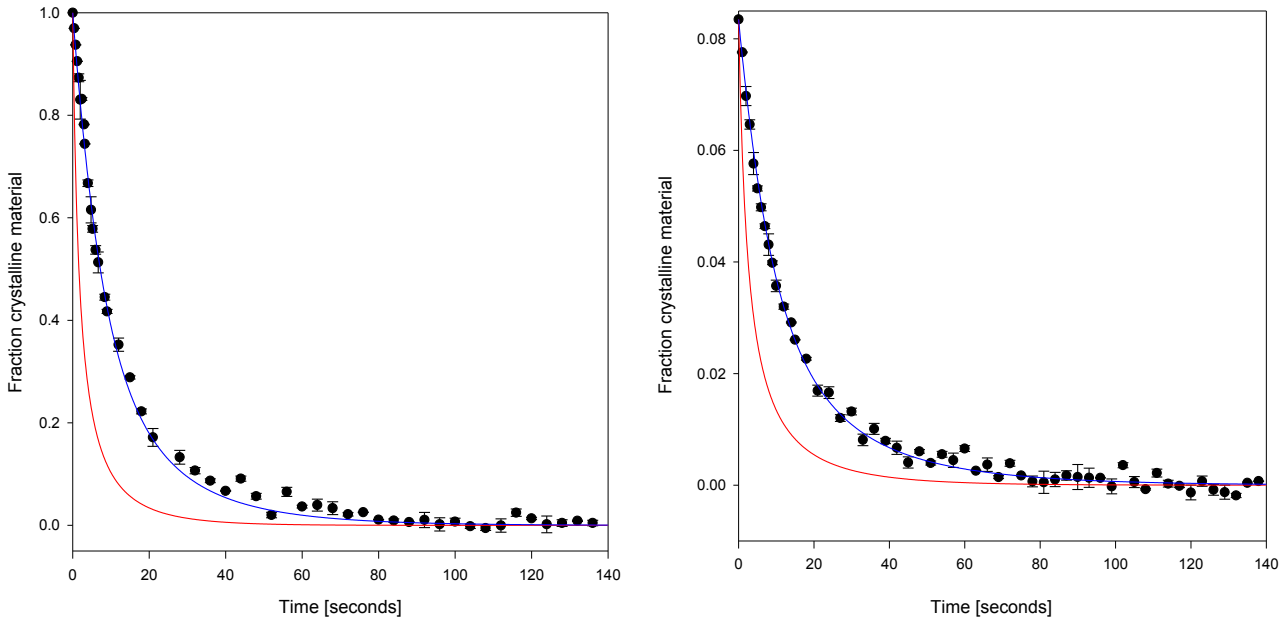

a) b)

Figure 5. Result from dissolution experiments on Linaprazan. The fraction crystalline material is plotted vs. time for a) 0.1μM initial crystals in water, the theoretical curve (red) corresponds to λ=0nm and (blue) λ=0.2μm, b) 0.1μM initial crystals and 1.15μM in the initial solution. The theoretical curve (red) corresponds to λ =0nm and (blue) λ=0.2μm. Note the difference in the y-axis.

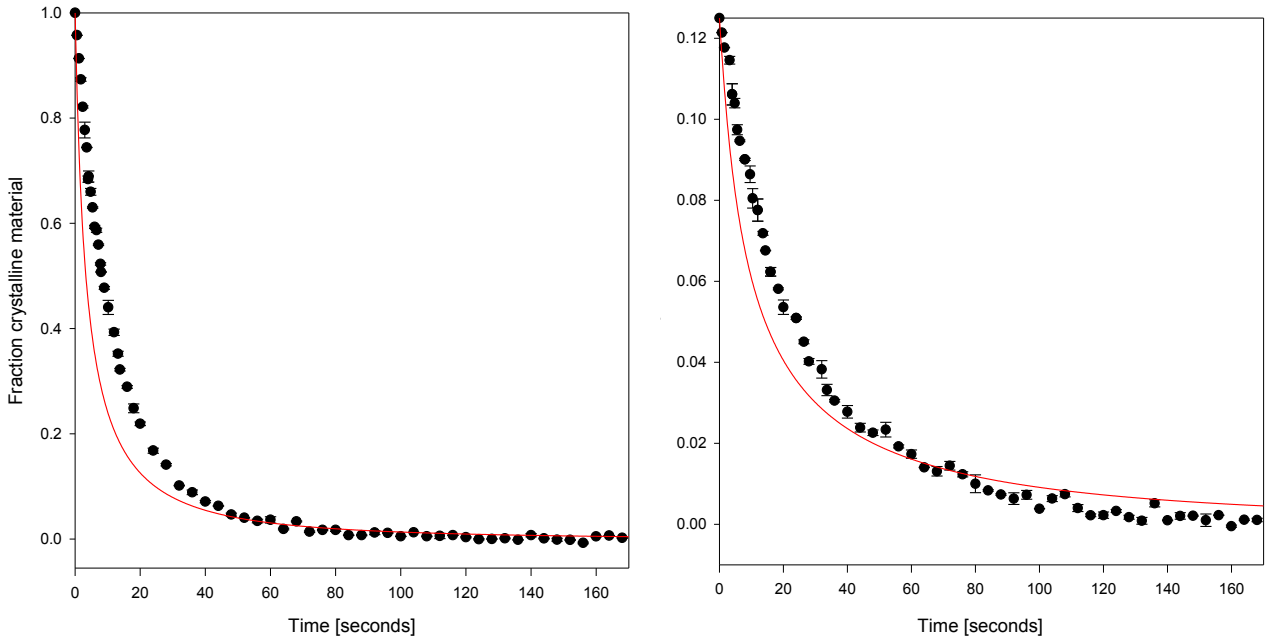

a) b)

Figure 6. Result from dissolution experiments on Felodipine. The fraction crystalline material is plotted vs. time for a) 0.2μM initial crystals in water, the theoretical curve (red) corresponds to λ =0nm, b) 0.2μM initial crystals and 1.6μM in the initial solution. The theoretical curve (red) corresponds to λ =0nm. Note the difference in the y-axis.

The results agree well with theory. Deviation between experimental results and theoretical results are mainly seen for Linaprazan. This is likely due to stabilization with polymer, and perhaps also a small error in the solubility. The solubility of Linaprazan was investigated; the previously determined solubility gave experimental dissolution that was faster than diffusion controlled dissolution. Since this is impossible, the solubility was questioned and thus measured in-house to get reliable data. The solubility of Linaprazan was determined to 3.7μM, compared to 1.5μM from previous data.

The same was also seen for Felodipine, but the solubility that made the experiments concur with the theory was within the margin of error of the known solubility and the edited value has thus been used throughout the entire report. The previous value was 2.1±0.5μM, when evaluating the dissolution data from Felodipine it became clear that the rate of dissolution corresponded to a higher solubility. The solubility that gave the best agreement was 2.5μM, and since this is within the margin of error this value was accepted as the correct.

4.2.4 Growth experiments

Growth experiments were performed as described in section 3.3.5. The results were normalized and display fraction of crystalline material as a function of time.

Normalized average curves with the standard error of the mean are to be seen for Bicalutamide in figure 7. The metastable zone, the concentration range where no increase in fluorescence was detected for 3 hours, was investigated. It was concluded that 17μM was the limit for Bicalutamide. This value was thus used in the normalization of the experimental results.

It can clearly be seen in the figure that the rate of growth decreases with lower supersaturations.

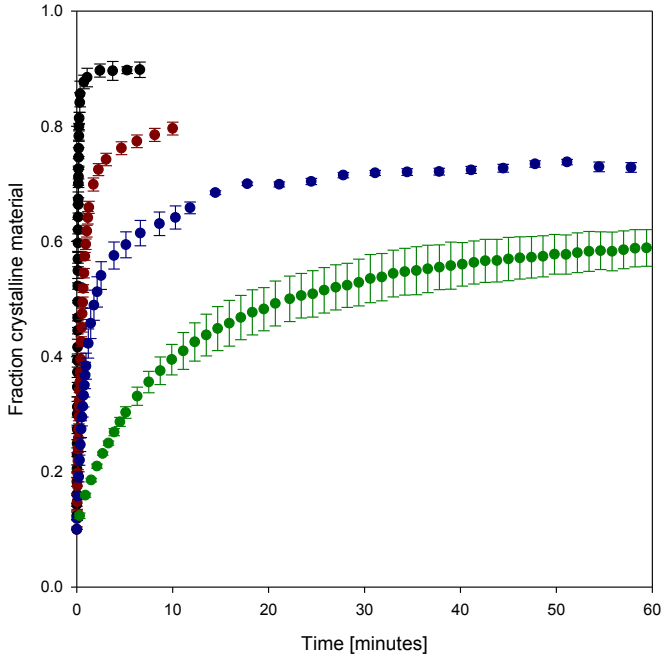

Figure 7. Normalized results for growth experiments performed on Bicalutamide. The figure display fraction crystalline material as a function of time.
Initial fraction of crystalline material is 0.1. The supersaturations are ● 150µM, ● 75µM, ● 60µM and ● 45µM.

The averaged curves with the standard error of the mean, for each supersaturation can be seen for Linaprazan in figure 8. The metastable zone, for 3 hours was determined to 5µM, the value was thus used in the normalization of the experimental results.

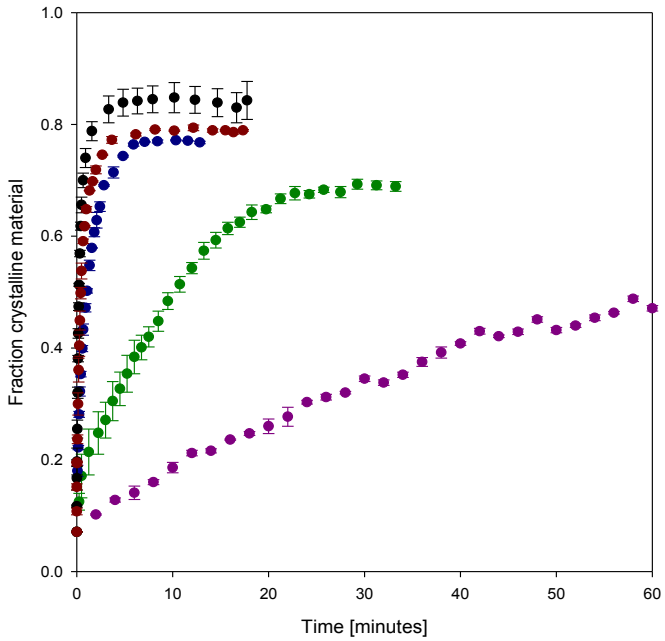

Figure 8. Normalized results for growth experiments performed on milled Linaprazan particles. The figure display fraction crystalline material as a function of time.
Initial fraction of crystalline material is 0.071. The supersaturations are ● 30µM, ●25µM, ● 20µM, ● 15µM and ● 10µM.

For Felodipine the metastable zone for growth was determined to 4µM. The averaged curves with the standard error of the mean for each supersaturation can be seen in figure 9.

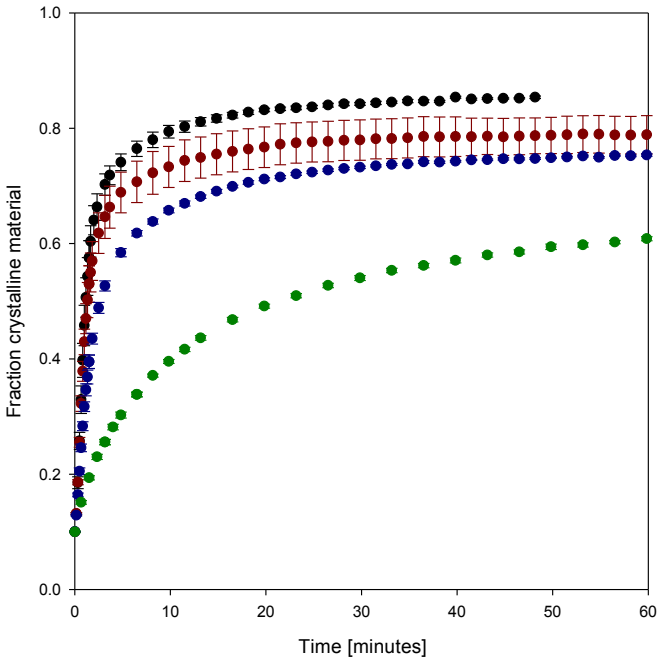

Figure 9. Normalized results for growth experiments performed on Felodipine. The figure display fraction crystalline material as a function of time.
Initial fraction of crystalline material is 0.1. The supersaturations are ● 25µM, ● 20µM, ● 15µM and ● 10µM.

The experiments gave very reproducible results between replicates for all substances; this indicates that the method is robust and reliable.

Calculation was performed in a computer program based on equation 20. In this equation the only unknown parameter is the surface integration factor. The fitting procedure was performed, trying to match the experimental data and the calculations in the beginning of the growth. This is due to that the growth rate is slower when the supersaturation decreases, and this is not included in the equation used in the theoretical comparison. In the beginning of the experiment the supersaturation can be seen as constant. The polydispersity of the samples are taken into account in the simulation.

Lindfors et al. have in previous experiments seen a good correlation between experimental results and the surface integration model. Those experiments did not cover a significant concentration range. [4] The aim in this report was to see how the experimental data correlates with theory in a large concentration range.

For Bicalutamide the results for each supersaturation can be seen in appendix 23. The average of the measurements at each supersaturation is displayed with the standard error of the mean.

In each graph the best simulated curve is showed as well. The experimental result and the best simulated curves for the highest and lowest supersaturation can be seen in figure 9.

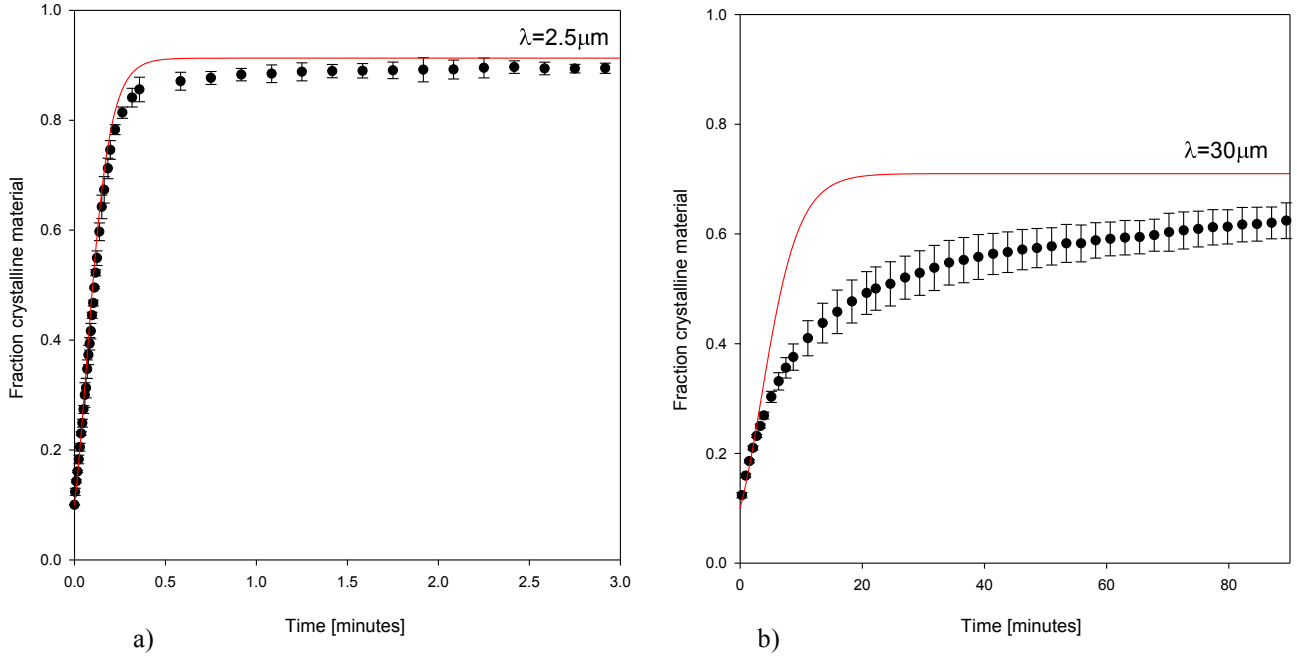

Figure 9. The fraction of crystalline material is plotted against time for a) 150μM Bicalutamide in the solution initially, and 10% crystals b) 45μM Bicalutamide in the solution initially, and 10% crystals. The simulated curves from the λ-model are also included. λ was set to 2.5μm for 150mM and 30μm for 45μM.

The λ values that were obtained from each fit are displayed in table 5, where they are related to the supersaturations.

Table 5. Results for the surface integration factor received from fitting of simulations based on classic nucleation theory to experimental growth results for Bicalutamide.

Conc. supersaturated solution [μM]	Supersaturation	λ [μm]
150	10	2.5
120	8	2.5
90	6	2.5
75	5	2.8
60	4	6
45	3	30

The λ values increases with decreasing supersaturation. This is expected and at concentrations near the solubility the λ value approaches infinity. It is expected, but does also show that the model does not describe crystal growth in a good way. If the agreement had been good, the theoretical model should be able to describe the growth at all initial concentrations and the entire growth curves. This is not valid here.

Since the surface integration model seem to work reasonable for high supersaturations, i.e. the λ-value is constant, the lowest λ value that is obtained from the simulations are thus used in the simulations for the crystal nucleation experiments, where higher supersaturations are used, see below.

For Linaprazan the results for each supersaturation can be seen in appendix 24. The average of the measurements at each supersaturation is displayed with the standard error of the mean and the best simulated curves. The highest and lowest investigated supersaturations can also be seen in figure 10 below.

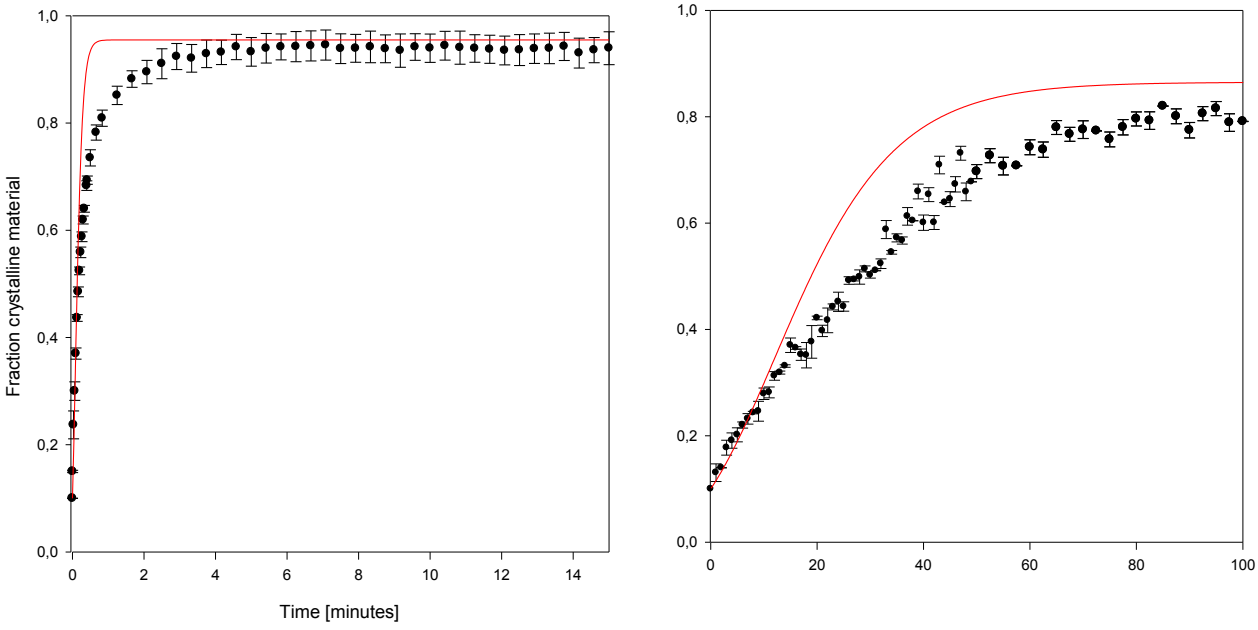

a) b)

Figure 10. The fraction of crystalline material is plotted against time for a) 30μM Linaprazan in the solution initially, and 7.1% crystals b) 10μM Linaprazan in the solution initially, and 7.1% crystals. The simulated curves from the λ-model are also included. λ was set to 0.5μm for 30mM and 20μm for 10μM.

The λ values that were obtained from each fit are displayed in table 6. The values are quite stable at high supersaturations, $C/S_0 \geq 5.4$. At lower supersaturations the values begin to increase.

Table 6. Results for the surface integration factor received from fitting of simulations based on classic nucleation theory to experimental growth results for Linaprazan.

Conc. supersaturated solution [μM]	Supersaturation	λ [μm]
30	8.1	0.5
25	6.8	0.5
20	5.4	0.6
15	4.1	1.6
10	2.7	20

For Felodipine the results for each supersaturation can be seen more clearly in appendix 25, and for the highest and lowest supersaturations the experimental results and best simulated curves can be seen in figure 11 below as well.

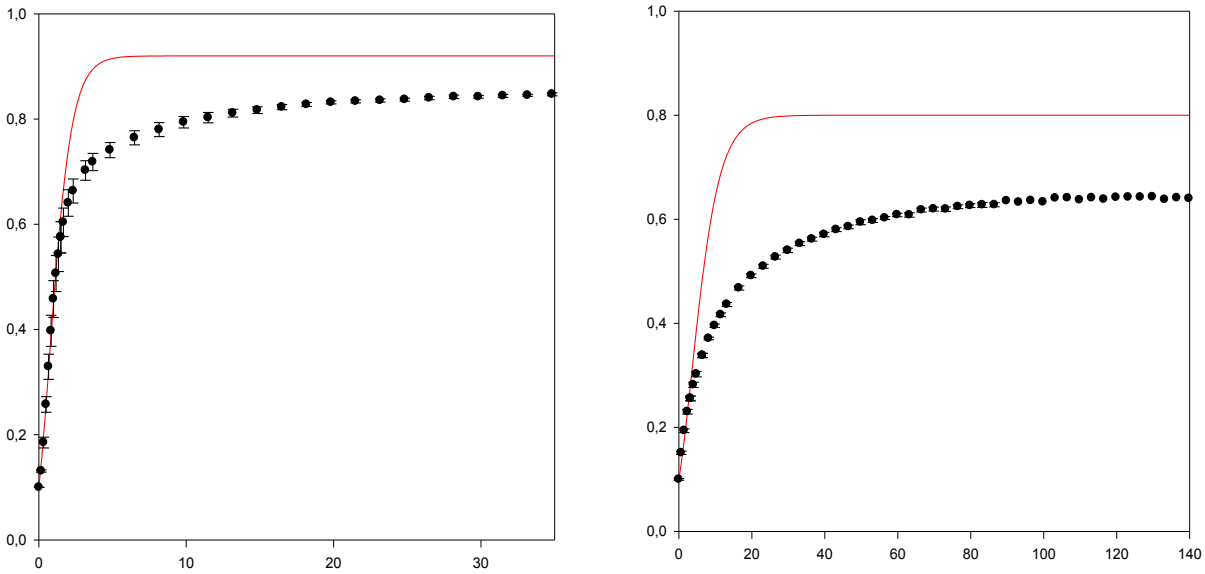

a) b)

Figure 11. The fraction of crystalline material is plotted against time for a) 25μM Felodipine in the solution initially, and 10% crystals b) 10μM Felodipine in the solution initially, and 10% crystals. The simulated curves from the λ-model are also included. λ was set to 3.5μm for 30mM and 7μm for 10μM.

The λ values that were obtained from each fit are displayed in table 7. The results deviate some and do not show a significant increase in l at the lowest supersaturation. This might however be due not investigating at as low supersaturations as for the other two substances.

Table 7. Results for the surface integration factor received from fitting of simulations based on classic nucleation theory to experimental growth results for Felodipine.

Conc. supersaturated solution [μM]	Supersaturation	λ [μm]
25	10	3.5
20	8	2.8
15	6	3.0
10	4	7

The trend, that the λ values are low at the highest supersaturation and increases with lower supersaturation, can be seen for all three substances. This indicates that there is a barrier for crystal growth, the same way as for crystal nucleation. This does in turn indicate that growth as well might be a nucleation based process. Here the nucleation would be two dimensional surface nucleation. For nucleation the barrier decreases with increasing supersaturation, and this would for crystal growth be related to the faster rate at higher supersaturations.

The λ-model can describe dissolution properly, but not growth. This might be due to that when a crystal dissolves; the shape goes from a characteristic, for example cubic to more and more spherical. This indicates that the dissolution will be a faster process that is diffusion controlled. The growth on the other hand, has a more complex mechanism. [29]

Due to the poor agreement with the λ-model, comparison between experimental results and polynuclear surface nucleation theory as described by Hillig and Nielsen has also been done. This comparison gives a frequency ν_{in} and an interfacial tension, γ_{3D}, see equation 30. The frequency is thought to reflect the incorporation of monomer and the γ_{sl} is the apparent three dimensional interfacial tension for crystal growth.

The calculation is based on equation 30 and the polydispersity is taken into account. For Bicalutamide the simulated curves fit fairly well to the experimental results, se figure 12. Though, it can clearly be seen that the theoretical curves are too fast at low supersaturations.

The theoretical values that presented the best agreement were a frequency of 7e6Hz and γ_{sl} 6.5mN/m.

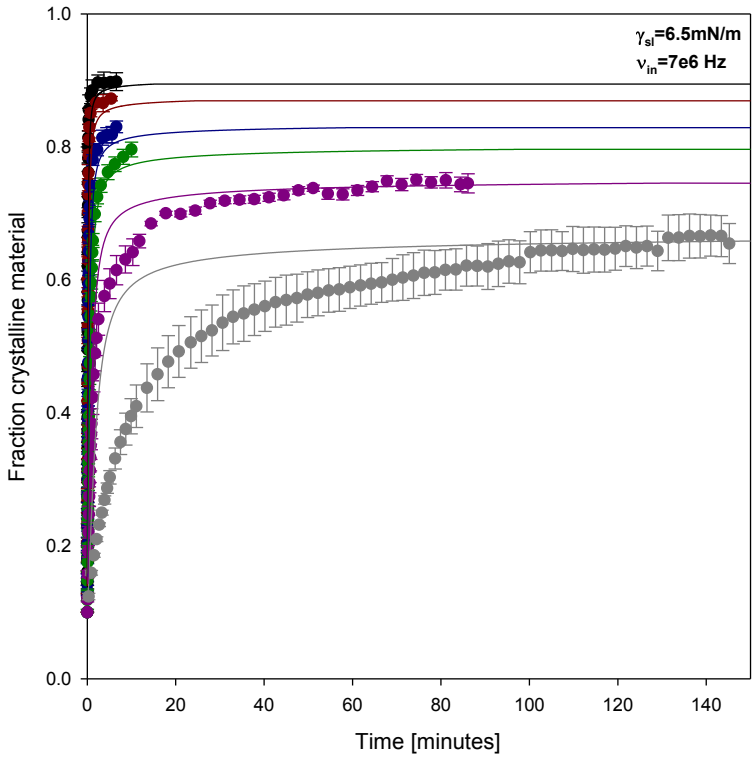

Figure 12. The fraction of crystalline material is plotted against time for Bicalutamdie with initial concentrations in the solution; ● 150µM, ● 120 µM ● 90µM ● 75µM ● 60µM ● 45µM. The initial crystal fraction was 10%. γ_{sl} was set to 6.5 mN/m and ν_{in} was set to 7e6 Hz, the theoretical curves are the solid lines in the figure.

For Linaprazan it has been difficult to get good correlation between experimental and simulated curves. The best fit can be seen in figure 13, where the theoretical curves corresponds to the following parameters; ν_{in} is 1e7 Hz and γ_{sl} is 6.0mN/m.

The difficulty to fit the simulated curves to the experiments results are thought to be increased by use of polymer in the experimental system.

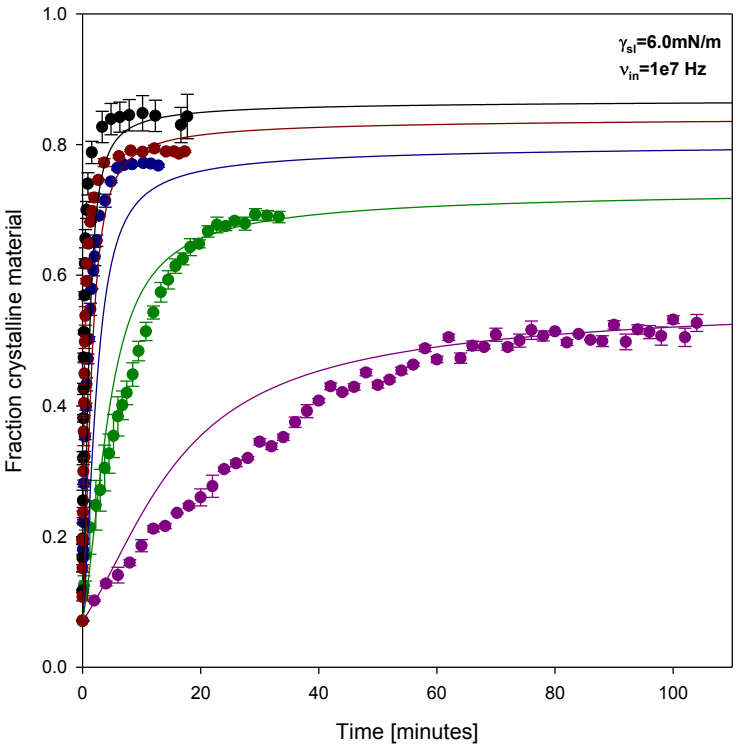

Figure 13. The fraction of crystalline material is plotted against time for Linaprazan with initial concentrations in the solution; • 30µM, • 25µM • 20µM • 15µM • 10µM. The initial crystal fraction was 7.1%. γ_{sl} was set to 6.0 mN/m and ν_{in} was set to 1e7 Hz, the theoretical curves are the solid lines in the figure.

For Felodipine the calculated results and the experimental data agree very well. This is very encouraging and is hopefully and indication that 2D nucleation is the right track regarding crystal growth theories.

The fit between experimental data and simulated curves can be seen in figure 14, ν_{in} is 6e7 Hz and γ_{sl} is 10.4 mN/m.

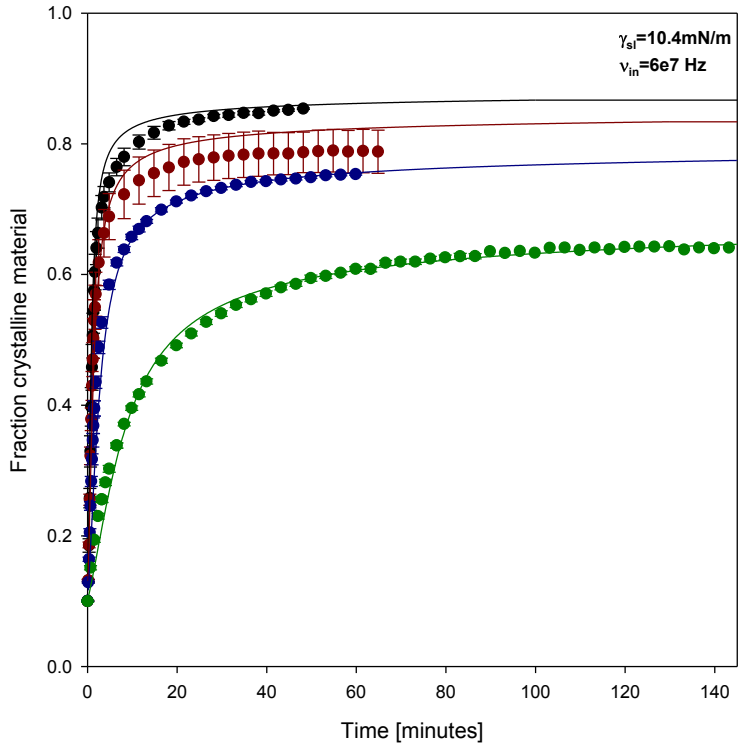

Figure 14. The fraction of crystalline material is plotted against time for Felodipine with initial concentrations in the solution; •25µM, •20µM • 15µM • 10µM. The initial crystal fraction was 10%. γ_{sl} was set to 10.4mN/m and ν_{in} was set to 6e7 Hz, the theoretical curves are the solid lines in the figure.

To summarize the results above, nanocrystal growth for Felodpine can be described nicely by the Hillig-Nielsen theory, Bicalutamide and Linaprazan does however not coincide entirely with theoretical calculations.

It can be seen that the simulated curves cannot describe all supersaturations with the same values of γ_{sl} and ν_{in}. This might be due to this model being based on poly nuclear growth. This mechanism is thought to be true for high supersaturations, but probably is not valid at low supersaturations. The Hillig-Nielsen model will thus give theoretical curves that go to fast at low supersaturations.

It can however be seen that the model is better, and also that it takes into consideration the decrease in concentration of the supersaturated solution. The simulated curves do not continue to solubility, it continues to the metastable zone for growth. This should when the parameters are set properly also coincide with the experimentally received values.

Due to the observations above, that the Hillig-Nielsen model works well at high supersaturations, but is too fast at low supersaturations, might indicate a different mechanism depending on the supersaturation. The theoretical Obretenov interpolation model, which combines both poly and mono nuclear growth was used in calculations. The results for all substances and supersaturations are to be seen below. The Obretenov interpolation model can be simulated by equation 35 and the polydispersity is taken into account.

For Bicalutamide γ_{sl} was determined to 4mN/m and υ_{in} was determined to 1e6 Hz. The curves do coincide fairly well, se figure 15. It can be seen that the model can describe the growth at high supersaturations in a much better way than at low ones. It can also be seen that the agreement is better here, than for the Hillig-Nielsen model.

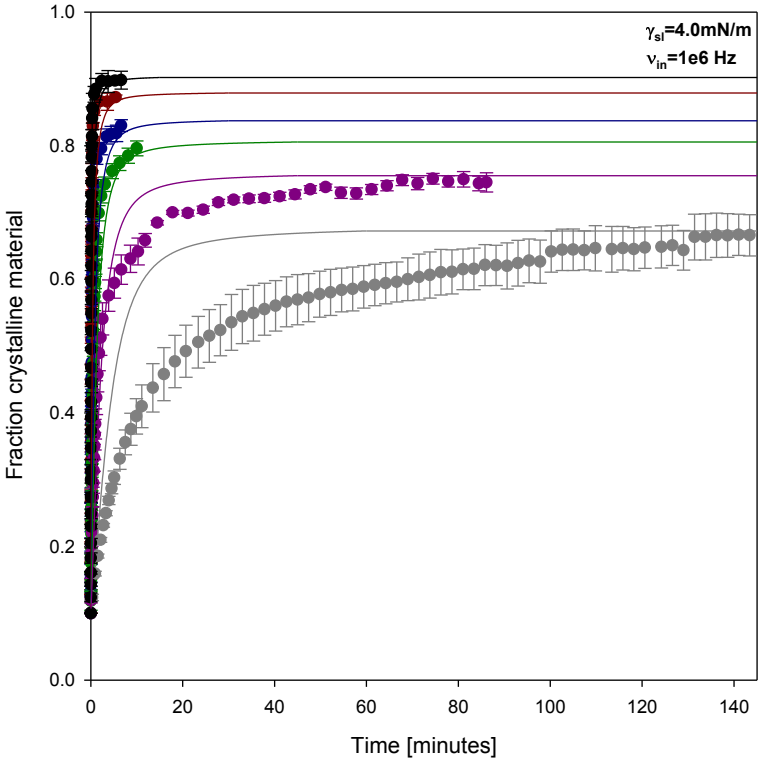

Figure 15. The fraction of crystalline material is plotted against time for Bicalutamdie with initial concentrations in the solution; ● 150µM, ●120 µM ● 90µM ● 75µM ● 60µM ● 45µM. The initial crystal fraction was 10%. γ_{sl} was set to 4.0 mN/m and ν_{in} was set to 1e6 Hz, the theoretical curves are the solid lines in the figure.

For Linaprazan γ_{sl} was determined to 5.5 mN/m and υ_{in} was determined to 1e7 Hz. The curves coincide fairly well, se figure 16. Here, as for Bicalutamide it can be seen that the model has poor agreement at low supersaturations, but better than the Hillig-Nielsen model.

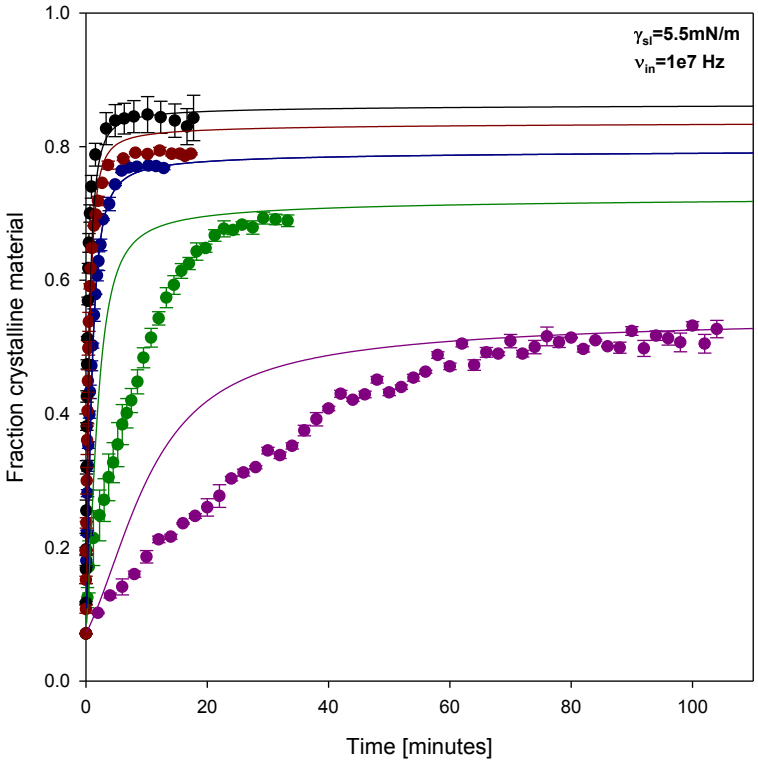

Figure 16. The fraction of crystalline material is plotted against time for Linaprazan with initial concentrations in the solution; ● 30µM, ● 25µM ● 20µM ● 15µM ● 10µM. The initial crystal fraction was 7.1%. γ_{sl} was set to 5.5 mN/m and ν_{in} was set to 1e7 Hz, the theoretical curves are the solid lines in the figure.

For Felodipine γ_{sl} was determined to 8.0 mN/m and υ_{in} was determined to 1e7 Hz. The curves do coincide fairly well, se figure 17. The agreement between theory and experimental results is about as good as it was for the Hillig Nielsen, polynuclear growth theory.

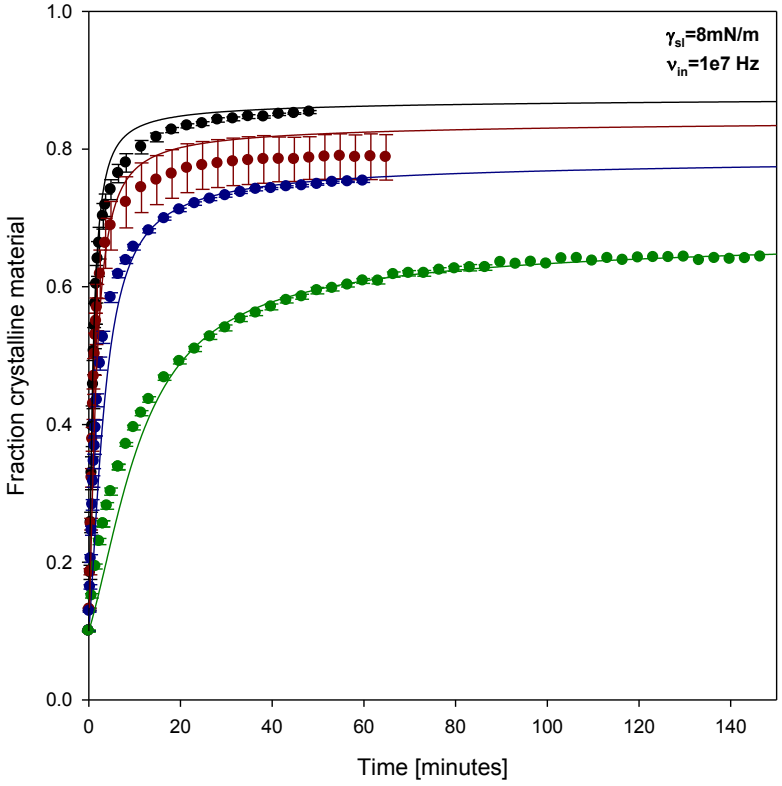

Figure 17. The fraction of crystalline material is plotted against time for Felodipine with initial concentrations in the solution; ● 25µM, ● 20µM ● 15µM ● 10µM. The initial crystal fraction was 10%. γ_{sl} was set to 8.0 mN/m and ν_{in} was set to 1e7 Hz, the theoretical curves are the solid lines in the figure.

The Obretenov interpolating theory is the model that describes crystal growth best for all three substances so far. It can be seen that the experimental curves and the simulated curves nicely go to the same final concentration; the metastable zone for growth is the same in the simulation as in the experiments.

The deviation between experiments and theory might be due to assumptions, such as a spherical molecular shape, and how mono and polynuclear growth models are combined. The deviations might also be due to that the mono and poly nuclear growth models are not the ones that will be able to describe the growth mechanisms. The growth might occur by some other mechanism, such as spiral growth.

Linaprazan show the most significant deviations between theory and experiments, which might be due to polymer being present in the experimental system.

The difference in growth rate between the different substances might partly be due to the crystal shapes.

Bicalutamide and Linaprazan crystals grow like diamonds/cubes, while Felodipine particles grow like cylinders, see figure 25. This gives rather deviating surface tension between the two morphologies. Felodipine crystals have high surface tension on the cylinder ends and low on the long sides, where growth mainly takes place. This is however thought to be true for all substances, that the surface tension is not equal at all sides. This would thus give a γ value that is not true for all or for two of the sides, but an apparent interfacial tension.

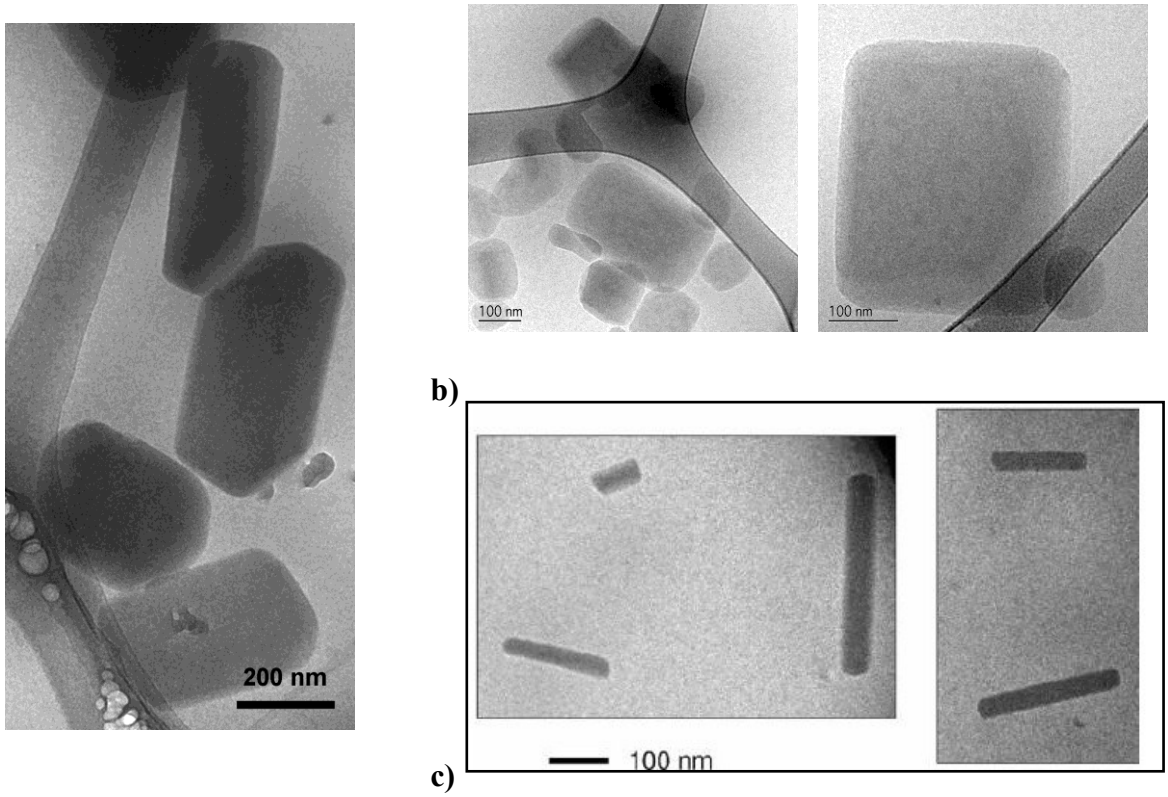

Figure 18. Cryo-TEM images of a) 1mM (ultrasonically prepared) crystalline nanosuspension of Bicalutamide. [30] b) milled particles of Linaprazan. [31 and c) 1mM (ultrasonically prepared) crystalline nanosuspension of Felodipine. [4]

The Bicalutamide and Felodipine particles produced in these studies have been stabilized with AOT. Prior measurements of the growth rate have been performed by Lindfors et al. Bicalutamide particles used in those experiments were stabilized with SDS. The λ value was determined to 6.5μm. [5] The difference in λ value is probably due to use of different stabilizators and/or use of Millex-GV filters.

For Felodipine previous growth experiments have been performed by Lindfors et al. The λ value was 2.5μm for particles ultrasonically prepared with 0.2% (w/w) PVP and 0.25mM SDS as stabilization. [4] The value determined in this study was 3μm. The difference here is probably due to different stabilization. Previously, Felodipine particles have been milled as well, with PVP/AOT, this gave λ= 4μm. The difference between these experiments also indicates that the stabilization affects the growth rate to some extent.

For Linaprazan prior measurements have been performed by Lindfors et al. on milled particles that were stabilized with 1.33 % (w/w) PVP (K30) and 0.067 % (w/w) AOT. The λ value for these particles was determined to 2μm. [32] The same has been done here, due to problems when trying to perform the experiments on ultrasonically prepared particles. From the performed experiments the λ value was determined to 0.5μm. The difference is probably due to use of different filters.

Interesting experimental observations were made during growth experiments on Linaprazan. When at the end of an experiment, the final intensity should be measured; the vessel was turned gently once. The turn resulted in lower intensity then before. If the procedure was repeated and the more violent the turning was made, the lower the final intensity was.

This result might be an indication that the growing dendrites that falls of easily when the vessel is turned.

The particles used in these studies showed rather different stabilities. For example Bicalutamide particles were stable for several weeks while Felodipine was only stable for 2 days.

The growth rate for Bicalutamide was significantly faster compared to results presented by Lindfors et al [5]. The λ value determined in that paper was 6.5 μm compared to 2.5 in this studie. This is partly due to the filtration performed by Lindfors et al was performed with Millex-GV filters.

4.4.5. Growth experiments with different amount of stabilization

Growth experiments with different stabilization were performed the same way as the growth experiments above. The experiments were performed to see how the stabilization affects the growth rate.

For Bicalutamide these experiments were performed with 0.05% AOT, 0.2% AOT, 1% AOT and 0.25mM SDS.

The results are displayed below, where fraction crystalline material is plotted against time, see figure 26.

The experiments were performed before the effect of the used filter was known, and thus the results are affected by the use of Millex-GV filters. Since these results are only used for subjective comparison to experiments with 0.1% AOT also performed with filtration with Millex-GV filter the comparison is still valid.

The substance concentration in the supersaturated solution was 150µM Bicalutamide and initially there was 10% nanocrystals.

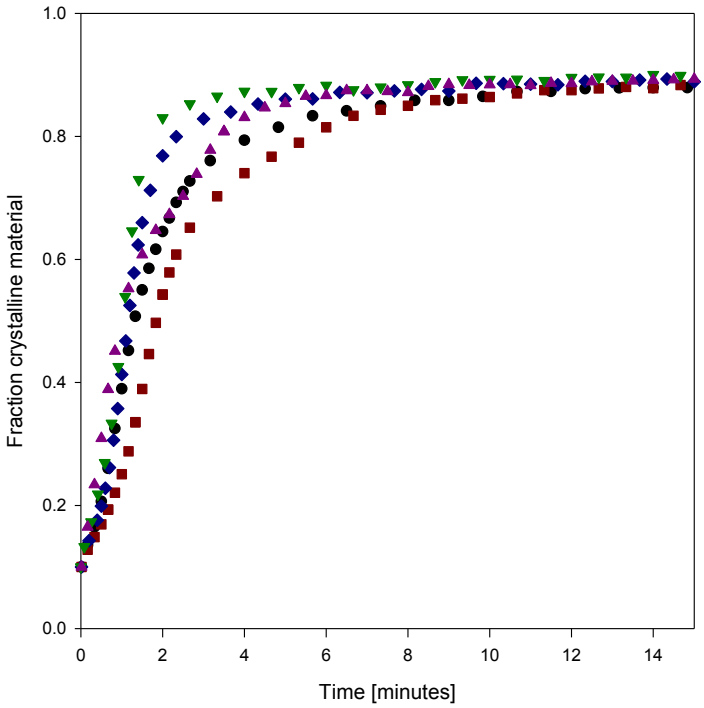

Figure 19. Millex-GV filter were used for the filtration, the concentration was, 150mM Bicalutamide, with 10% initial crystals. The particles were stabilized as follows; • 0.1% AOT, ■ 0.05% AOT, ♦ 0.2% AOT, ▼1% AOT, ▲0.25mM SDS. The different stabilization does not seem to impact the growth rate significantly

The results from these experiments show that the amount of surfactant does not affect the crystal growth rate significantly within the range 0.05-0.2% AOT. This result is very good and shows that the effect of the amount of surfactant is limited.

That use of more surfactant, 1%, gives a faster growth rate is unexpected. But it might be due to the surfactant lowering the surface tension for nucleation. The effects of surfactants are not well investigated. This effect can be seen for 0.05 and 0.2% AOT as well.

The result from experiments performed with SDS also shows a slight increase in growth rate. But the difference is rather limited.

For Linaprazan an experiment with 30µM Substance, 1% initial crystals and 10 times as much stabilizator was performed. The experiment was conducted on milled particles and PTFE-filters were used to filter the supersaturated solutions. The experimental results can be seen below.

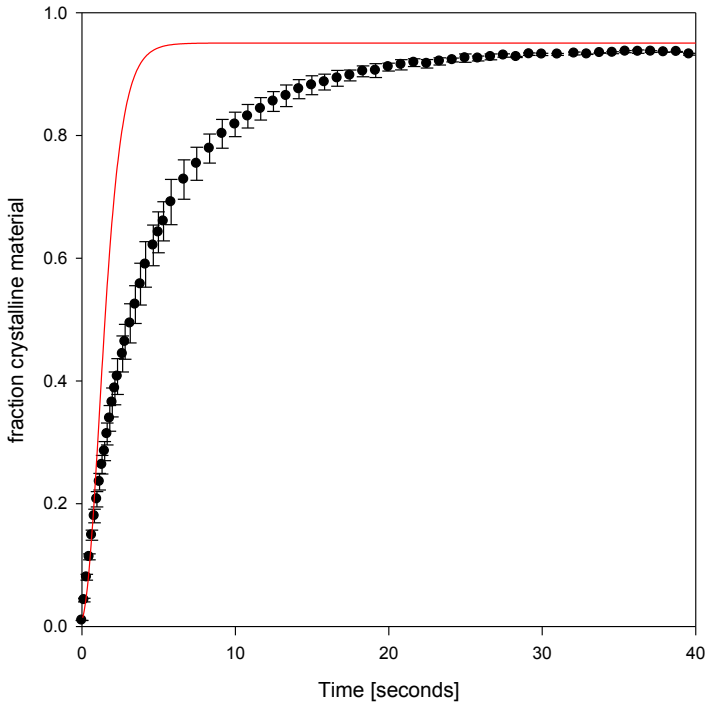

Figure 20. 30µM Linaprazan, 1% initial crystals, 10*stabilisator, λ=0.9µm.

The growth rate is somewhat decreased, which is reasonable. The decrease is probably due to a larger amount of polymer being present.

4.3 Crystal Nucleation

4.3.1 Metastable zone experiments

Metastable zone experiments were performed in order to determine up to what concentration no nucleation takes place in the chosen time range. This concentration range is, as written above, referred to as the metastable zone for crystal nucleation.

The chosen experimental time was 72 hours for Bicalutamide and Linaprazan. The time range was established in the prior report. [1] The experiments had to be redone due to use of the Millex-GV filters. The new results using PTFE-filters are to be seen below.

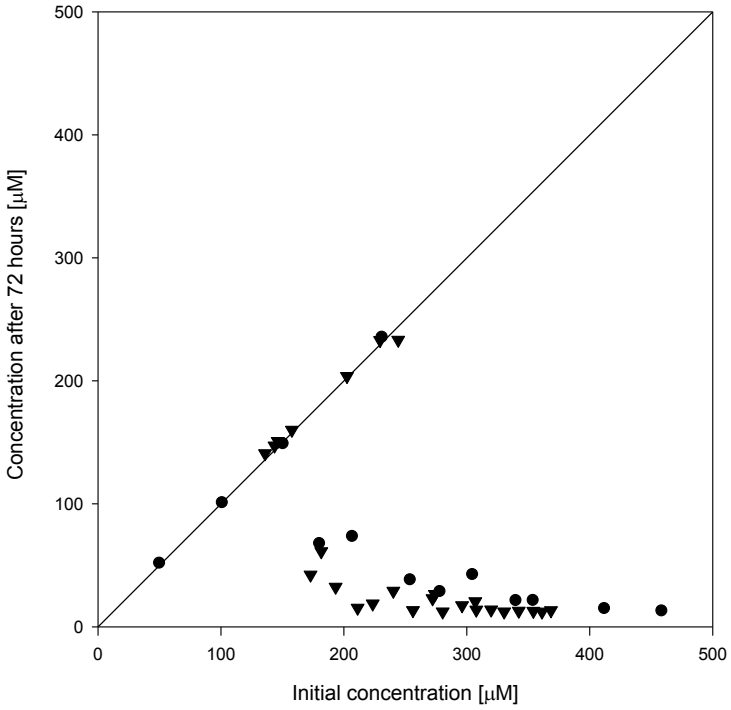

Figure 21. Result for metastable zone experiments for Bicalutamide, the concentration after 72 hours (the nucleation time) is plotted against the initial concentration. The final concentrations have been compensated for loss by filtration. The solid line is a guide to the eye. Different symbols indicate different occasions.

The metastable zone reaches up to about 220μM for 72 hours. It can also be seen in the figure that above 200μM there are almost no symbols in the middle region. All samples, but few, have either the same concentration as initially or a low concentration, about 25μM. This "birfucation" might indicate that the crystallization process for Bicalutamide is affected by secondary nucleation.

If the primary nucleation takes place, secondary nucleation follows and rapidly gives a large amount of crystals. This phenomenon is not well understood theoretically, but might be due to existing nuclei stabilizing the formation of new nuclei, or that pieces of larger crystals falls of giving new nuclei that can continue to grow. What is known is however that secondary nucleation can exist and that it gives a cascade reaction in terms of amount of crystals.

For Linaprazan the metastable zone reaches up to slightly above 20μM with initial filtration. At higher concentrations the amount after 72 hours is lower than the initial, see figure 22.

There is no "bifurcation" seen in this experiment. This is probably an indication that secondary nucleation is not as evident as for Bicalutamide.

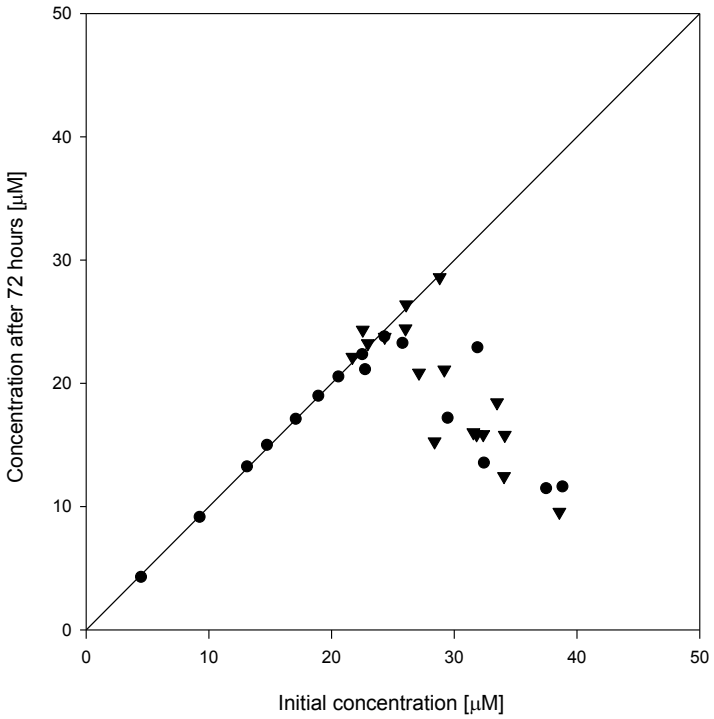

Figure 22. Result for metastable zone experiments for Linaprazan, the concentration after 72 hours (the nucleation time) is plotted against the initial concentration. The final concentrations have been compensated for loss by filtration. The solid line is a guide to the eye. Different symbols indicate different occasions.

For Felodipine no decrease in concentration was seen after 72 hours nucleation, see figure 23a). Thus the experiment was conducted with longer nucleation, to determine a metastable zone.

Unexpected results were seen. At longer nucleation times the concentration drops regardless of initial concentration, see figure 23 b).

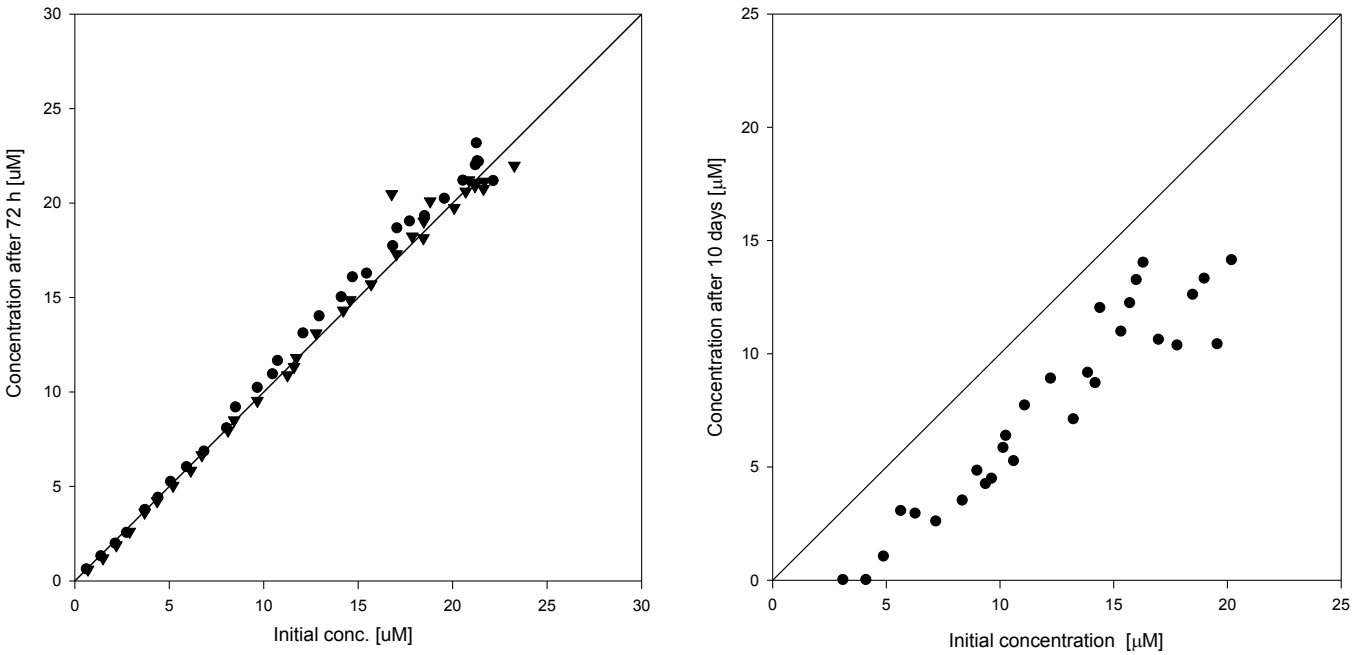

a) b)

Figure 23. Result for metastable zone experiments for Felodipine. a) the concentration after 72 hours (the nucleation time) is plotted against the initial concentration. The solid line is a guide to the eye. Different symbols indicate different occasions. b) the concentration after 10 days (the nucleation time) is plotted against the initial concentration. The final concentrations have been compensated for loss by filtration.

This indicated that there might be adsorption or heterogeneous nucleation on the walls. Due to this, different modified glass vials were tested. The results can be seen in figure 24.

All three sorts of glass, borosilicate, silianized and borosilicate coated with nanosuspension, showed a significant prop in concentration in the entire concentration range. This result shows that these different glass types cannot prevent surface adsorption or heterogeneous nucleation, or else there is some other problem arising.

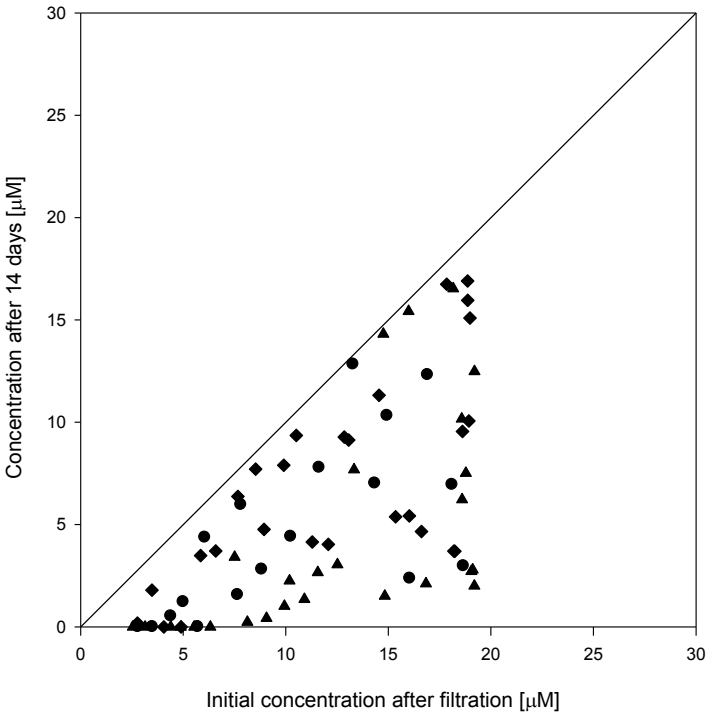

Figure 24. Result for metastable zone experiments for Felodipine performed in different glass vials. ● represents ordinary borosilicate vials, ▲ vials coated with nanosuspension and ♦, silanized vials. The final concentrations have been compensated for loss by filtration.

It was thought that there might be something that affects the samples when they are standing on the anti-vibration table, and thus experiments were conducted simultaneously on the anti-vibration table and an ordinary table, both situated in the same room. The experiment were performed in ordinary glass vials, and the loss was for some reason not as significant as before, but still there is some loss and no clear drop, see figure 25 below.

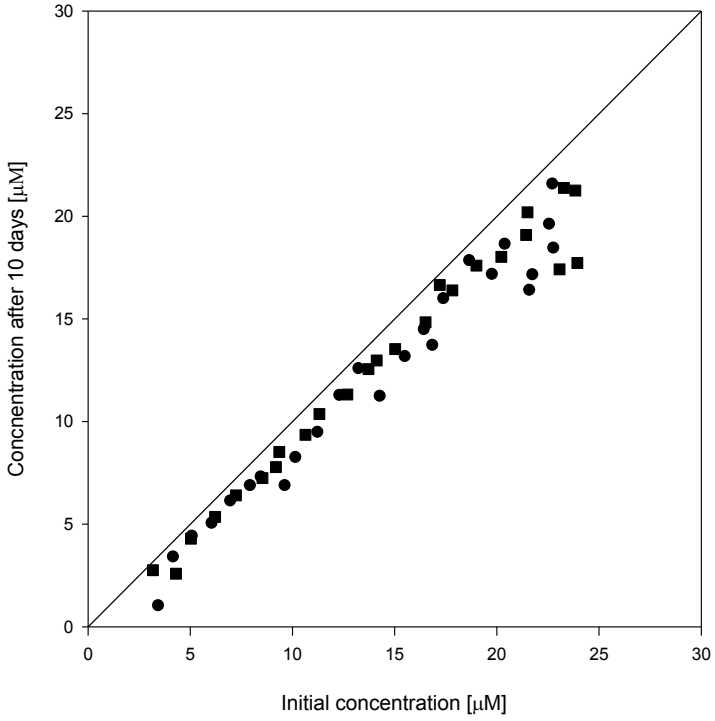

Figure 25. Result for metastable zone experiments for Felodipine performed on different tables. ● represents samples that nucleated on the anti-vibration table, ■ are samples that nucleated on the ordinary table. The final concentrations have been compensated for loss by filtration.

The crystallization and growth processes have been simulated by use of equation 13 and 20. For Bicalutamide the surface integration factor, λ, used was 2.5 μm, based on the results from the simulations and the experimental growth results. The γ_{sl} value was determined to 20±1 mN/m. The experimental results and the theoretical fits are displayed in figure 26. The dots are experimental results and the solid line is the calculated curve.

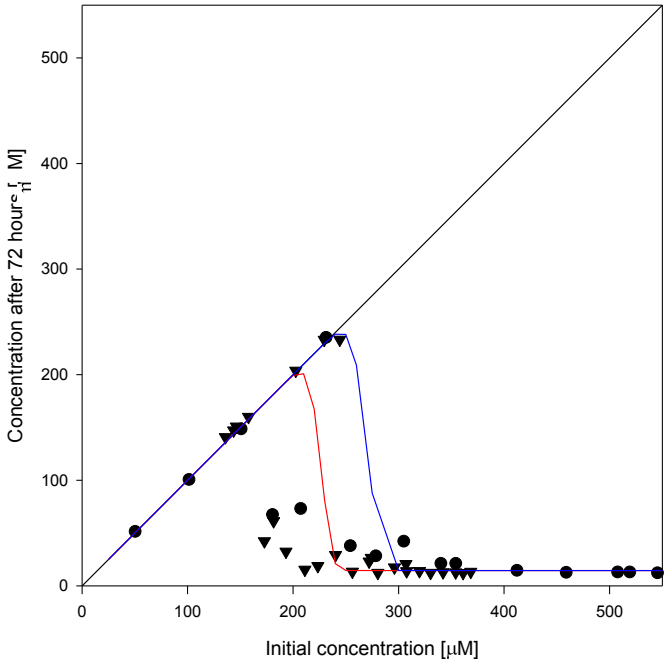

Figure 26. Experimental result and simulated curves for metastable zone experiments on Bicalutamide. The concentration after 72 hours is plotted against the initial concentration. The concentrations after 72 hours have been compensated for loss caused by filtration. Curves for λ=2.5 and γ_{sl}=20.0 (red), 21.0 (blue) and 22.0 (blue) mN/m.

The reason for giving an average value, a highest value and a lowest value is that there can be reasons for choosing either of them. The average could be seen as the right value since it is natural with some deviation from the "true" value in experimental results. Thus presenting it with a deviation is reasonable.

The reason for choosing the lowest value would be that it is here that crystallization begins to occur with three days nucleation time. Below this concentration nothing happens and thus this is the limit where nucleation starts.

The reason for choosing the highest value is that the concentration can be raised to this level without crystallizing in the chosen time range.

The obtained interfacial tension is smaller than expected, when comparing to previous results received by Lindfors et al. [5] This might be due to the sensitivity of the experiments giving slightly deviating results and this, combined with the interpretation of where the metastable

zone is, gives the difference in the γ_{sl} value. The deviation may also be due to those experiments being affected by both nucleation and growth.

For Linaprazan the surface integration factor, λ was determined to 0.5μm. The surface tension received from the theoretical calculations was 15.8±0.7mN/m. In figure 27, the experimental results are showed by dots and the calculated curve by a solid line.

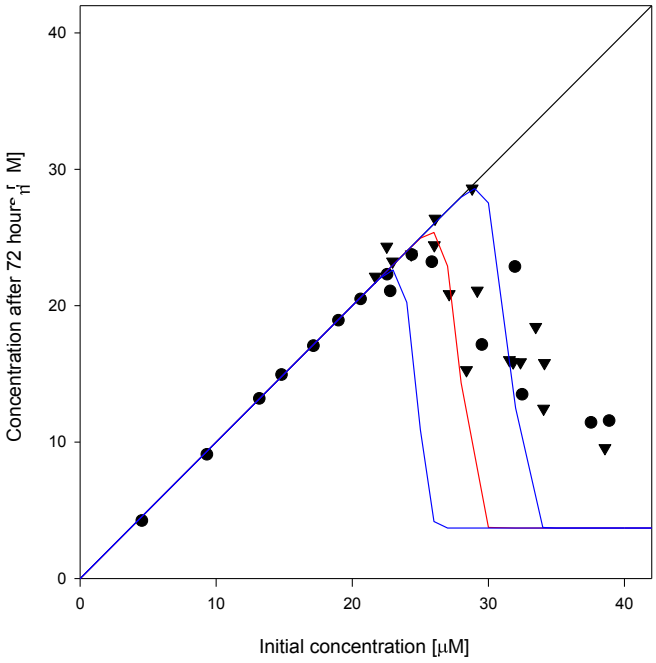

Figure 27. Experimental results and simulated curves for metastable zone experiments on Linaprazan. The concentration after 72 hours is plotted against the initial concentration. The experimental values have been compensated for loss caused by filtration. Curves for λ=0.5 and γ_{sl}=15.8 (red), 16.5 (blue) and 15.1 (blue) mN/m.

The slope of the calculated curves is much steeper than the experimental slopes, especially seen for Linaprazan, this is due to the theory not taking into consideration that the nucleation and growth rate is slower when the concentration is lower. This is also the reason for not reaching the solubility in the metastable zone experiments for both Bicalutamide and Linaprazan.

The surface tension for Linaprazan was determined to be smaller than for Bicalutamide. This indicates that the nucleation barrier for Linaprazan is lower and that primary nucleation occurs more easily.

For Linaprazan γ_{sl} has been determined previously by F. Engström, in his thesis work, γ_{sl} was determined by measuring the induction time in stirred experiments. The experimental values can be seen in figure 28 below, and the values does fairly well correspond to γ_{sl} between

15.7mN/m and 16.0mN/m, compared to 15.8mN/m in this report. The values of the surface tension has been received by using λ=0.5μm, as found in this report.

These values are very similar and do thus indicated that the value is in the correct region.

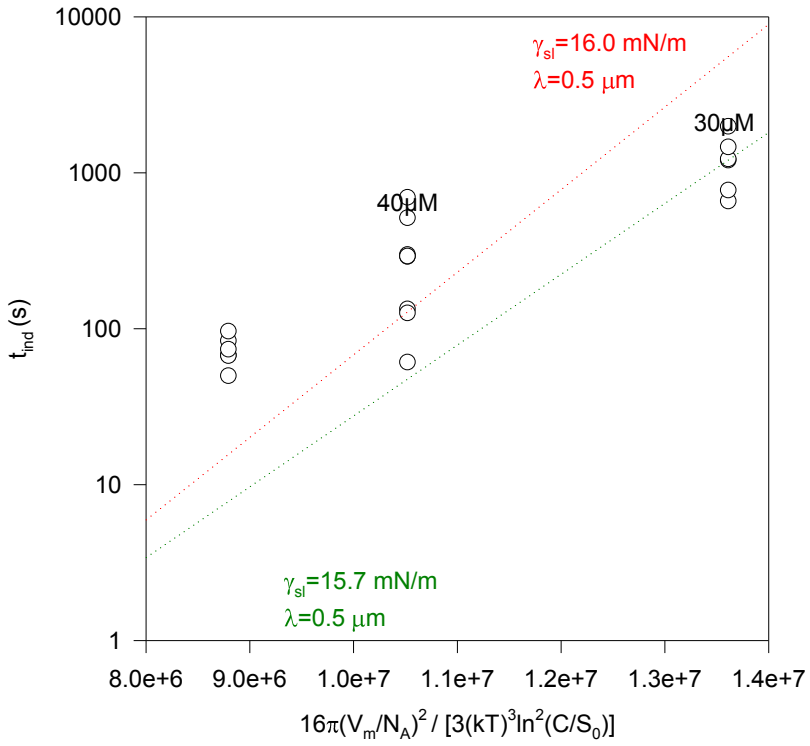

Figure 28. Experimental values for the induction time for Linaprazan are plotted in the figure. The dotted lines are theoretical curves, corresponding to ····· λ=0.5mm and γ_{sl}=15.7mN/m and ····· λ=0.5mm and γ_{sl}=16.0 mN/m.

For Felodipine the correct metastable zone has been difficult to determine. There has been substantial substance loss in the experiments, regardless of which method was used to eliminate large particles in the beginning of the experiment. The loss was difficult to get an understanding of. The main problem is most likely due to surface adsorption and/or heterogeneous nucleation. It was however surprising that change of glass vessels did not impact the results in a positive direction. The silanized vials were thought to minimize interactions, but no change was seen in the results.

Since no well established metastable zone has been determined, the γ_{sl} value is instead presented as a "lowest value". The metastable zone seems to reach higher than what can be detected in the experiments and the values presented below are thus detecting the limit where no nucleation has begun in the chosen time range.

The result below presents both 72 hours nucleation time, figure 29 a) and 14 days nucleation time, figure 29 b).

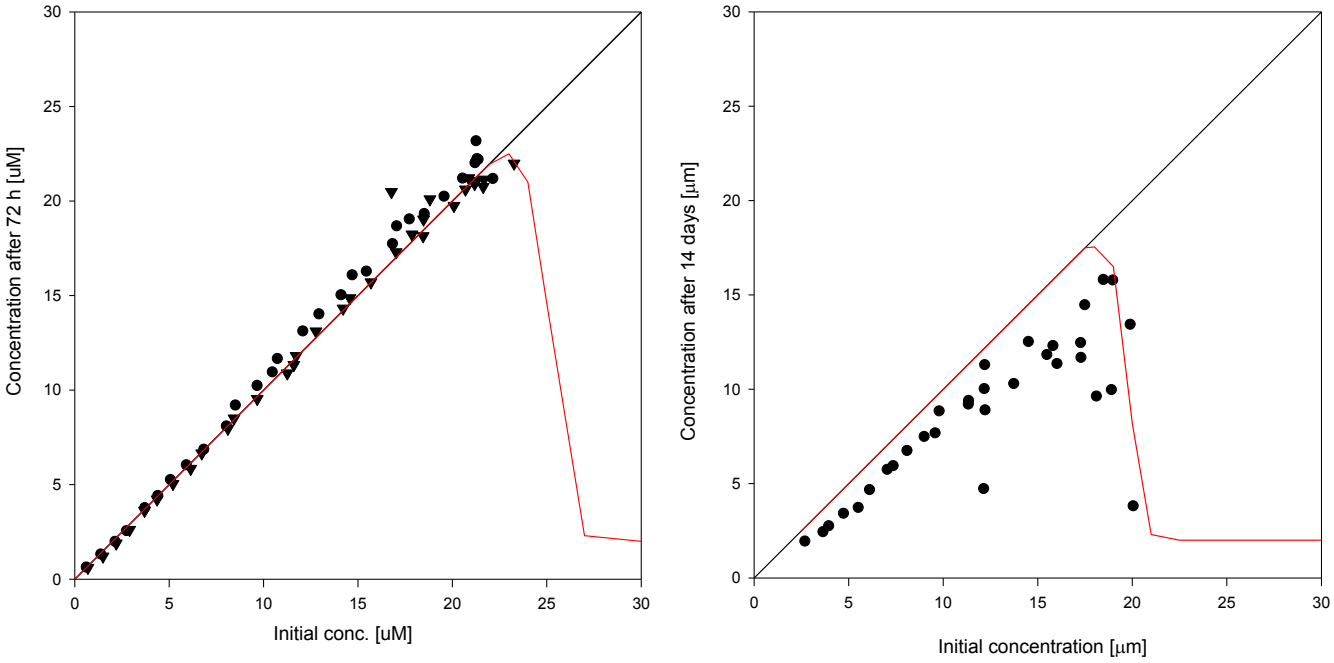

a) b)

Figure 29. Experimental results and simulated curves for metastable zone experiments on felodipine. The concentration after the nucleation time is plotted against the initial concentration. The experimental values have been compensated for loss caused by filtration. a) nucleation time=72 hours, λ= 2.8µm gave γ_{sl}=18.5mN/m, b) nucleation time=14days, λ= 2.8µm gave γ_{sl}=18.0mN/m.

The values differ slightly, but when looking at the experimental results it can be seen that the experiment that has been conducted for 14 days have more deviation from the expected line. These results are thus more uncertain. It is easier to evaluate the results from the experiment that has been conducted for 72 hours. It can thus be concluded that the γ_{sl} value for Felodipine is at the lowest 18.5mN/m.

4.3.3 Crystal nucleation experiments

Crystal nucleation experiments have been performed on Bicalutamide for one nucleation concentration, 440µM. The experiments have been performed according to the procedure in section 3.11.7 and evaluated according to section 3.11.8.

The nucleation times ranged from zero minutes (metastable zone) to one hour and fifteen minutes. The concentration during the growth was 175µM, which is within the determined

metastable zone for three days time. Images of typical detected crystals are to be seen in appendix 26. The results from the initial nucleation experiments can be seen in figure 30.

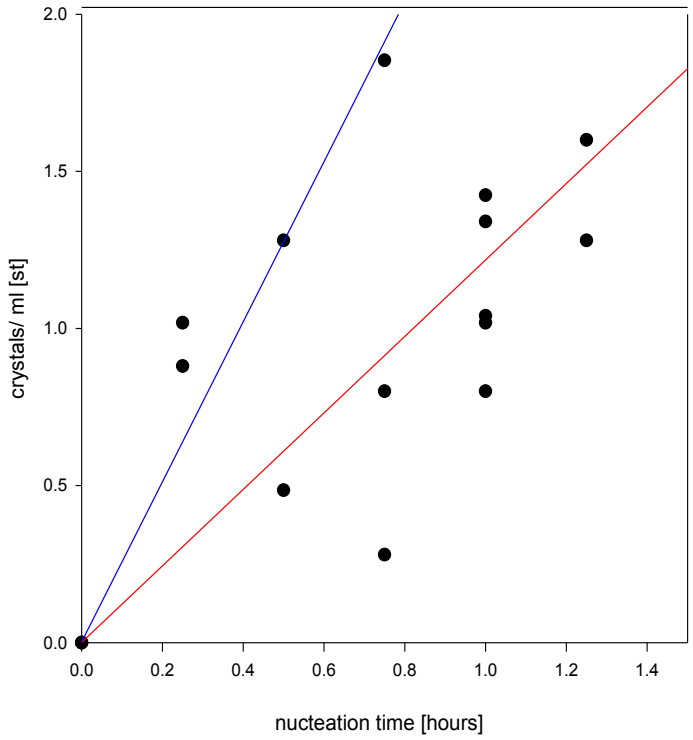

Figure 30. The number of crystals per milliliter for nucleation experiments on Bicalutamide is plotted against the nucleation time. The nucleation concentration was 440µM and growth concentration was 175 µM. Different symbols indicate different experiments. The solid lines represent theoretical values of the surface tension. The red line corresponds to γ_{sl}=24.6, and the blue lines are ±0.1mN/m.

The nucleation experiments gave γ_{sl}=24.6±0.1mN/m. The experimental deviation might appear large when looking in the figure, the deviation between the red average line at 24.6mN/m and the blue lines, presenting a highest and lowest value is 0.1mN/m. Almost all values are within this region. This gives the information that the γ_{sl} value is well determined and that the method used is robust and reliable.

There is some difference between the γ_{sl} values for Bicalutamide, determined from the metastable zone experiments and the nucleation experiments. This might be due to the metastable zone experiments including growth and secondary nucleation as well as primary nucleation, that is the only contributor to the surface tension in the nucleation experiments.

To determine whether secondary nucleation influence the outcome of the nucleation experiments, an experiment was conducted where two series of samples were made, the difference between these was the nucleation volume. One series had 4ml samples, and the other had 1ml samples.

The idea was that if secondary nucleation is present in the experiments there would be significantly more crystals in the samples that had nucleated in 4 ml. However, no significant difference could be seen between the two volumes. This was very good, and strengthens the method reliability. Secondary nucleation is still believed to have a significant influence for Bicalutamide but with clusters of as small size as the ones that are created within the nucleation time in the experiments there are no stabilizing effects or dendrites falling off.

Monte Carlo simulations on Bicalutamide has been conducted by R. Persson, this has given γ_{sl} values around 27mN/m, se figure 31 below.

There is a good agreement between the simulations and the experiments performed in this thesis work. This is interesting and indicates that the results are in the correct region.

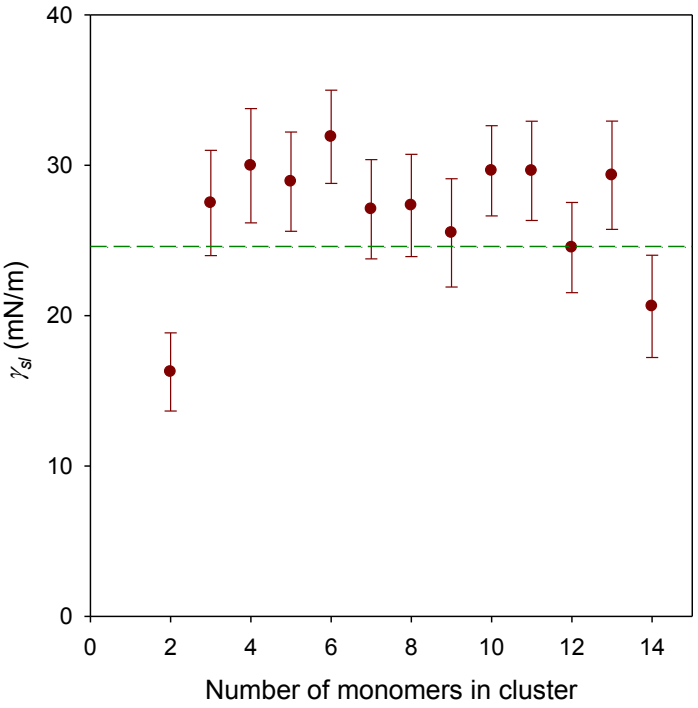

Figure 31. Theoretical values for γ_{sl} for Bicalutamide are plotted against the number of monomers in the cluster. The values originates from Monte Carlo Studies.

Initial experiments have also been performed on Linaprazan. The nucleation time ranged up to eight hours. The nucleation concentration was 30μM and the crystals were allowed to grow for three days at 18μM.

The first experiment gave crystals where the nucleation time was above 4 hours. The crystals were long and narrow, see appendix 27. The shape made them very difficult to count and thus it was tested to have some surfactant present during the nucleation time. In this

experiment no crystals were seen and thus the initial experiment was repeated, this time no crystals were to be seen.

These initial experiments have only given the information that Linaprazan crystals can be detected.

The new nucleation method presented above, with its initial results is believed to be a good method.

The experiments are fairly easy to perform. The results seem to be reliable and robust. The method does also present many opportunities to perform these experiments with some modifications to receive a lot of new information. The experimental setup can be used with different additives in the supersaturated solutions, to see how nucleation is affected. It is also possible to introduce a single crystal into the solution at t=0, to see how this affects the crystallization rate, i.e. the effect of secondary nucleation.

5. Conclusions

Experimental method development has been an important part of this thesis work. The result is several experimental setups that feel reliable and very informative.

The crystal nucleation experimental setup seems reliable and the experiment is relatively easy to perform. From this experiment the surface tension can be determined.

The growth and dissolution experiments give concurring results between different experiments and do thus seem reliable. These experiments give information about the surface integration kinetics.

The metastable zone experiments gave valuable information about the limit of nucleation for a certain time and thus the surface tension.

The surface tension was determined to 20±1mN/m for Bicalutamide from the metastable zone experiments. From the nucleation experiments the value was determined to 24.6±0.1mN/m. These values do not agree and this might be due to secondary nucleation.

Nucleation of Bicalutamide seems to be largely influenced by secondary nucleation. This is seen in the metastable zone experiments where a bifurcation clearly is seen. It has however successfully been determined that secondary nucleation is not present when the crystals are very small. This has given a solid base for the crystal nucleation experiments that has been carried out.

Agreement between the nucleation results and performed Monte Carlo simulations do also indicate that the results are reliable.

The surface tension for Linaprazan was determined to 15.8±0.7 mN/m. This indicates that the barrier for nucleation is slightly lower for Linaprazan than for Bicalutamide.

Felodipine results indicate a barrier for nucleation that is above 18.5mN/m. The true value has been very difficult to find. The reason for this is partially due to the low amorphous solubility. This makes it difficult to make solutions of high supersaturation.

The growth experiments have given significantly lower values in this thesis work than in the prior. This is thought to mainly be due to working with more unaffected systems and avoiding Millex GV-filters.

The understanding of the filters large impact on the nucleation related processes was an important finding in this report.

The λ values that have been determined are 2.5μm for Bicalutamide, 0.5μm for Linaprazan and 2.8μm for Felodipine. The surface integration model is not able to describe growth in a satisfactory way, especially not at low supersaturations.

The Hillig Nielsen, polynuclear model, had better agreement, and gave γ_{sl} 6.5 mN/m and $7*10^6$ Hz for Bicalutamide. For Linaprazan the corresponding values were 6.0 mN/m and $1*10^7$ Hz. For Felodipine the frequency was $6*10^7$ Hz and the surface tension was 10.4mN/m. The model was able to describe all growth curves well for Felodipine and fairly well for Linaprazan and Bicalutamide.

The Obretenov interpolation model, where both mono- and polynuclear growth are included gave γ_{sl} 4.0mN/m and $1*10^6$ Hz for Bicalutamide. For Linaprazan the corresponding values were 5.5 mN/m and $1*10^7$ Hz. For Felodipine the frequency was $1*10^7$ Hz and the surface tension was 8.0mN/m. The Obretenov interpolation model was the best at describing all growth curves well for all substances.

The difference between the three substances might be due to different shapes of the crystals when growing.

It was very interesting to find that within reasonable limits, the growth is unaffected by the amount of stabilizator and only slightly affected by the type used.

The crystal dissolution experiments have showed that the process is diffusion controlled. This is probably due to no shape maintenance during the dissolution.

6. Future Work

More crystal nucleation experiments need to be performed, primarily on more substances and also on different nucleation concentrations for each of these substances.

Further, secondary nucleation experiments are an interesting extension that would be possible to continue with. A crystal would then be added to the supersaturated solution at t=0, and removed at $t=t_{nuc}$, and the solution would then be diluted into the metastable zone.

This type of experiment would give information about secondary nucleation. And the experiment could be performed with and without mixing, to determine the influence of mass transfer.

With a well-functioning method where the rate of nucleation can be measured the opportunity to investigate the effects of additives arises, so this is also a natural following step.

Growth and dissolution has been fairly well investigated. It might be of interest to compare milled particles of Bicalutamide and Felodipine with the results from the ultrasonically prepared particles used in this report.

It would also be of great interest to further investigate why it was impossible to work with ultrasonically prepared nanoparticles of Linprazan. This could preferably be done by trying to determine the polymorph of the ulrasonically prepared particles to make sure that the polymorph is the one that is expected, and also that the particles are crystalline.

7. Acknowledgements

Lennart, thanks for all help and support. Your enthusiasm and true interest has been inspiring. Your holistic perspective, great knowledge and critical review of my work has thought me a lot, not only on crystal nucleation and crystal growth but on structured lab work and the importance of keeping notes (if you can't keep everything in mind, and I can't.)

Pia, thanks for time, knowledge and space that you have given me. Your support, input and help in the lab and regarding experiments has been very valuable to me. I have learned a lot about how to think, plan and work in a good way in a lab. Don't think that I could have had a better teacher.

Everyone else on Astra Zeneca that I have met, you have been very helpful and welcoming.

Ulf, thanks for giving me a good start by the reading course and for helping me to find a place to do my diploma work by talking to Lennart.

Jonathan, thanks for your support and patience during this time. It has meant a lot to me to be able to talk to you about my work, the problems everything else going on. Thank you.

8. Definitions

A	surface area
A_{121}	Hammaker constant
a	cross sectional area of a molecule
C	concentration, in molar
Cb	bulk concentration
C’	concentration at the boundary layer outside a crystal
c	speed of light
D	diffusion coefficient
D_0	diffusion coefficient for monomers in water
Dn*	diffusion coefficient for a cluster of critical size
DM	diffusion coefficient of monomers in water
dC/dX	concentration gradient
dM/dt	molar flow of monomers to the particle surface
E	energy
f	frequency
G_L	Line energy
h	Planck’s constant
I_0	incident intensity
J	nucleation rate
J_D	flow of monomers
J_{2D}	rate of 2D nucleation
$J_{D\infty}$	net flow of monomers to the crystal
k_B	Boltzmann coefficient
k_+	surface integration factor
kn^{*+}	forward rate for the formation of a cluster of critical size
l	distance between a nucleus and a crystal
logP	a measure of the hydrophobicity of a molecule
M	monomer
M*	the critical number of monomers
M_n	n monomers
M_{n*}	the number of monomers in a critical cluster

M_{n^*+1} the number of molecules in a supercritical cluster

m ratio between the refractive index of the particle and the solvent

Mw molecular weight

N number of crystals

$\langle N \rangle$ average number of crystal

N_{tot} total number of crystals or nuclei

n number of molecules

n* number of molecules in a cluster of critical size

nc number of aggregating molecules

n_p refractive index of the particle

n_s refractive index of the solvent

P Poisson distribution

pKa a measure of the charge of a molecule

R molar gas constant

R radius of particle

R^* radius of a nucleus of critical size

Rn* radius of a cluster of critical size

R_M radius of a monomer

[S] concentration of substance

$[S]_{crystal}$ concentration of crystalline substance

$S_{amorphous}$ apparent solubility of amorphous state

S(r) the concentration at the surface of the particle

S_0 intrinsic solubility

T temperature in Kelvin

V volume

w spreading velocity of a monoatomic step during 2D nucleation and lateral spreading

β numerical constant, regarding Obretenov interpolated growth, that is 0.97 when using Hillig-Nielsen for the polynuclear growth

ν molar volume

ν_{in} the frequency by which molecules attach to a 2D nuclei

dX/dt flow of substance

x_c equilibrium solubility of the substance

χ_0 average distance between kink positions at the edge of a 2D nuclei

ΔG difference in free energy

$\Delta G_{surfnuc}$ difference in free energy for 2D nucleation

ΔG^* free energy barrier

γ interfacial tension

γsl interfacial tension, surface free energy between the solid and liquid phase

η viscosity

λ surface integration constant

λ line tension

λ wavelength

θ contact angle

$\nabla C(r)$ gradient concentration as a function of distance from the center of a spherical particle

[] concentration of

ψ $r/(\lambda+r)$

μ^0 standard chemical potential in the crystalline state

μ^* standard chemical potential in solution

μ_n chemical potential of n molecules in the condensed layer

μ_l chemical potential of n molecules in solution

9. References

[1] A.Franzén, *Crystal nucleation of poorly soluble drugs, I Method development and initial results, 2011*

[2] R.H. Müller, C. Jacobs, O. Kayser, *Nanosuspensions as particulate drug formulations in therapy Rationale for development and what we can expect from the future*, Elsevier, 2001

[3] B.C. Hancock, M. Parks, *What is the true Solubility Advantage for amorphous Pharmacuticals?*, Pharmaceutical Research, vol 17, no 4, 2000

[4] L. Lindfors, P. Skantze, U. Skantze, J. Westergren, U.Olsson, *Amorphous Drug Nanosuspensions. 3. Particle Dissolution and Crystal Growth*, Langmuir, vol. 23, 2007, 9866

[5] L. Lindfors, S. Forssén, J. Westergren, U. Olsson, *Nucleation and crystal growth in supersaturated solutions of a model drug*, Journal of Colloid and Interface Science, vol. 325, 2008, 404-413

[6] I. V Markov, *Crystal growth for beginners, Fundamentals of Nucleation, crystal Growth and epitaxy*, 2:nd edt, 2008, World Scientific Publishing Co. Pte. Ltd., Singapore

[7] R.A. Granberg, C. Ducreux, S. Gracin et al. *Primary nucleation of paracetamol in acetone-water mixtures*. Chemical Enginering. Sci. vol. 56, 2001, 2305-2313

[8] B.A. Hendriksen, DJW Grant, *The effect of structurally related substances on the nucleation kinetics of paracetamol (acetaminophen),* Journal of Crystal Growth, vol. 156, 1995, 252-260

[9] AM Kulkarni, CF Zukoski, *Nanoparticle crystal nucleation: Influence of solution conditions*, Langmuir, vol. 18, 2002, 3090-3099

[10] O Galkin, PG Vekilov. *Are nucleation kinetics of protein crystals similar to those of liquid*
droplets? J. Am. Chem. Soc. vol 122, 2000, 156-163

[11] O Galkin, PG Vekilov. *Direct determination of the nucleation rates of protein crystals,* J.

Phys. Chem. B, vol. 103, 1999, 10965-10971

[12] O Galkin, PG Vekilov. *Nucleation of protein crystals: critical nuclei, phase behavior, and control pathways,* J. Crystal Growth vol. 232, 2001, 63-76

[13] PG Vekilov, O Galkin. *On the methods of determination of homogeous nucleation rates of protein crystals. Colloids and Surfaces A*: Physiochem. Eng. Aspects 00, 2002, 1-6

[14] T. Koop, B. Luo, A. Tsias, T. Peter, *Water activity as the determinant for homogeneous ice nucleation in aqueous solutions, Letters to Nature,* vol. 406, 2000, 611-614

[15] A.E. Nielsen, *Electrolyte crystal growth mechanism*, J. of Crystal Growth 67, 1984, 289-310

[16] W. Obretenov, D. Kashchiev, V. Bostanov, *Unified description of the rate of nucleation-mediated crystal growth*, J. of Crystal Growth 96, 1989, 843-848

[17] J. Park, V. Privman, E. Matejevic, *Model of Formation of Monodisperse Colloids*, J. Phys Chem. vol. 105, 2001, 11630-11635

[18] U.Olsson, *Surface nucleation – a simple model of layer-by-layer crystal growth***,** Lund University

[19] R. Persson, *Generalized Hillig-Nielsen Theory for crystalline nanoparticel growth*, 2008

[20] T.P Melia, W.P. Moffit, *Secondary nucleation from aqueous solution*, I&EC Fundamentals, vol. 3, no. 4, 1964, 313-317

[21] S.V. Amel'kin, *The role of van der Waals Forces in the Kinetics of Mass Crystallization*, Colloid Journal, vol. 63, no. 3, 2001, 263-269

[22] Astra Zeneca, In-house data report

[23] G.Ruecroft, D.Hippkiss, T. Ly, N. Maxted, P.W. Cains, Sonocrystallization: *The use of ultrasound for improved industrial crystallization*, Organic Process Research & Development, vol. 9, 2005, 923-932

[24] V. Kharb, M. Bhatia, H. Dureja, D. Kaushik, *Nanoparticle technology for the delivery of poorly water-soluble drugs*, feb 2006, Pharmtech.com

[25] L.Gao, D. Zhang, M. Chen, Drug *nanocrystals for the formulation of poorly soluble drugs and its application as a potential drug delivery system*, J. Nanopart. Res. Vol. 10, 2008, 845-862

[26] R. Fossheim, *Crystal Structure of the Dihydropyridine Ca2+ Antagonist Felodipine. Dihydropyridine Binding Prerequisites Assessed from Crystallographic Data*, J. Med. Chem. vol. 29, 1986, 305-307

[27] P.Skantze, U.Skantze, *Nanosuspensions and early phase formulation-a practical guide*, version 2, in-house report Astra Zeneca Mölndal, 2008

[28] D. Xia, P. Quan, H. Piao, S. Sun, Y. Yin, F. Cui, *Preparation of stable nitrendipine nanosuspensions using the precipitation-ultrasonication method for enhancement of dissolution and oral bioavailability*, European Journal of Pharmaceutical Sciences, vol. 40, 2010, 325-334

[29] R. Snyder, S. Veesler, M. F. Doherty, *The Evolution of Crystal Shape During Dissolution, Predictions and Experiments*, Crystal Growth & Design, vol. 8, no. 4, 2008, 1100-1101

[30] Astra Zeneca, In-house Cryo-TEM pictures, L. Lindfors

[31] Astra Zeneca and U. Olsson, Cryo-TEM images of particles milled in-House, and the Cryo-Tem was performed at Lund University by help from U. Olsson.

[32] S. Carlert, *"Predicting Intestinal Precipitation-A case Example for Basic BCS Class II Drug"*, Pharm Res, 2010

Appendix 1

The structures of the model substances used in the thesis work. a) Bicalutamide, b) Linaprazan and c) Felodipine.

a)

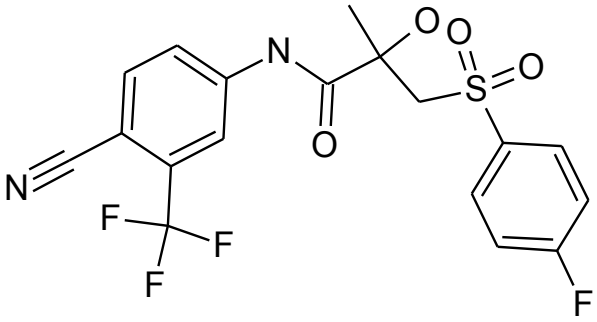

b)

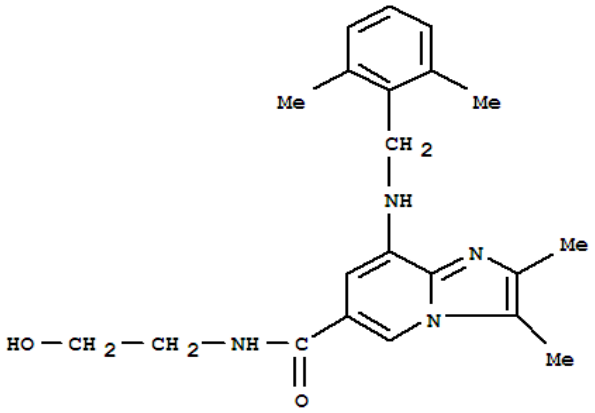

c)

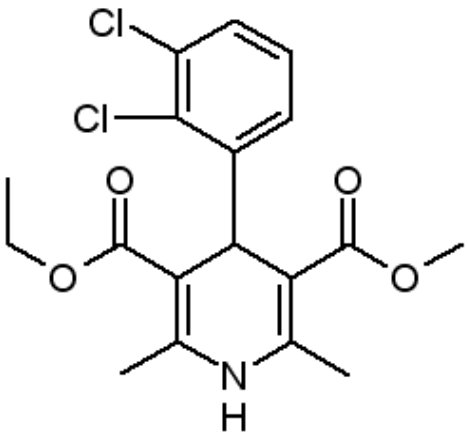

Appendix 2

Nanocrystals of Bicalutamide

Preparations

- Fill the water bath belonging to the S2 from Covaris with fresh MilliQ-water
- Start the degas on the S2, at least 30 minutes prior to use

Prepare the stabilizer solution, 0.1(w/w) % AOT

- Add 9 ml of MilliQ-water to a vial
- Add one ml of 1(w/w) % AOT, wash the tip five times
- Stir for 10 minutes
- Filtrate the solution with a PTFE filter, 0.2μm

Make the nanocrystals, 1mM Bicalutamide, 0.1(w/w) % AOT, 0.8(w/w) % DMSO

- Add 1982μL 0.1(w/w) % AOT solution to a Biotage microwave vial
- Close the vial with parafilm
- Put it in the S2
- Prepare the addition of the stock solution, use a Hamilton syringe with a tall needle
  - Pull up the stock solution in the syringe, 16μL 125mM Bicalutamide in DMSO
  - Draw some air into the needle
  - Dry the needle with Kleenex
- Start the ”Ultrasonic” treatment
- Rapidly add the stock solution
- Put more parafilm on top of the vial
- Put the lid on
- When the run is finished measure the size

Appendix 3

Nanocrystals of Linaprazan

Preparations

- Milling vessels, 1.2ml
- Weigh in substance (~57mg)
    - Add thawed vehicle, 1.33 (w/w) % PVP (K30), 0.067% (w/w) AOT to give 10 (w/w) % substance (~570mg)
    - Add a magnet and let it stir over night
- Weigh in 0.6-0.8mm zirconium beads (2*2.4g)

Milling

- Add the "slurry" that has been stirred over night (or water) to the milling vessel (510mL)
- Add the beads
- Put the lid on
- Put on parafilm to ensure tight closure of the vessles
- Put the vessles in to the mill, Fritsch, Pulverisette, and attach them thoroughly
- Start the Milling procedure
    - 700rpm
    - 4*30 minutes
    - 15 minute brakes in-between
- When finished, pull out the nanosuspension with a syringe and needle
- Clean the beads with water; 3*1/2 volume (3*250µL) to get as much compound as possible
- Use LC to determine the batch concentration
- Measure the particle size

Appendix 4

Nanocrystals of Felodipine

Preparations

- Fill the water bath belonging to the S2 from Covaris with fresh MilliQ-water
- Start the degas on the S2, at least 30 minutes prior to use
- Fill an ordinary ultrasound water bath with fresh MilliQ-water
- Run for 5 minutes

Prepare the stabilizer solution, 0.1(w/w) % AOT

- Add 9 ml of MilliQ-water to a vial
- Add one ml of 1(w/w) % AOT, wash the tip five times
- Mix it on a magnetic stirrer for 10 minutes
- Filtrate the solution with a PTFE filter, 0.2μm

Make the nanocrystals, 0.5mM Felodipine, 0.1(w/w) % AOT, 0.8(w/w) %DMSO

- Add 1984μL stabilizer solution to a Biotage microwave vial
- Put the Biotage microwave vial in the ordinary ultrasonic bath, start it
- Prepare the addition of the stock solution
  - Use a Hamilton syringe
  - Pull up the stock solution in the syringe, 16μL 62.5mM Felodipine in DMSO
  - Draw some air into the needle
  - Dry the needle with Kleenex
- Rapidly add the 16 μL to the Biotage microwave vial
- Put the lid on
- Stop the ultrasound
- Rapidly move it to the S2
- Start the ”Ultrasonic” treatment
- Put the lid on
- When the run is finished measure the size

Appendix 5

Growth experiments on Bicalutamide

Settings

- Excitation: 234 nm, slith width: 5 nm
- Emission: 323 nm, slith width: 2.5 nm
- Data interval: 1 second
- Response width: 3 seconds
- No “single read”
- Concentrations: 150, 120, 90, 75, 60, 45µM
- 10% initial crystals

Procedure

- Use nanocrystals prepared according to the instructions in appendix 2
- Turn the crystal solution four times and ultrasonicate for 30 seconds prior to use (if not completely fresh)
- Measure the size of the particles using the zetasizer nano
- Add 10 (w/w) % crystals to the bottom of the quarts cuvette using a Hamilton syringe
- Put the cuvette into the fluorometer, close and start the measurement
- Make the supersaturated solution, stock solutions described above are to be used
  - Add 3968 uL filtrated MilliQ water to a 10 ml vial
  - Add 32 uL stock solution, turn twice
  - Filter the solution with a PTFE filter, 0.20µm
- Rapidly add the supersaturated solution, $V_{supersat.. sol.}=(2000-V_{crystal})$ µL
- Measure until stable or negative slope, take out and turn the sample twice, insert again to measure the final value

Appendix 6

Growth experiments on Linaprazan

Settings

- Excitation: 300 nm, slith width: 5 nm
- Emission: 378 nm, slith width: 2.5 nm
- Data interval: 1 second
- Response width: 3 seconds
- No “single read”
- Concentrations: 30, 25, 20, 15, 10µM
- 7.1% initial crystals

Procedure

- Use nanocrystals prepared according to the instructions in appendix 3
- Turn the crystal solution four times and ultrasonicate for 30 seconds prior to use (if not completely fresh)
- Measure the size of the particles using the zetasizer nano
- Add 7.1(w/w) % crystals to the bottom of the quarts cuvette using a Hamilton syringe
- Put the cuvette into the fluorometer, close and start the measurement
- Make the supersaturated solution, stock solutions described above are to be used
    - Add 3968 uL filtrated MilliQ water to a 10 ml vial
    - Add 32 uL stock solution, turn twice
    - Filter the solution with a PTFE filter, 0.20µm
- Rapidly add the supersaturated solution, $V_{supersat.. sol.}=(2000-V_{crystal})$ µL
- Measure until stable or negative slope, take out and turn the sample twice, insert again to measure the final value

Appendix 7

Growth experiments on Felodipine

Settings

- Excitation: 370 nm, slith width: 2.5 nm
- Emission: 430 nm, slith width: 2.5 nm
- Data interval: 1 second
- Response width: 3 seconds
- No “single read”
- Concentrations: 25, 20, 15, 10, 8µM
- 10% initial crystals

Procedure

- Use nanocrystals prepared according to the instructions in appendix 4
- Turn the crystal solution four times and ultrasonicate for 30 seconds prior to use (if not completely fresh)
- Measure the size of the particles using the zetasizer nano
- Add 10(w/w) % crystals to the bottom of the quarts cuvette using a Hamilton syringe
- Put the cuvette into the fluorometer, close and start the measurement
- Make the supersaturated solution, stock solutions described above are to be used
    - Add 3968 uL filtrated MilliQ water to a 10 ml vial
    - Add 32 uL stock solution, turn twice
    - Filter the solution with a PTFE filter, 0.20µm
- Rapidly add the supersaturated solution, $V_{supersat.. sol.}=(2000-V_{crystal})$ µL
- Measure until stable or negative slope, take out and turn the sample twice, insert again to measure the final value

Appendix 8

Dissolution experiments on Bicalutamide

Settings

- Excitation: 234 nm, slith width: 5 nm
- Emission: 323 nm, slith width: 5 nm
- Data interval: 0.02 seconds
- Response width: 0.06 seconds
- No “single read”
- Concentrations: 11.5, 8.5, 5.5, 2.5, 0µM in the solution
- 1.5µM initial crystals

Procedure

- Use nanocrystals prepared according to the instructions in appendix 2
- Turn the crystal solution four times and ultrasonicate for 30 seconds prior to use (if not completely fresh)
- Measure the size of the particles using the mastersizer
- Add 1.5µM crystals to the bottom of the quarts cuvette using a Hamilton syringe
- Put the cuvette into the fluorometer, close and start the measurement
- Make the undersaturated solution
    - Add 3968 uL filtrated MilliQ water to a 10 ml vial
    - Add 32 uL stock solution, turn twice
    - Filter the solution with a PTFE filter, 0.20µm
- Rapidly add the supersaturated solution to a total of 2ml
- Measure until there is no slope

Appendix 9

Dissolution experiments on Linaprazan

Settings

- Excitation: 300 nm, slith width: 5 nm
- Emission: 378 nm, slith width: 5 nm
- Data interval: 0.02 seconds
- Response width: 0.06 seconds
- No “single read”
- Concentrations: 1.15, 0.85, 0.55, 0.35, 0.1, 0μM in the solution
- 0.1μM initial crystals

Procedure

- Use nanocrystals prepared according to the instructions in appendix 3
- Turn the crystal solution four times and ultrasonicate for 30 seconds prior to use (if not completely fresh)
- Measure the size of the particles using the mastersizer
- Add 0.15μM crystals to the bottom of the quarts cuvette using a Hamilton syringe
- Put the cuvette into the fluorometer, close and start the measurement
- Make the undersaturated solution
    - Add 3968 uL filtrated MilliQ water to a 10 ml vial
    - Add 32 uL stock solution, turn twice
    - Filter the solution with a PTFE filter, 0.20μm
- Rapidly add the supersaturated solution to a total of 2ml
- Measure until there is no slope

Appendix 10

Dissolution experiments on Felodipine

Settings

- Excitation: 370 nm, slith width: 5 nm
- Emission: 430 nm, slith width: 5 nm
- Data interval: 0.02 seconds
- Response width: 0,06 seconds
- No “single read”
- Concentrations: 1.6, 1.2, 0.8, 0.4, 0.2, 0μM in the solution
- 0.2μM initial crystals

Procedure

- Use nanocrystals prepared according to the instructions in appendix 4
- Turn the crystal solution four times and ultrasonicate for 30 seconds prior to use (if not completely fresh)
- Measure the size of the particles using the mastersizer
- Add 0.2μM crystals to the bottom of the quarts cuvette using a Hamilton syringe
- Put the cuvette into the fluorometer, close and start the measurement
- Make the undersaturated solution
    - Add 3968 uL filtrated MilliQ water to a 10 ml vial
    - Add 32 uL stock solution, turn twice
    - Filter the solution with a PTFE filter, 0.20μm
- Rapidly add the supersaturated solution to a total of 2ml
- Measure until there is no slope

Appendix 11

Crystal nucleation experiments on Bicalutamide – 440µM /175µM

Coat the plate

- Prepare 1 (w/w) % (w/w) PVP solution (360 kDa), stir for a couple of hours
- Filter with PTFE filter, 0,2µm
- Add 400µL to each well on the 96 microwell plate
- Leave for two hours
- Rinse ten times with tap-water
- Rinse 5 times with MilliQ water
- Put on a shaking table in a MilliQ water bath for a couple of hours
- Rinse 5 times with MilliQ water
- Dry the wells with nitrogen gas
- Dry the plate in vacuum over night
- Store upside down

Prepare the growth solution

- Add 17.84 mL MilliQ water to a 20ml vial
- Add 2000uL 0,21(w/w) % PVP (360 kDa), wash the tip five times
- Carefully add 160 µL 1.825mM Bicalutamide, turn twice
- Filter with a PTFE filter, 0.2µm
- ⇒ 14.6µM Bicalutamide, 0.021(w/w) % PVP 360kDa, 0.8(w/w) % DMSO

Nucleation experiment, nucleation at 440µM, growth at 175µm, to be performed on antivibration table

- Check the plate, using the microscope
- Add 193.1µL of growth solution to each well by use of a manual pipette
- Make supersaturated solutions, 440µM
  - 3968µL filtered MilliQ water in a 10ml vial
  - Carefully add 32µL, 55mM Bicalutamide, mix gently three times
  - Filter with a PTFE filter, 0.2µm, in to a 4ml vial
- t_{nuc}

- Transfer the solution to the plate
- Calmly pull up the supersaturated solution, 116.9μL, with a manual pipette
- Put the solution down into a well, against the wall, calm and decisive. Pull up from the bottom and down again against the wall
- 16 wells per nucleation time, 4 wells from each batch.
- Growth time, 72 hours (film+ cover + tinfoil)

  6 series/ plate $\Rightarrow$ 0 min (reference), 15min, 30 min, 45 min, 60 min och 75 min.

Harvest the nucleation experiment

- 72 hours after the nucleation was terminated
- Look at the wells by use of a light microscope, count the crystals and take photos of each well
- Evaluate using Sigma Plot and the Poisson distribution

Appendix 12

Crystal nucleation experiments on Linprazan – 30μM /18μM

Coat the plate

- Prepare 1 (w/w) % HPMC solution (6 cPs), stir for a couple of hours
- Filter with PTFE filter, 0,2μm
- Add 400μL to each well on the 96 microwell plate
- Leave for two hours
- Rinse ten times with tap-water
- Rinse 5 times with MilliQ water
- Put on a shaking table in a MilliQ water bath for a couple of hours
- Rinse 5 times with MilliQ water
- Dry the wells with nitrogen gas
- Dry the plate in vacuum over night
- Store upside down

Prepare the growth solution

- Add 19.22 mL 1μM NaOH to a 20ml vial
- Add 500uL, 4(w/w) % HPMC (6 cPs), wash the tip five times
- Carefully add 160 μL 0.20mM Linprazan, turn twice
- Filter with a PTFE filter, 0.2μm
- ⇒ 1.5μM Linaprazan, 0.1(w/w) % HPMC (6cPs), 0.8(w/w) % DMSO, 1μM NaOH

Nucleation experiment, nucleation at 30μM, growth at 18μm, to be performed on antivibration table

- Check the plate, using the microscope
- Add 130.5μL of growth solution to each well by use of a manual pipette
- Make supersaturated solutions, 30μM
  - 3968μL filtered 1μM NaOH in a 10ml vial
  - Carefully add 32μL, 4mM Linaprazan, mix gently three times
  - Filter with a PTFE filter, 0.2μm, in to a 4ml vial
- t_{nuc}

- Transfer the solution to the plate
- Calmly pull up the supersaturated solution, 179.5μL, with a manual pipette
- Put the solution down into a well, against the wall, calm and decisive. Pull up from the bottom and down again against the wall
- 16 wells per nucleation time, 4 wells from each batch.
- Growth time, 72 hours (film+ cover + tinfoil)
  6 series/ plate $\Rightarrow$ 0 min (reference), 1, 2, 4, 6 and 8 hours.

Harvest the nucleation experiment

- 72 hours after the nucleation was terminated
- Look at the wells by use of a light microscope, count the crystals and take photos of each well
- Evaluate using Sigma Plot and the Poisson distribution

Appendix 13

Result from the mastersizer measurement on Bicalutamide nanoparticles- after editing.

MASTERSIZER 2000

Result Analysis Report

Sample Name: A110504 Bic
SOP Name:
Measured: den 4 maj 2011 09:48:56
Sample Source & type:
Measured by: HP8765
Analysed: den 4 maj 2011 10:08:11
Sample bulk lot ref:
Result Source: Edited

Particle Name: Polystyrene latex
Accessory Name: Hydro 2000μP (A)
Analysis model: General purpose (spherical)
Sensitivity: Enhanced
Particle RI: 1.590
Absorption: 0
Size range: 0.020 to 2.201 um
Obscuration: 2.36 %
Dispersant Name: Water
Dispersant RI: 1.330
Weighted Residual: 1.961 %
Result Emulation: Off

Concentration: 0.0053 %Vol
Span : 1.482
Uniformity: 0.463
Result units: Volume
Specific Surface Area: 55.7 m²/g
Surface Weighted Mean D[3,2]: 0.103 um
Vol. Weighted Mean D[4,3]: 0.137 um

d(0.1): 0.062 um **d(0.5):** 0.120 um **d(0.9):** 0.240 um

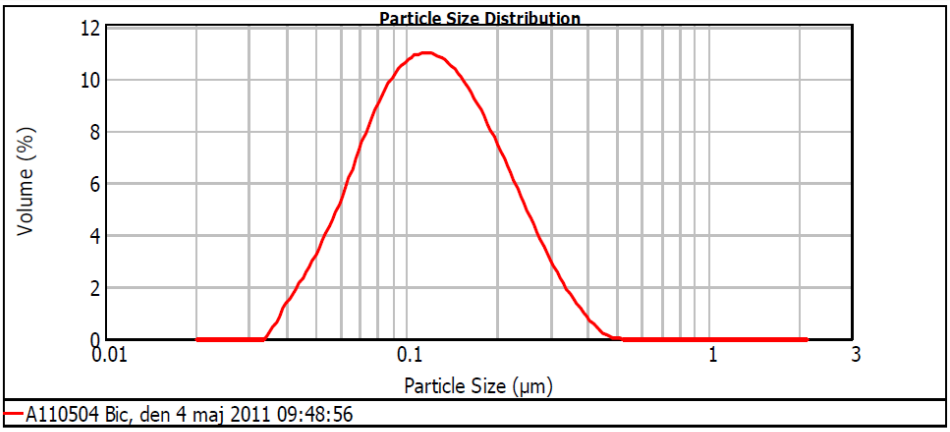

Size (μm)	Volume In %	Size (μm)	Volume In %	Size (μm)	Volume In %	Size (μm)	Volume In %	Size (μm)	Volume In %	Size (μm)	Volume In %
0.010	0.00	0.105	9.91	1.096	0.00	11.482	0.00	120.226	0.00	1258.925	0.00
0.011	0.00	0.120	9.79	1.259	0.00	13.183	0.00	138.038	0.00	1445.440	0.00
0.013	0.00	0.138	9.21	1.445	0.00	15.136	0.00	158.489	0.00	1659.587	0.00
0.015	0.00	0.158	8.25	1.660	0.00	17.378	0.00	181.970	0.00	1905.461	0.00
0.017	0.00	0.182	7.01	1.905	0.00	19.953	0.00	208.930	0.00	2187.762	0.00
0.020	0.00	0.209	5.63	2.188	0.00	22.909	0.00	239.883	0.00	2511.886	0.00
0.023	0.00	0.240	4.21	2.512	0.00	26.303	0.00	275.423	0.00	2884.032	0.00
0.026	0.00	0.275	2.90	2.884	0.00	30.200	0.00	316.228	0.00	3311.311	0.00
0.030	0.00	0.316	1.75	3.311	0.00	34.674	0.00	363.078	0.00	3801.894	0.00
0.035	0.00	0.363	0.86	3.802	0.00	39.811	0.00	416.869	0.00	4365.158	0.00
0.040	0.64	0.417	0.23	4.365	0.00	45.709	0.00	478.630	0.00	5011.872	0.00
0.046	1.68	0.479	0.00	5.012	0.00	52.481	0.00	549.541	0.00	5754.399	0.00
0.052	2.74	0.550	0.00	5.754	0.00	60.256	0.00	630.957	0.00	6606.934	0.00
0.060	4.06	0.631	0.00	6.607	0.00	69.183	0.00	724.436	0.00	7585.776	0.00
0.069	5.60	0.724	0.00	7.586	0.00	79.433	0.00	831.764	0.00	8709.636	0.00
0.079	7.31	0.832	0.00	8.710	0.00	91.201	0.00	954.993	0.00	10000.000	0.00
0.091	8.66	0.955	0.00	10.000	0.00	104.713	0.00	1096.478	0.00		
0.105	9.54	1.096	0.00	11.482	0.00	120.226	0.00	1258.925	0.00		

Operator notes: *0,1mM Bicalutamide sp m vatten före upplösningsexperiment*

Malvern Instruments Ltd.
Malvern, UK
Tel := +[44] (0) 1684-892456 Fax +[44] (0) 1684-892789

Mastersizer 2000 Ver. 5.60
Serial Number : MAL100079

File name: A110504
Record Number: 13
2011-08-17 13:39:20

Appendix 14

Result from Mastersizer measurement on Bicalutamide nanoparticles- before editing.

MASTERSIZER 2000

Result Analysis Report

Sample Name: A110504 Bic	**SOP Name:**	**Measured:** den 4 maj 2011 09:48:56	
Sample Source & type:	**Measured by:** HP8765	**Analysed:** den 4 maj 2011 09:48:59	
Sample bulk lot ref:	**Result Source:** Measurement		
Particle Name: Polystyrene latex	**Accessory Name:** Hydro 2000μP (A)	**Analysis model:** General purpose (spherical)	**Sensitivity:** Enhanced
Particle RI: 1.590	**Absorption:** 0	**Size range:** 0.020 to 2000.000 um	**Obscuration:** 2.36 %
Dispersant Name: Water	**Dispersant RI:** 1.330	**Weighted Residual:** 1.961 %	**Result Emulation:** Off
Concentration: 0.0053 %Vol	**Span :** 1.612	**Uniformity:** 4.67	**Result units:** Volume
Specific Surface Area: 54.1 m²/g	**Surface Weighted Mean D[3,2]:** 0.106 um	**Vol. Weighted Mean D[4,3]:** 0.654 um	

d(0.1): 0.062 um **d(0.5):** 0.122 um **d(0.9):** 0.260 um

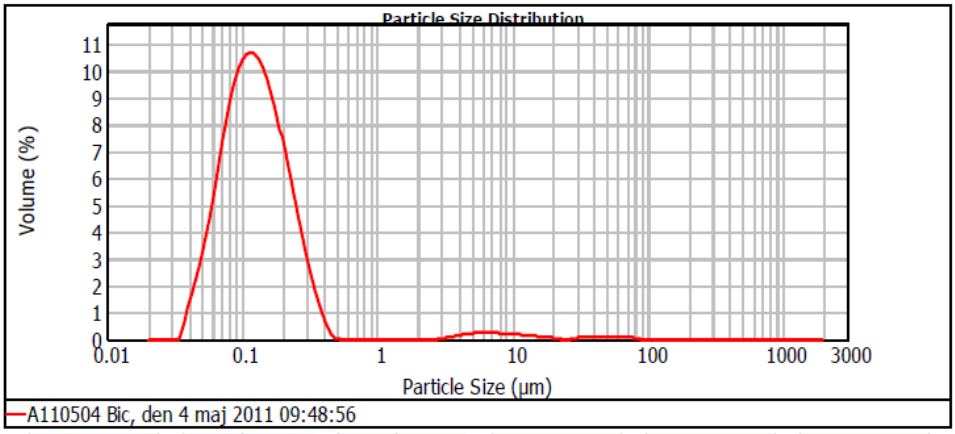

Size (μm)	Volume In %	Size (μm)	Volume In %	Size (μm)	Volume In %	Size (μm)	Volume In %	Size (μm)	Volume In %	Size (μm)	Volume In %
0.010	0.00	0.105	9.63	1.096	0.00	11.482	0.15	120.226	0.00	1258.925	0.00
0.011	0.00	0.120	9.51	1.259	0.00	13.183	0.12	138.038	0.00	1445.440	0.00
0.013	0.00	0.138	8.95	1.445	0.00	15.136	0.09	158.489	0.00	1659.587	0.00
0.015	0.00	0.158	8.02	1.660	0.00	17.378	0.08	181.970	0.00	1905.461	0.00
0.017	0.00	0.182	6.81	1.905	0.00	19.953	0.02	208.930	0.00	2187.762	0.00
0.020	0.00	0.209	5.47	2.188	0.00	22.909	0.00	239.883	0.00	2511.886	0.00
0.023	0.00	0.240	4.09	2.512	0.00	26.303	0.02	275.423	0.00	2884.032	0.00
0.026	0.00	0.275	2.81	2.884	0.04	30.200	0.08	316.228	0.00	3311.311	0.00
0.030	0.00	0.316	1.70	3.311	0.10	34.674	0.08	363.078	0.00	3801.894	0.00
0.035	0.00	0.363	0.84	3.802	0.15	39.811	0.10	416.869	0.00	4365.158	0.00
0.040	0.63	0.417	0.22	4.365	0.19	45.709	0.10	478.630	0.00	5011.872	0.00
0.046	1.63	0.479	0.00	5.012	0.22	52.481	0.10	549.541	0.00	5754.399	0.00
0.052	2.67	0.550	0.00	5.754	0.23	60.256	0.09	630.957	0.00	6606.934	0.00
0.060	3.94	0.631	0.00	6.607	0.22	69.183	0.07	724.436	0.00	7585.776	0.00
0.069	5.44	0.724	0.00	7.586	0.21	79.433	0.01	831.764	0.00	8709.636	0.00
0.079	7.10	0.832	0.00	8.710	0.19	91.201	0.00	954.993	0.00	10000.000	0.00
0.091	8.42	0.955	0.00	10.000	0.17	104.713	0.00	1096.478	0.00		
0.105	9.27	1.096	0.00	11.482		120.226	0.00	1258.925	0.00		

Operator notes: *0,1mM Bicalutamide sp m vatten före upplösningsexperiment*

Malvern Instruments Ltd.
Malvern, UK
Tel := +[44] (0) 1684-892456 Fax +[44] (0) 1684-892789

Mastersizer 2000 Ver. 5.60
Serial Number : MAL100079

File name: A110504
Record Number: 1
2011-08-17 13:38:20

Appendix 15

Result from the mastersizer measurement on Linaprazan nanoparticles- after editing.

MASTERSIZER 2000

Result Analysis Report

Sample Name: A110504 Linaprazan	**SOP Name:**	**Measured:** den 4 maj 2011 15:38:35	
Sample Source & type:	**Measured by:** HP8765	**Analysed:** den 4 maj 2011 15:51:21	
Sample bulk lot ref:	**Result Source:** Edited		
Particle Name: Polystyrene latex	**Accessory Name:** Hydro 2000µP (A)	**Analysis model:** General purpose (spherical)	**Sensitivity:** Enhanced
Particle RI: 1.590	**Absorption:** 0	**Size range:** 0.020 to 0.763 um	**Obscuration:** 2.10 %
Dispersant Name: Water	**Dispersant RI:** 1.330	**Weighted Residual:** 1.898 %	**Result Emulation:** Off
Concentration: 0.0034 %Vol	**Span :** 1.675	**Uniformity:** 0.52	**Result units:** Volume
Specific Surface Area: 51.3 m²/g	**Surface Weighted Mean D[3,2]:** 0.111 um	**Vol. Weighted Mean D[4,3]:** 0.156 um	

d(0.1): 0.065 um **d(0.5):** 0.132 um **d(0.9):** 0.286 um

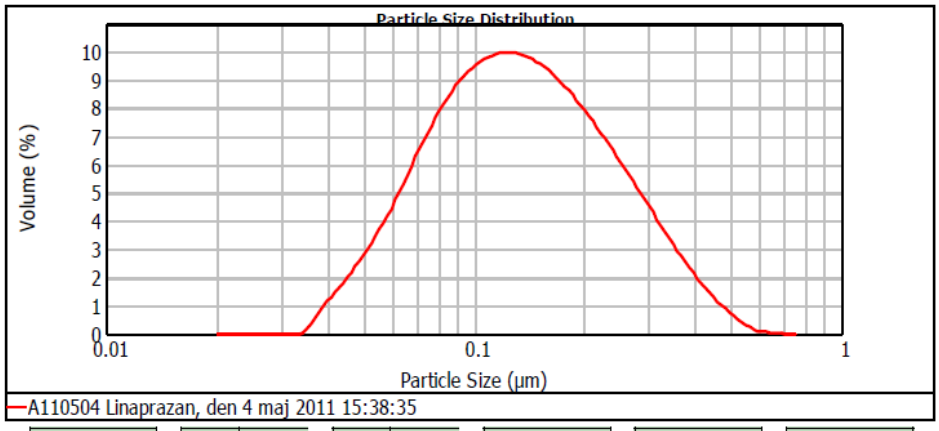

Size (µm)	Volume In %	Size (µm)	Volume In %	Size (µm)	Volume In %	Size (µm)	Volume In %	Size (µm)	Volume In %	Size (µm)	Volume In %
0.010	0.00	0.105	8.92	1.096	0.00	11.482	0.00	120.226	0.00	1258.925	0.00
0.011	0.00	0.120	9.00	1.259	0.00	13.183	0.00	138.038	0.00	1445.440	0.00
0.013	0.00	0.138	8.72	1.445	0.00	15.136	0.00	158.489	0.00	1659.587	0.00
0.015	0.00	0.158	8.14	1.660	0.00	17.378	0.00	181.970	0.00	1905.461	0.00
0.017	0.00	0.182	7.33	1.905	0.00	19.953	0.00	208.930	0.00	2187.762	0.00
0.020	0.00	0.209	6.37	2.188	0.00	22.909	0.00	239.883	0.00	2511.886	0.00
0.023	0.00	0.240	5.31	2.512	0.00	26.303	0.00	275.423	0.00	2884.032	0.00
0.026	0.00	0.275	4.20	2.884	0.00	30.200	0.00	316.228	0.00	3311.311	0.00
0.030	0.00	0.316	3.09	3.311	0.00	34.674	0.00	363.078	0.00	3801.894	0.00
0.035	0.00	0.363	2.07	3.802	0.00	39.811	0.00	416.869	0.00	4365.158	0.00
0.040	0.50	0.417	1.19	4.365	0.00	45.709	0.00	478.630	0.00	5011.872	0.00
0.046	1.43	0.479	0.56	5.012	0.00	52.481	0.00	549.541	0.00	5754.399	0.00
0.052	2.35	0.550	0.10	5.754	0.00	60.256	0.00	630.957	0.00	6606.934	0.00
0.060	3.49	0.631	0.01	6.607	0.00	69.183	0.00	724.436	0.00	7585.776	0.00
0.069	4.83	0.724	0.00	7.586	0.00	79.433	0.00	831.764	0.00	8709.636	0.00
0.079	6.34	0.832	0.00	8.710	0.00	91.201	0.00	954.993	0.00	10000.000	0.00
0.091	7.59	0.955	0.00	10.000	0.00	104.713	0.00	1096.478	0.00		
0.105	8.45	1.096	0.00	11.482	0.00	120.226	0.00	1258.925	0.00		

Operator notes: *0,1mM Linaprazan, malda partiklar, spädda med 0,1uM NaOH*

Malvern Instruments Ltd.
Malvern, UK
Tel := +[44] (0) 1684-892456 Fax +[44] (0) 1684-892789

Mastersizer 2000 Ver. 5.60
Serial Number : MAL100079

File name: A110504_L
Record Number: 9
2011-08-17 13:51:06

Appendix 16

Result from the mastersizer measurement on Linaprazan nanoparticles- before editing.

MASTERSIZER 2000

Result Analysis Report

Sample Name: A110504 Linaprazan - Average	**SOP Name:**	**Measured:** den 4 maj 2011 15:38:35	
Sample Source & type:	**Measured by:** HP8765	**Analysed:** den 4 maj 2011 15:38:37	
Sample bulk lot ref:	**Result Source:** Averaged		
Particle Name: Polystyrene latex	**Accessory Name:** Hydro 2000μP (A)	**Analysis model:** General purpose (spherical)	**Sensitivity:** Enhanced
Particle RI: 1.590	**Absorption:** 0	**Size range:** 0.020 to 2000.000 um	**Obscuration:** 2.09 %
Dispersant Name: Water	**Dispersant RI:** 1.330	**Weighted Residual:** 1.923 %	**Result Emulation:** Off
Concentration: 0.0033 %Vol	**Span :** 1.799	**Uniformity:** 1.76	**Result units:** Volume
Specific Surface Area: 49.2 m²/g	**Surface Weighted Mean D[3,2]:** 0.116 um	**Vol. Weighted Mean D[4,3]:** 0.331 um	

d(0.1): 0.066 um **d(0.5):** 0.137 um **d(0.9):** 0.313 um

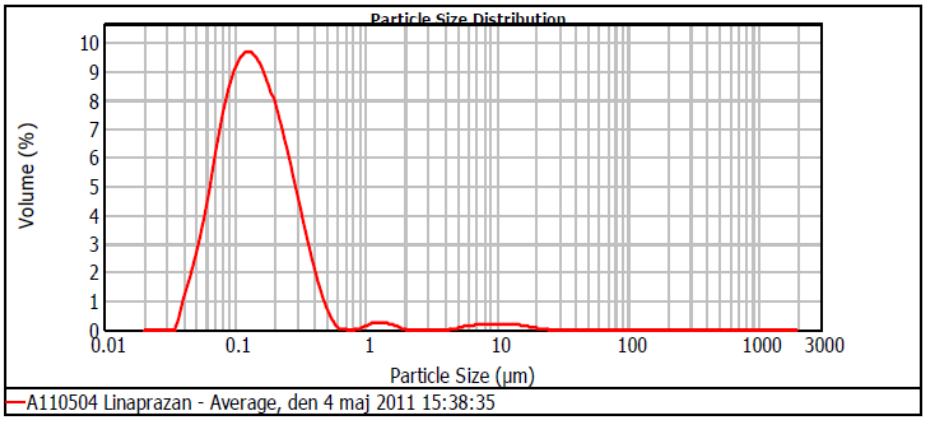

Size (μm)	Volume In %	Size (μm)	Volume In %	Size (μm)	Volume In %	Size (μm)	Volume In %	Size (μm)	Volume In %	Size (μm)	Volume In %
0.010	0.00	0.105	8.61	1.096	0.22	11.482	0.18	120.226	0.00	1258.925	0.00
0.011	0.00	0.120	8.75	1.259	0.22	13.183	0.15	138.038	0.00	1445.440	0.00
0.013	0.00	0.138	8.54	1.445	0.17	15.136	0.13	158.489	0.00	1659.587	0.00
0.015	0.00	0.158	8.03	1.660	0.10	17.378	0.08	181.970	0.00	1905.461	0.00
0.017	0.00	0.182	7.29	1.905	0.00	19.953	0.04	208.930	0.00	2187.762	0.00
0.020	0.00	0.209	6.38	2.188	0.00	22.909	0.01	239.883	0.00	2511.886	0.00
0.023	0.00	0.240	5.36	2.512	0.00	26.303	0.00	275.423	0.00	2884.032	0.00
0.026	0.00	0.275	4.29	2.884	0.00	30.200	0.00	316.228	0.00	3311.311	0.00
0.030	0.00	0.316	3.18	3.311	0.00	34.674	0.00	363.078	0.00	3801.894	0.00
0.035	0.40	0.363	2.15	3.802	0.00	39.811	0.00	416.869	0.00	4365.158	0.00
0.040	1.33	0.417	1.25	4.365	0.02	45.709	0.00	478.630	0.00	5011.872	0.00
0.046	2.20	0.479	0.58	5.012	0.08	52.481	0.00	549.541	0.00	5754.399	0.00
0.052	3.27	0.550	0.13	5.754	0.12	60.256	0.00	630.957	0.00	6606.934	0.00
0.060	4.54	0.631	0.00	6.607	0.15	69.183	0.00	724.436	0.00	7585.776	0.00
0.069	6.00	0.724	0.00	7.586	0.17	79.433	0.00	831.764	0.00	8709.636	0.00
0.079	7.22	0.832	0.03	8.710	0.18	91.201	0.00	954.993	0.00	10000.000	
0.091	8.10	0.955	0.14	10.000	0.18	104.713	0.00	1096.478	0.00		
0.105		1.096		11.482		120.226		1258.925			

Operator notes: *0,1mM Linaprazan, malda partiklar, spädda med 0,1uM NaOH*

Malvern Instruments Ltd.
Malvern, UK
Tel := +[44] (0) 1684-892456 Fax +[44] (0) 1684-892789

Mastersizer 2000 Ver. 5.60
Serial Number : MAL100079

File name: A110504_L
Record Number: 4
2011-08-17 13:50:06

Appendix 17

Result from the mastersizer measurement on Felodipine nanoparticles- after editing.

MASTERSIZER 2000

Result Analysis Report

Sample Name: 125uM Felo	**SOP Name:**	**Measured:** den 15 juni 2011 11:41:40	
Sample Source & type:	**Measured by:** HP8765	**Analysed:** den 1 juli 2011 08:11:00	
Sample bulk lot ref:	**Result Source:** Edited		
Particle Name: Polystyrene latex	**Accessory Name:** Hydro 2000μP (A)	**Analysis model:** General purpose (spherical)	**Sensitivity:** Enhanced
Particle RI: 1.590	**Absorption:** 0	**Size range:** 0.020 to 0.887 um	**Obscuration:** 3.82 %
Dispersant Name: Water	**Dispersant RI:** 1.330	**Weighted Residual:** 1.386 %	**Result Emulation:** Off
Concentration: 0.0045 %Vol	**Span :** 1.876	**Uniformity:** 0.604	**Result units:** Volume
Specific Surface Area: 47.2 m²/g	**Surface Weighted Mean D[3,2]:** 0.121 um	**Vol. Weighted Mean D[4,3]:** 0.181 um	

d(0.1): 0.068 um **d(0.5):** 0.144 um **d(0.9):** 0.338 um

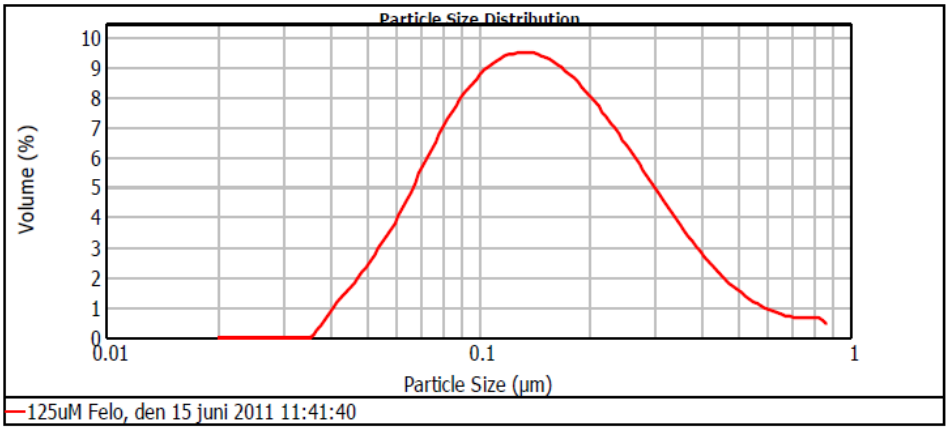

Size (μm)	Volume In %	Size (μm)	Volume In %	Size (μm)	Volume In %	Size (μm)	Volume In %	Size (μm)	Volume In %	Size (μm)	Volume In %
0.010	0.00	0.105	8.32	1.096	0.00	11.482	0.00	120.226	0.00	1258.925	0.00
0.011	0.00	0.120	8.57	1.259	0.00	13.183	0.00	138.038	0.00	1445.440	0.00
0.013	0.00	0.138	8.48	1.445	0.00	15.136	0.00	158.489	0.00	1659.587	0.00
0.015	0.00	0.158	8.07	1.660	0.00	17.378	0.00	181.970	0.00	1905.461	0.00
0.017	0.00	0.182	7.40	1.905	0.00	19.953	0.00	208.930	0.00	2187.762	0.00
0.020	0.00	0.209	6.56	2.188	0.00	22.909	0.00	239.883	0.00	2511.886	0.00
0.023	0.00	0.240	5.60	2.512	0.00	26.303	0.00	275.423	0.00	2884.032	0.00
0.026	0.00	0.275	4.59	2.884	0.00	30.200	0.00	316.228	0.00	3311.311	0.00
0.030	0.00	0.316	3.59	3.311	0.00	34.674	0.00	363.078	0.00	3801.894	0.00
0.035	0.23	0.363	2.68	3.802	0.00	39.811	0.00	416.869	0.00	4365.158	0.00
0.040	1.18	0.417	1.90	4.365	0.00	45.709	0.00	478.630	0.00	5011.872	0.00
0.046	1.97	0.479	1.30	5.012	0.00	52.481	0.00	549.541	0.00	5754.399	0.00
0.052	2.96	0.550	0.88	5.754	0.00	60.256	0.00	630.957	0.00	6606.934	0.00
0.060	4.15	0.631	0.65	6.607	0.00	69.183	0.00	724.436	0.00	7585.776	0.00
0.069	5.56	0.724	0.57	7.586	0.00	79.433	0.00	831.764	0.00	8709.636	0.00
0.079	6.79	0.832	0.27	8.710	0.00	91.201	0.00	954.993	0.00	10000.000	
0.091	7.72	0.955	0.00	10.000	0.00	104.713	0.00	1096.478	0.00		
0.105		1.096		11.482		120.226		1258.925			

Operator notes: *125uM felo, ulkade 110516*

Malvern Instruments Ltd.
Malvern, UK
Tel := +[44] (0) 1684-892456 Fax +[44] (0) 1684-892789

Mastersizer 2000 Ver. 5.60
Serial Number : MAL100079

File name: A110615_F
Record Number: 11
2011-08-17 13:55:59

Appendix 18

Result from the mastersizer measurement on Felodipine nanoparticles- before editing.

MASTERSIZER 2000

Result Analysis Report

Sample Name: 125uM Felo	**SOP Name:**	**Measured:** den 15 juni 2011 11:41:40	
Sample Source & type:	**Measured by:** HP8765	**Analysed:** den 15 juni 2011 11:41:42	
Sample bulk lot ref:	**Result Source:** Measurement		
Particle Name: Polystyrene latex	**Accessory Name:** Hydro 2000μP (A)	**Analysis model:** General purpose (spherical)	**Sensitivity:** Enhanced
Particle RI: 1.590	**Absorption:** 0	**Size range:** 0.020 to 2000.000 um	**Obscuration:** 3.82 %
Dispersant Name: Water	**Dispersant RI:** 1.330	**Weighted Residual:** 1.386 %	**Result Emulation:** Off
Concentration: 0.0045 %Vol	**Span :** 16.407	**Uniformity:** 5.71	**Result units:** Volume
Specific Surface Area: 41.1 m²/g	**Surface Weighted Mean D[3,2]:** 0.139 um	**Vol. Weighted Mean D[4,3]:** 1.036 um	

d(0.1): 0.071 um **d(0.5):** 0.163 um **d(0.9):** 2.753 um

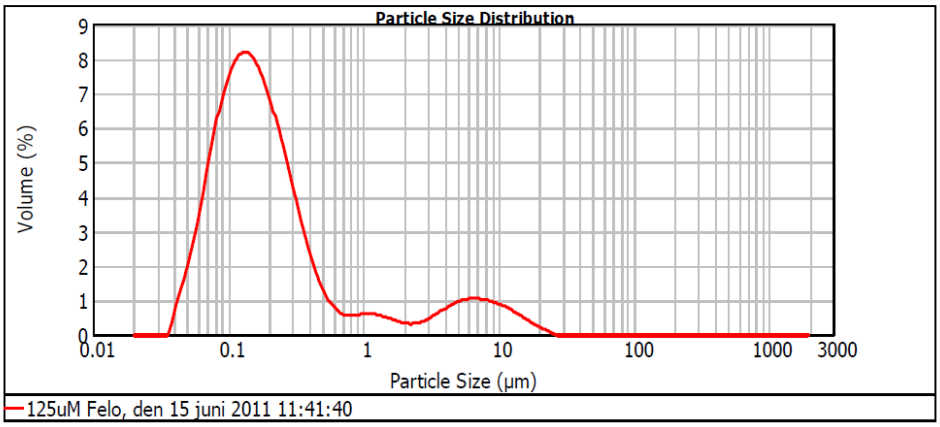

Size (μm)	Volume In %	Size (μm)	Volume In %	Size (μm)	Volume In %	Size (μm)	Volume In %	Size (μm)	Volume In %	Size (μm)	Volume In %
0.010	0.00	0.105	7.20	1.096	0.55	11.482	0.65	120.226	0.00	1258.925	0.00
0.011	0.00	0.120	7.42	1.259	0.50	13.183	0.52	138.038	0.00	1445.440	0.00
0.013	0.00	0.138	7.34	1.445	0.42	15.136	0.39	158.489	0.00	1659.587	0.00
0.015	0.00	0.158	6.98	1.660	0.35	17.378	0.27	181.970	0.00	1905.461	0.00
0.017	0.00	0.182	6.41	1.905	0.30	19.953	0.16	208.930	0.00	2187.762	0.00
0.020	0.00	0.209	5.68	2.188	0.29	22.909	0.06	239.883	0.00	2511.886	0.00
0.023	0.00	0.240	4.84	2.512	0.33	26.303	0.00	275.423	0.00	2884.032	0.00
0.026	0.00	0.275	3.97	2.884	0.43	30.200	0.00	316.228	0.00	3311.311	0.00
0.030	0.00	0.316	3.11	3.311	0.56	34.674	0.00	363.078	0.00	3801.894	0.00
0.035	0.20	0.363	2.32	3.802	0.70	39.811	0.00	416.869	0.00	4365.158	0.00
0.040	1.02	0.417	1.65	4.365	0.82	45.709	0.00	478.630	0.00	5011.872	0.00
0.046	1.71	0.479	1.13	5.012	0.91	52.481	0.00	549.541	0.00	5754.399	0.00
0.052	2.56	0.550	0.76	5.754	0.94	60.256	0.00	630.957	0.00	6606.934	0.00
0.060	3.59	0.631	0.56	6.607	0.94	69.183	0.00	724.436	0.00	7585.776	0.00
0.069	4.81	0.724	0.49	7.586	0.91	79.433	0.00	831.764	0.00	8709.636	0.00
0.079	5.87	0.832	0.51	8.710	0.85	91.201	0.00	954.993	0.00	10000.000	
0.091	6.68	0.955	0.56	10.000	0.76	104.713	0.00	1096.478	0.00		
0.105		1.096		11.482		120.226		1258.925			

Operator notes: *125uM felo, ulkade 110516*

Malvern Instruments Ltd.
Malvern, UK
Tel := +[44] (0) 1684-892456 Fax +[44] (0) 1684-892789

Mastersizer 2000 Ver. 5.60
Serial Number : MAL100079

File name: A110615_F
Record Number: 6
2011-08-17 13:55:08

Appendix 19

Original data received from excitation scan on Linaprazan crystals and supersaturated solutions. The intensity of crystals (black) and supersaturated solution of the same concentration is displayed below.

The lines are in the correct concentration order, from above; 20, 10, 5µM crystals. The supersaturated solutions have the same concentrations and the intensity is very low for all of them. The emission was measured at 378nm.

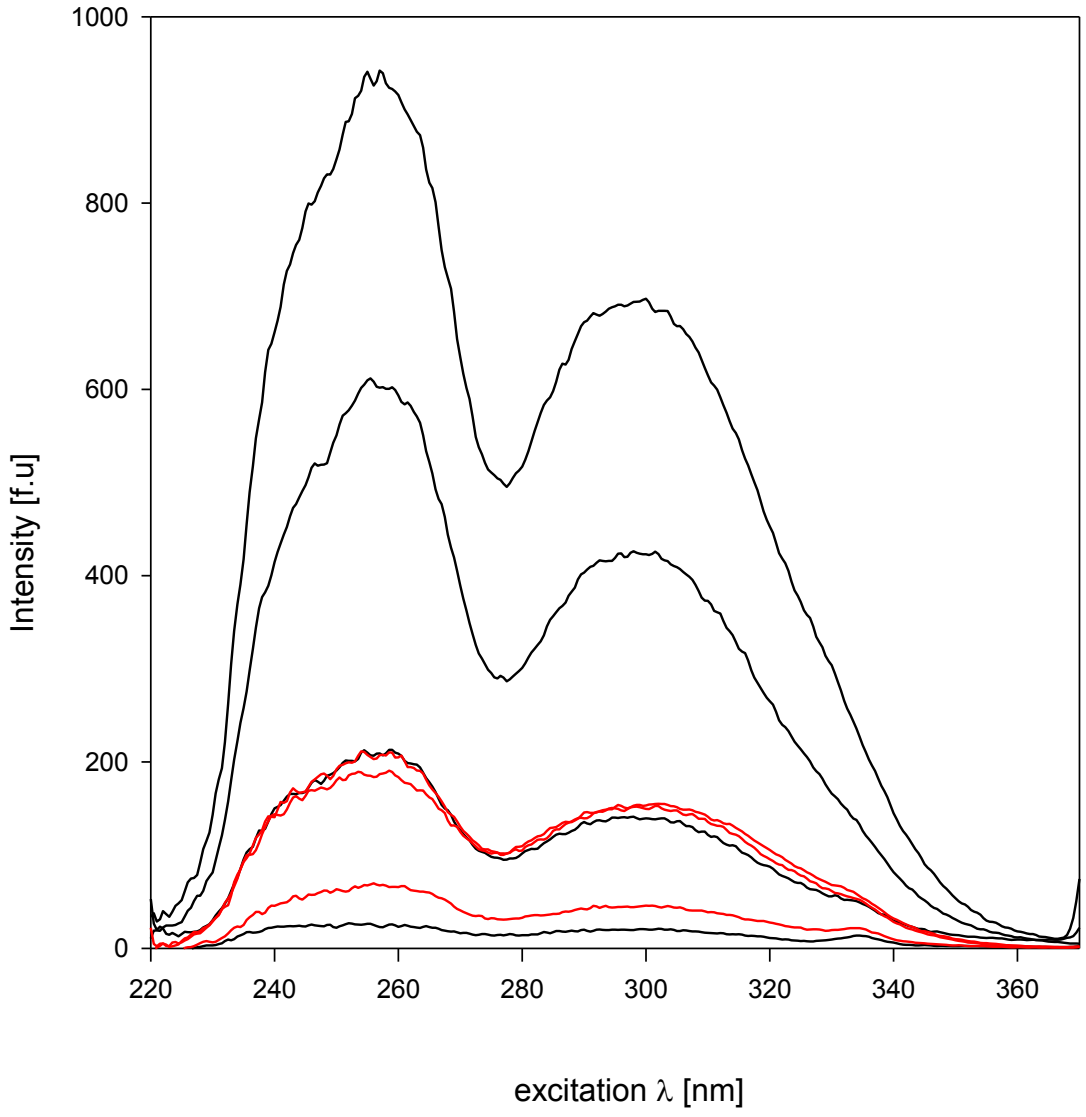

Appendix 20

Results from the comparison between the crystal dissolution experiments on Bicalutamide and classic nucleation theory. The mean value is displayed along with the standard error of the mean. The solid lines are the simulated curves. Note the difference in scale of the y-axis.

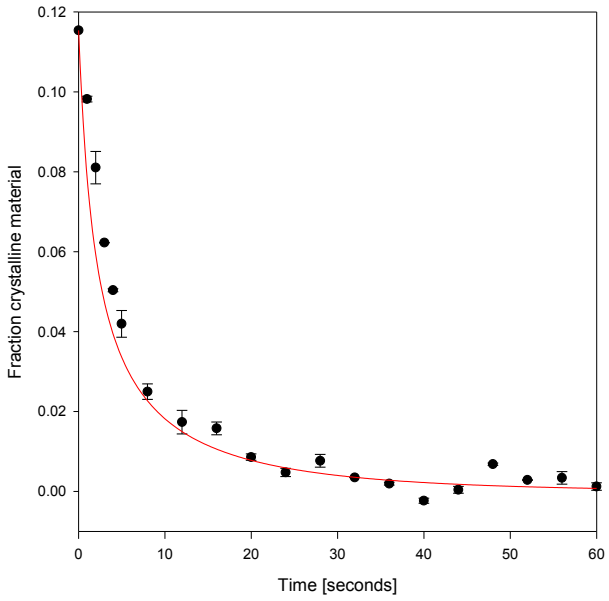

a)

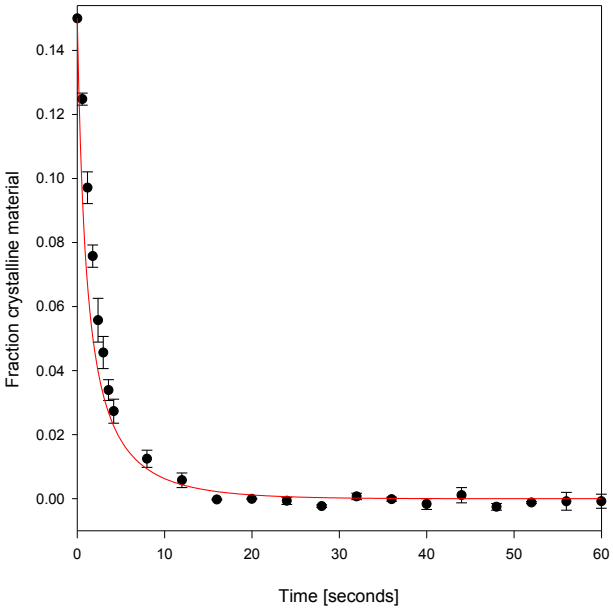

b)

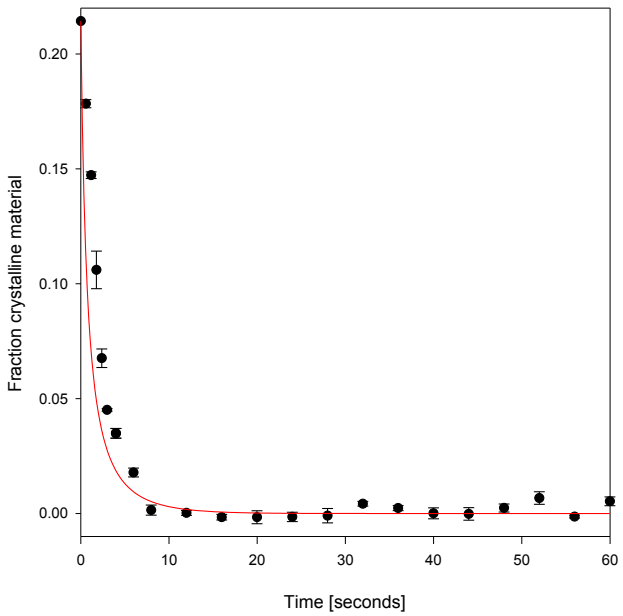

c)

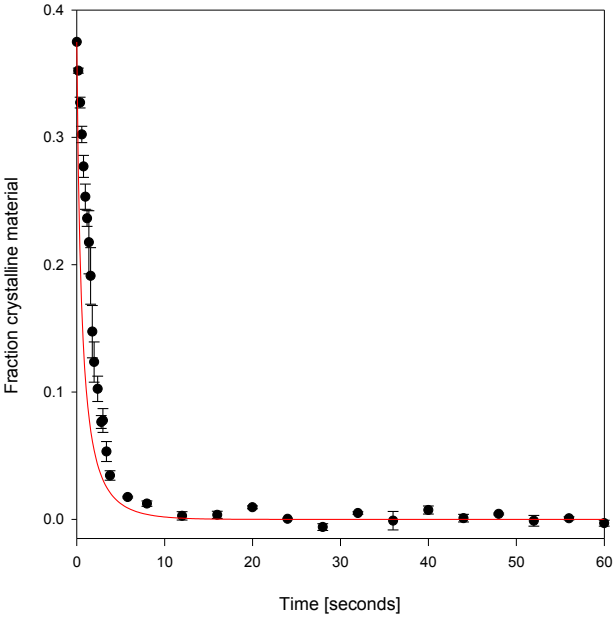

d)

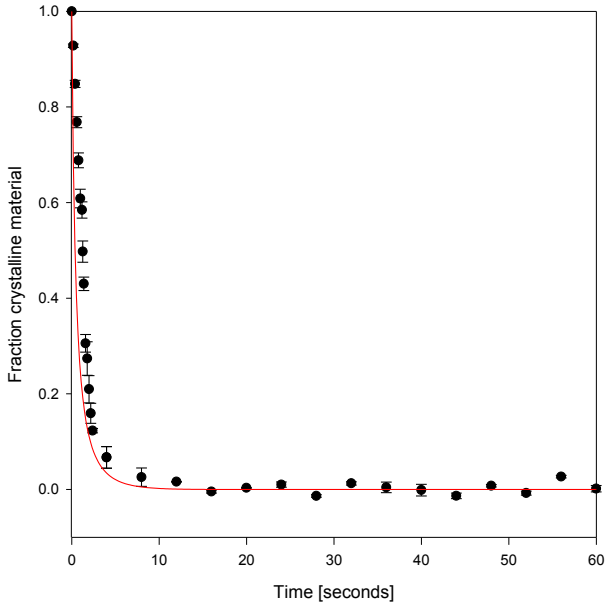

e)

a) 11.5μM Bicalutamide in the solution and 1.5μM initial crystals, λ=0μm
b) 8.5μM Bicalutamide in the solution and 1.5μM initial crystals, λ=0μm
c) 5.5μM Bicalutamide in the solution and 1.5μM initial crystals, λ=0μm
d) 2.5μM Bicalutamide in the solution and 1.5μM initial crystals, λ=0μm
e) 0μM Bicalutamide in the solution and 1.5μM initial crystals, λ=0μm

Appendix 21

Results from the comparison between the crystal dissolution experiments on Linaprazan and classic nucleation theory. The mean value is displayed along with the standard error of the mean. The solid lines are the simulated curves, red λ=0μm, blue λ=0.2μm. Note the difference in scale of the y-axis.

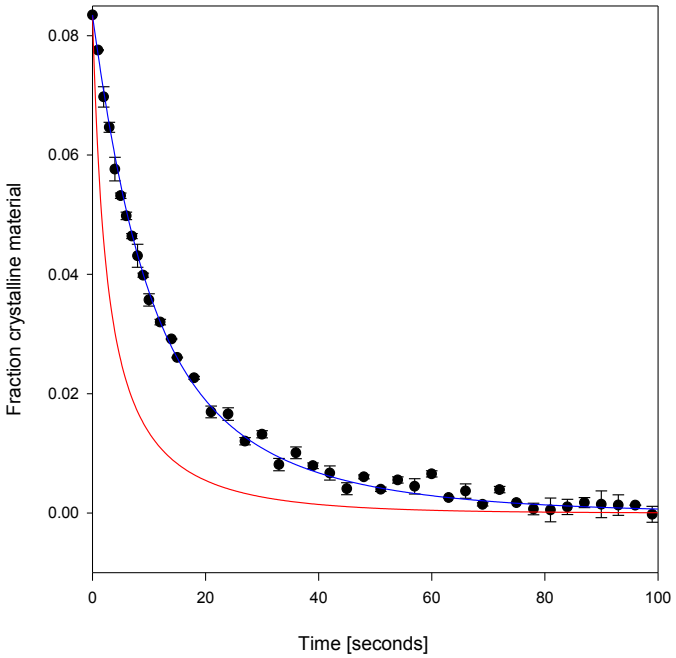

a)

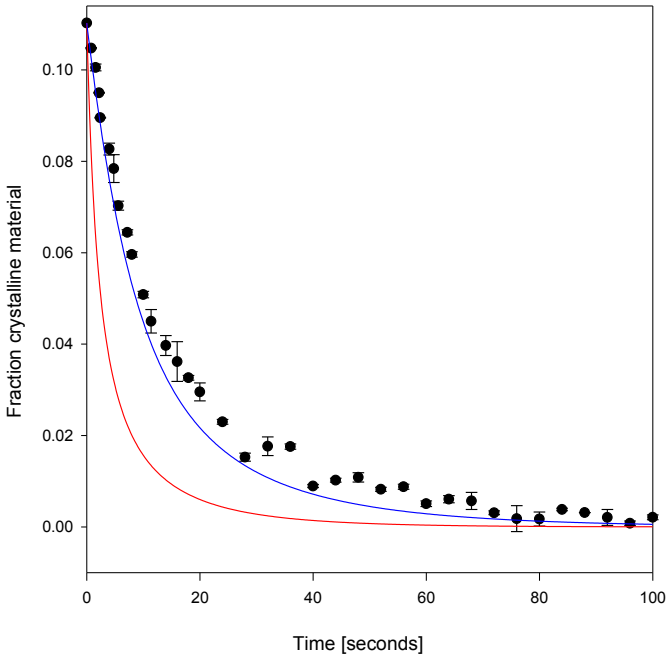

b)

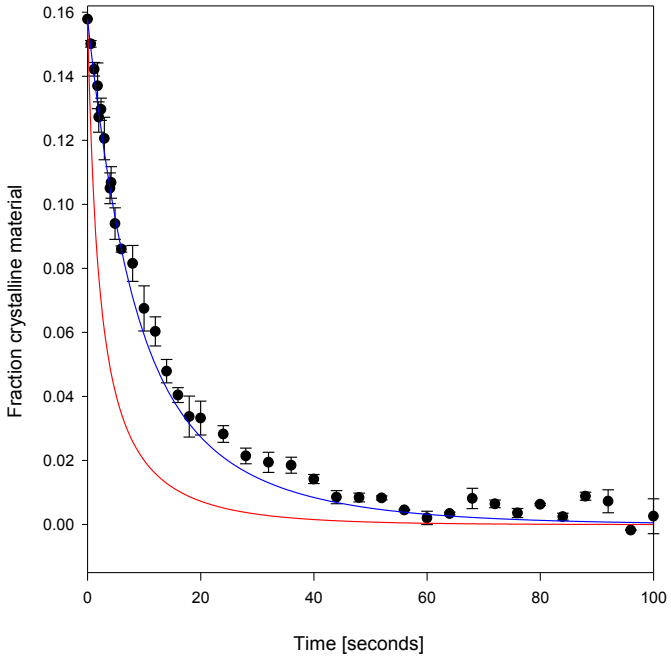

c)

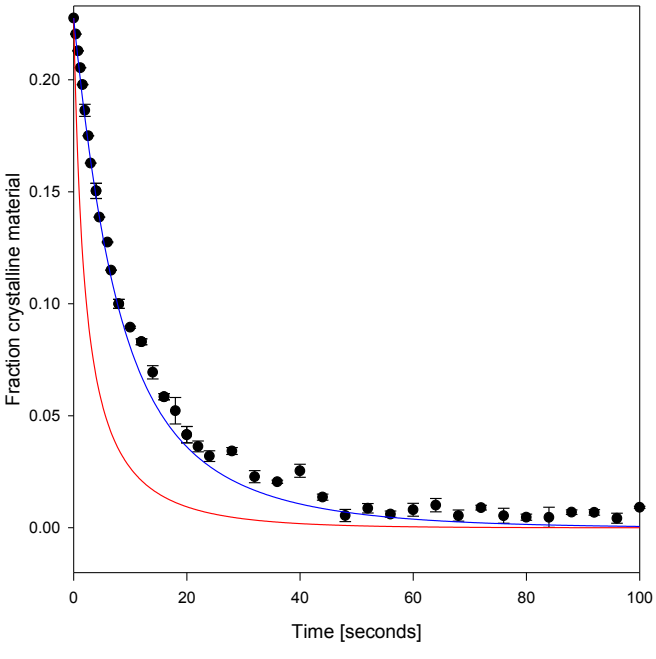

d)

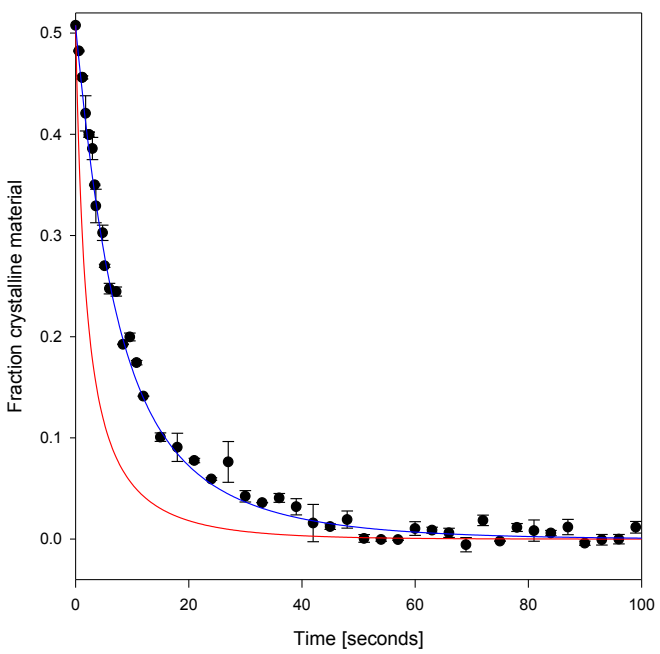

e)

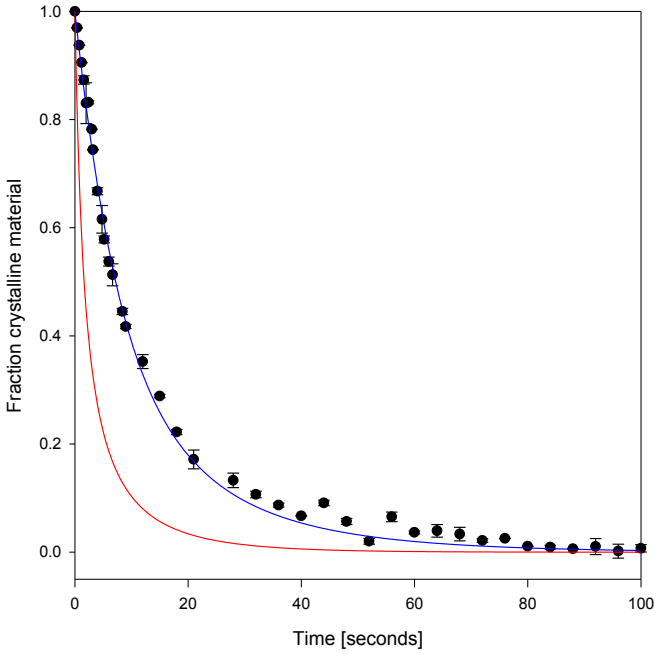

f)

a) 1.15µM Linaprazan in the solution and 0.15µM initial crystals, λ=0µm
b) 0.85µM Linaprazan in the solution and 0.15µM initial crystals, λ=0µm
c) 0.55µM Linaprazan in the solution and 0.15µM initial crystals, λ=0µm
d) 0.35µM Linaprazan in the solution and 0.15µM initial crystals, λ= µm
e) 0.1µM Linaprazan in the solution and 0.15µM initial crystals, λ=0µm
f) 0µM Linaprazan in the solution and 0.15µM initial crystals, λ=0µm

Appendix 22

Results from the comparison between the crystal dissolution experiments on Linaprazan and classic nucleation theory. The mean value is displayed along with the standard error of the mean. The solid lines are the simulated curves. Note the difference in scale of the x and y-axis.

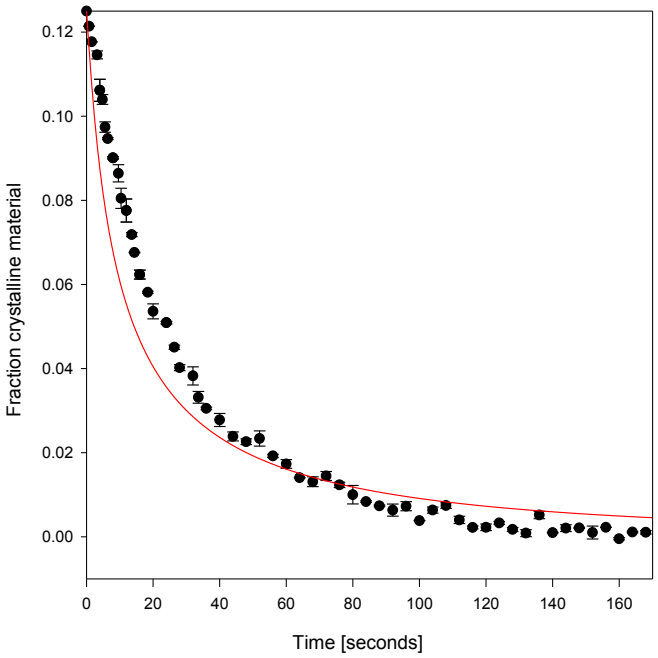

a)

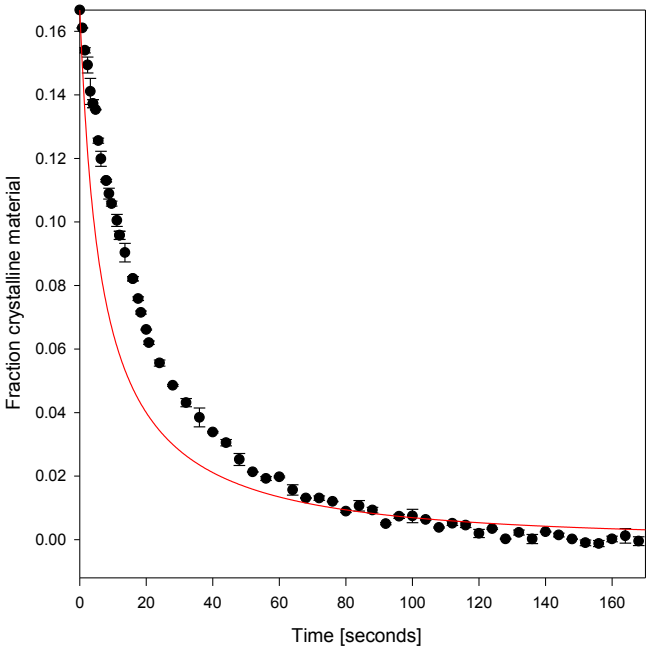

b)

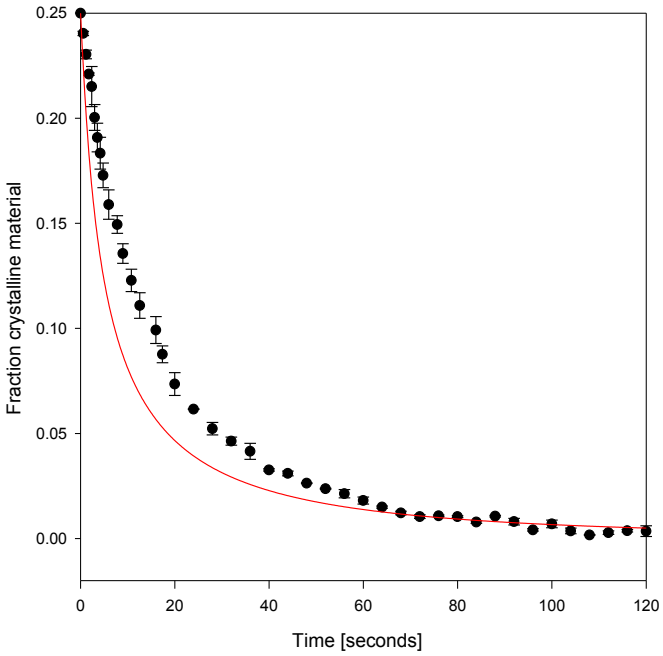

b)

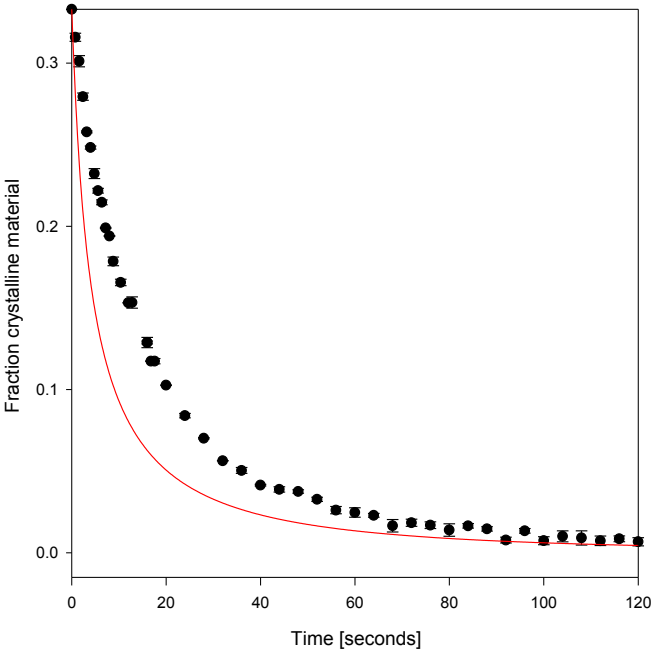

d)

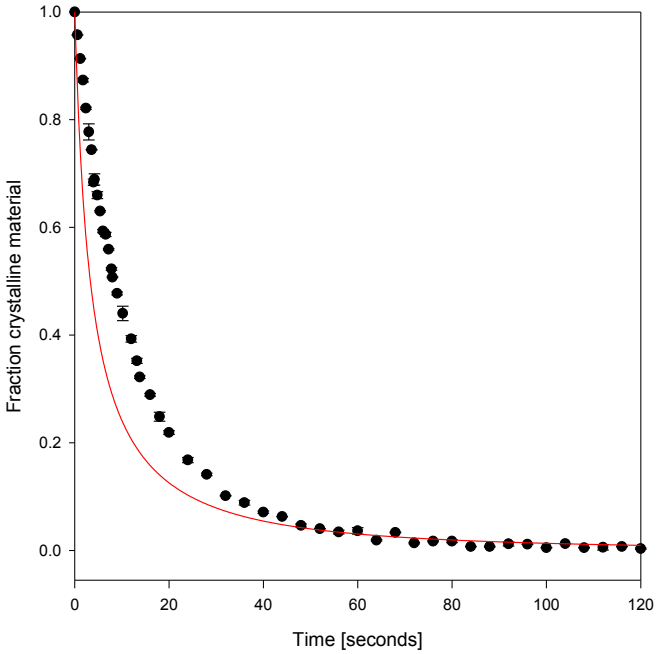

e)

a) 1.6μM Felodipine in the solution and 0.2μM initial crystals, λ=0μm
b) 1.2μM Felodipine in the solution and 0.2μM initial crystals, λ=0μm
c) 0.8μM Felodipine in the solution and 0.2μM initial crystals, λ=0μm
d) 0.4μM Felodipine in the solution and 0.2μM initial crystals, λ=0μm
e) 0μM Felodipine in the solution and 0.2μM initial crystals, λ=0μm

Appendix 23

Results from the comparison between the crystal growth experiments on Bicalutamide and classic nucleation theory. The mean value is displayed along with the standard error of the mean. The solid lines are the simulated curves.

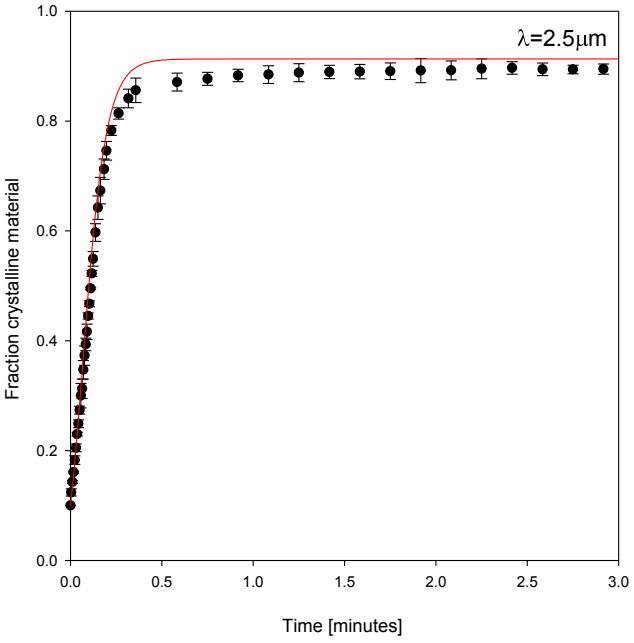

a)

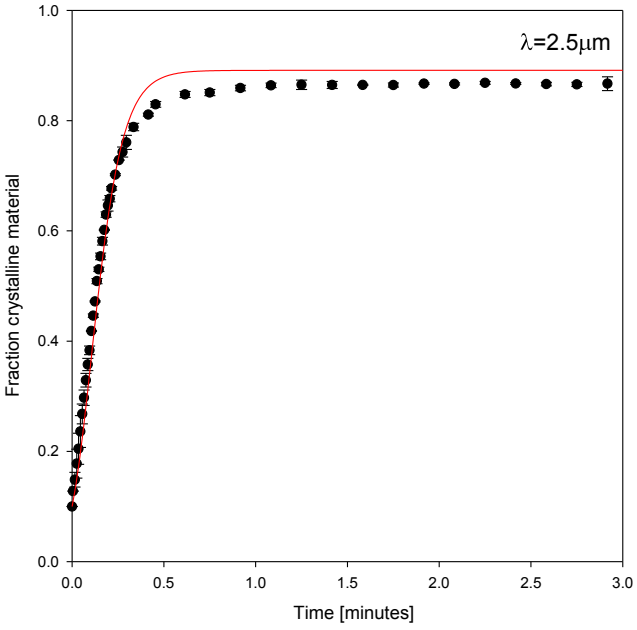

b)

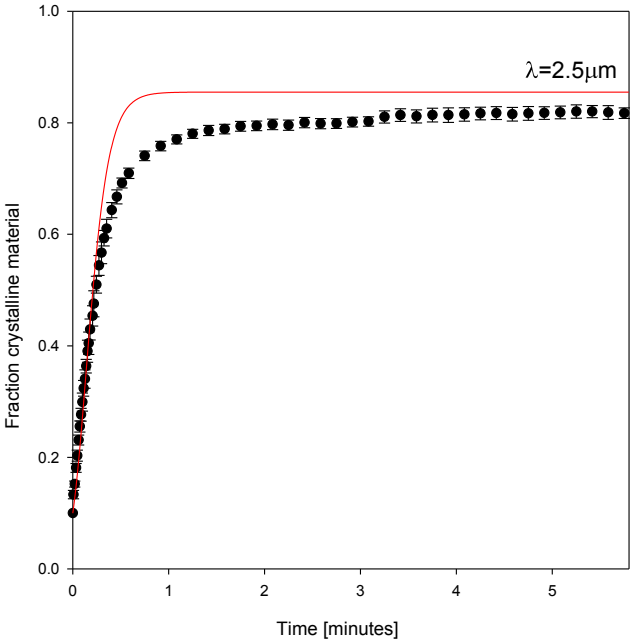

c)

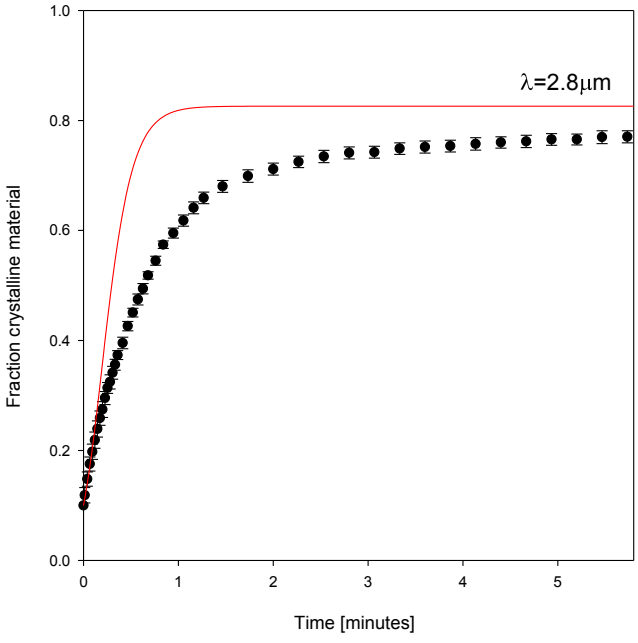

d)

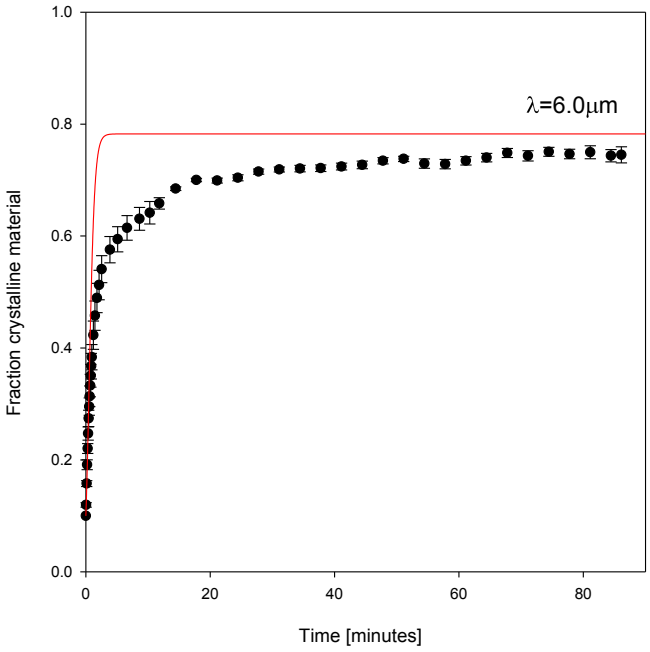

e)

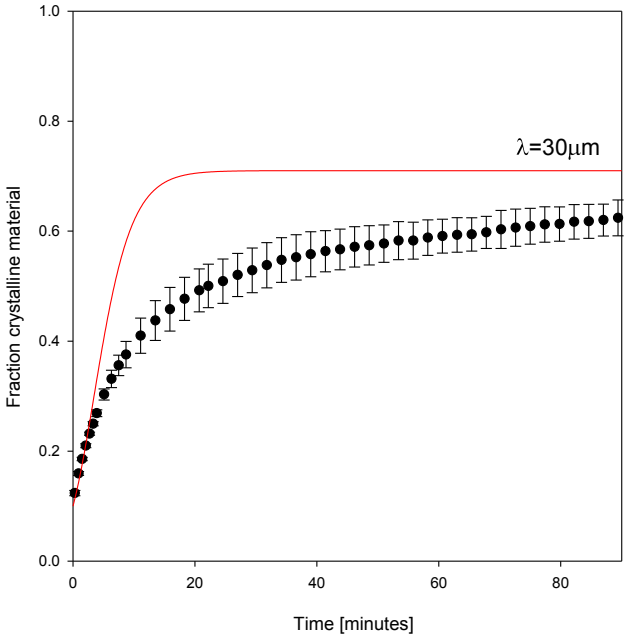

f)

a) 150μM supersaturated solution with 10% initial crystalline material, λ=2.5μm

b) 120μM supersaturated solution with 10% initial crystalline material, λ=2.5μm

c) 90 μM supersaturated solution with 10% initial crystalline material, λ=2.5μm

d) 75μM supersaturated solution with 10% initial crystalline material, λ=2.5μm

e) 60μM supersaturated solution with 10% initial crystalline material, λ=6μm

f) 45μM supersaturated solution with 10% initial crystalline material, λ=30μm.

Appendix 24

Results from the comparison between the crystal growth experiments on Linaprazan and classic nucleation theory. The mean value is displayed along with the standard error of the mean. The solid lines are the simulated curves.

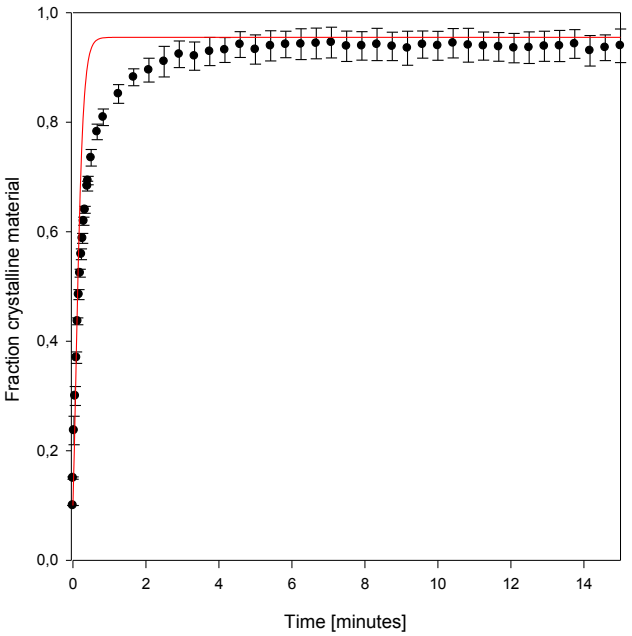

a)

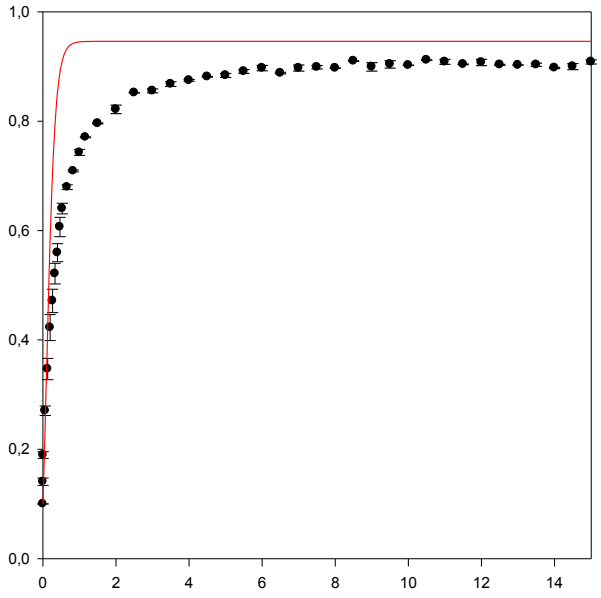

b)

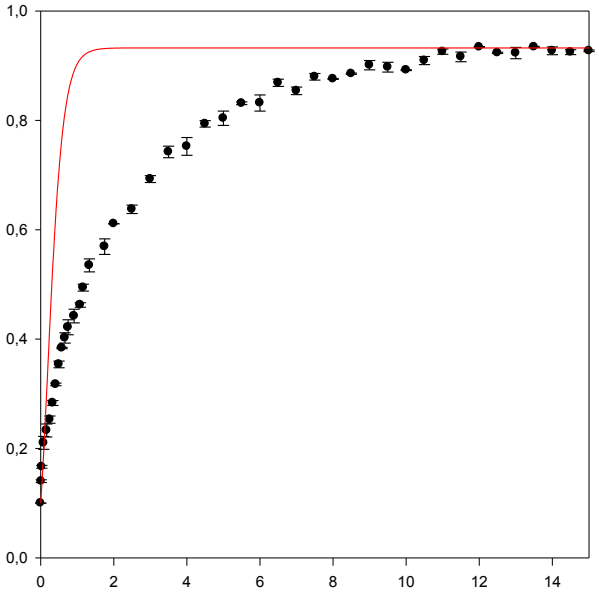

c)

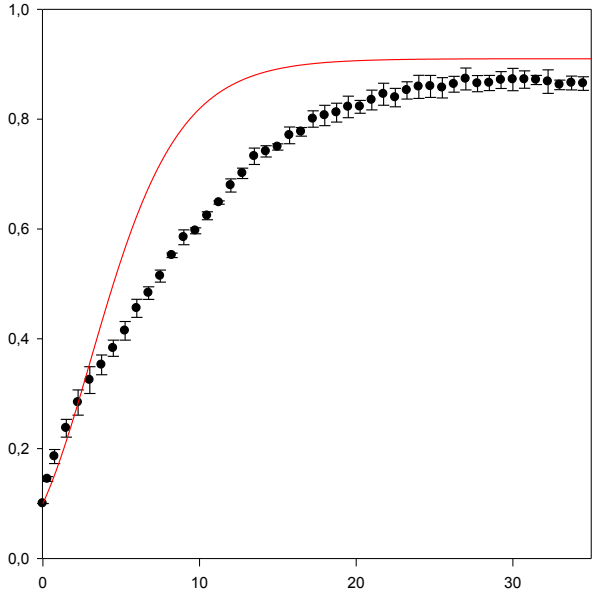

d)

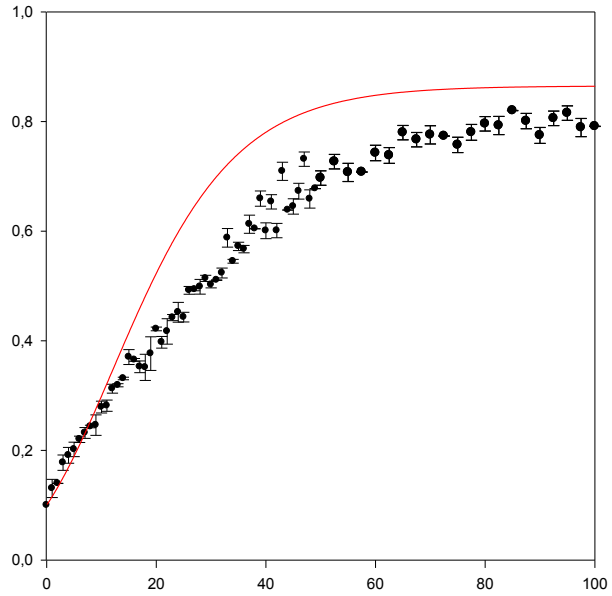

e)

a) 30μM supersaturated solution with 10% initial crystalline material, λ=0.5μm.

b) 25μM supersaturated solution with 10% initial crystalline material, λ=0.5μm.

c) 20 μM supersaturated solution with 10% initial crystalline material, λ=0.6μm.

d) 15μM supersaturated solution with 10% initial crystalline material, λ=1.6μm.

e) 10μM supersaturated solution with 10% initial crystalline material, λ=20μm.

Appendix 25

Results from the comparison between the crystal growth experiments on Felodipine and classic nucleation theory. The mean value is displayed along with the standard error of the mean. The solid lines are the simulated curves.

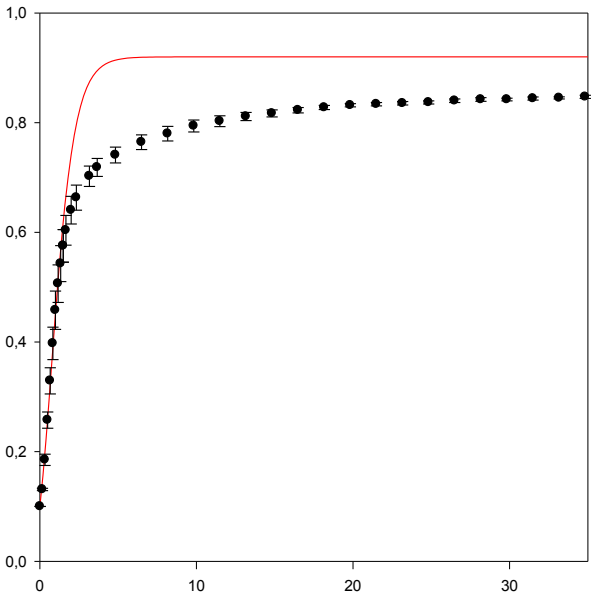

a)

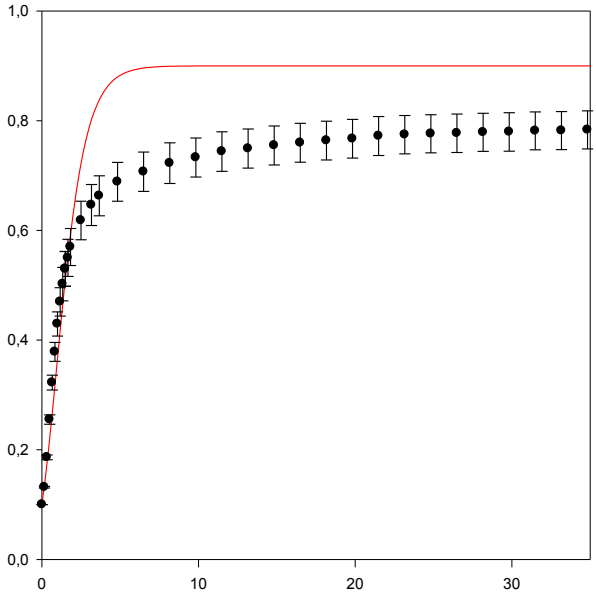

b)

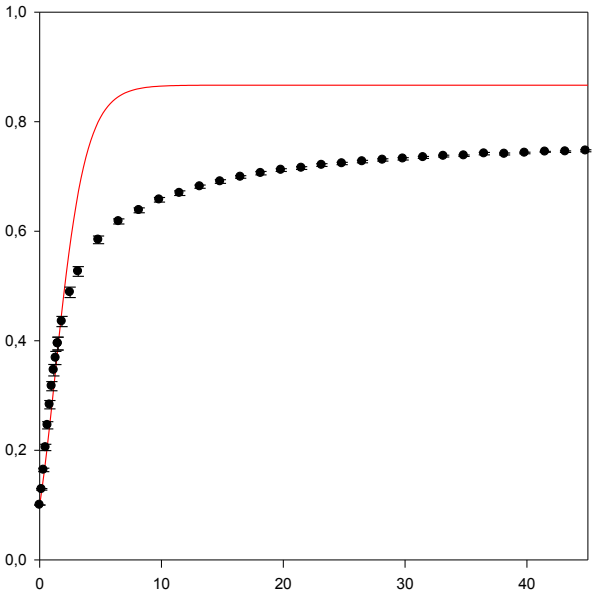

c)

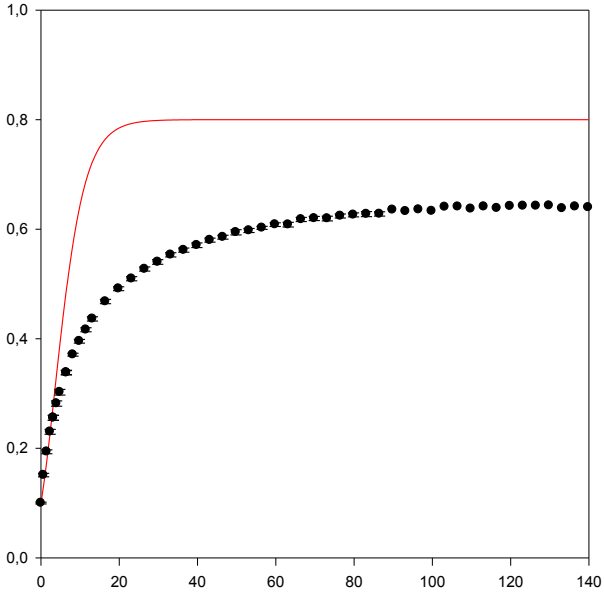

d)

a) 25μM supersaturated solution with 10% initial crystalline material, λ=3.5μm.
b) 20μM supersaturated solution with 10% initial crystalline material, λ=2.8μm.
c) 15 μM supersaturated solution with 10% initial crystalline material, λ=3.0μm.
d) 10μM supersaturated solution with 10% initial crystalline material, λ=7μm.

Appendix 26

Microscope images of crystals detected in the wells in the crystal nucleation experiments of Bicalutamide. The images displays typical crystals and typical wells, however many wells are empty as well.

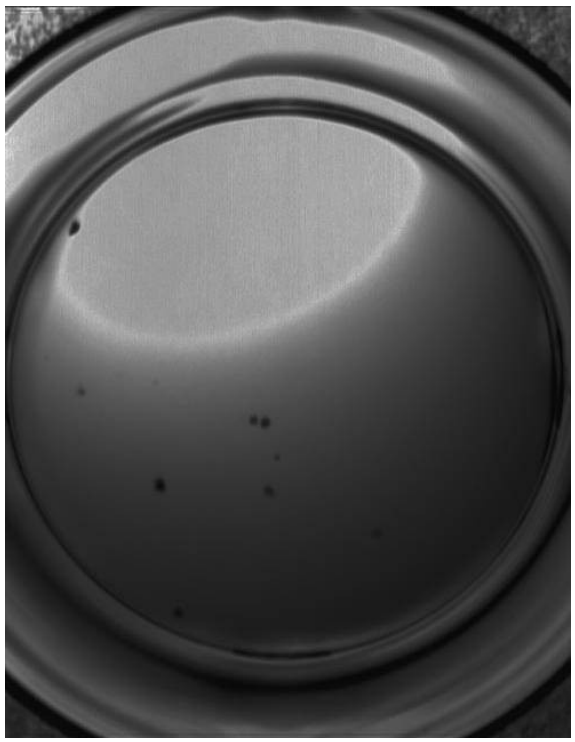

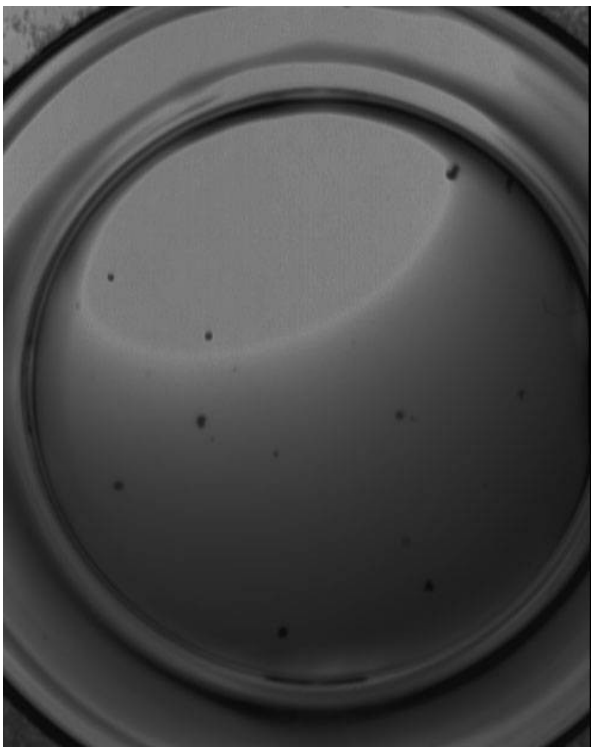

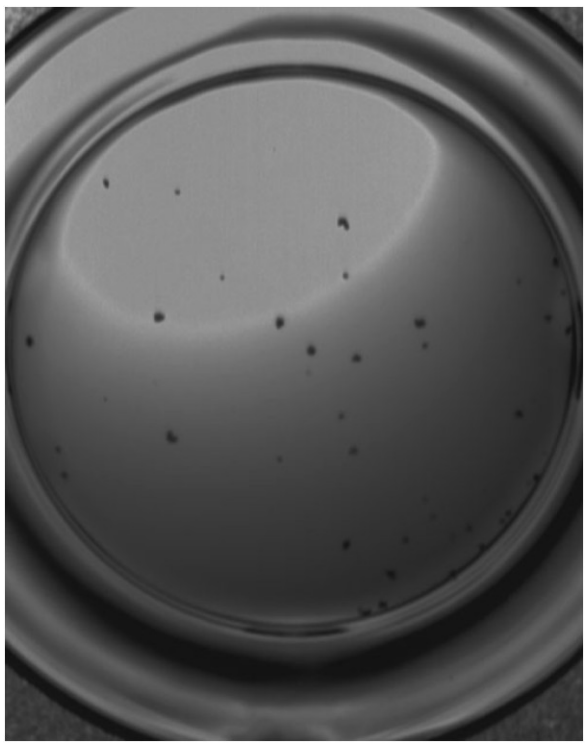

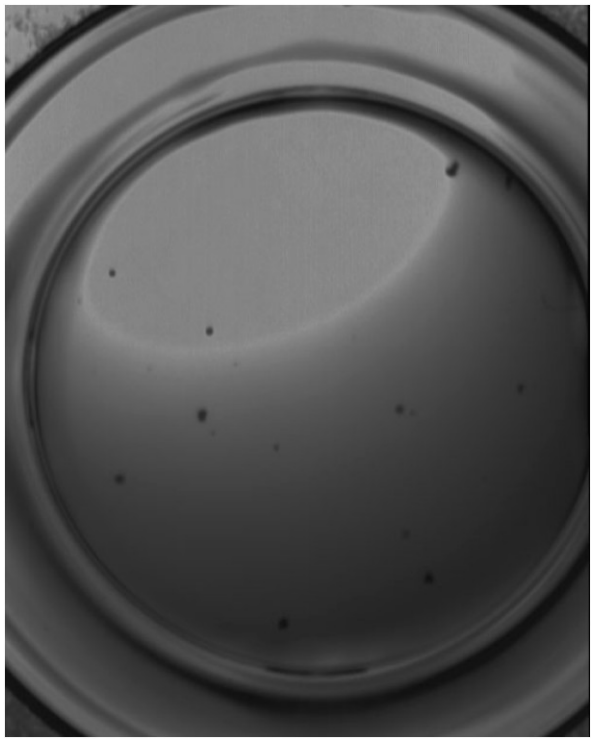

Appendix 27

Microscope images of crystals detected in the wells in the crystal nucleation experiments of Linaprazan. The images displays typical crystals and typical wells, however many wells are empty as well.